Influence of Ionic Characteristics of Inorganic Salt Solutions and Mechanical Loading on Attenuation and Self-sealing Ability of Compacted Bentonites

Thesis

Submitted in the partial fulfilment of the requirements for the degree of

Doctor of Philosophy

By

Partha Das

Roll No. 146104039

Under the supervision of

Dr. TV Bharat

Department of Civil Engineering

Indian Institute of Technology Guwahati

Certificate

This is to certify that the thesis entitled "Influence of Ionic Characteristics of Inorganic Salt Solutions and Chemo-mechanical Loading on Attenuation and Self-sealing Ability of Compacted Bentonites", submitted by Partha Das (146104039), a research scholar in the Department of Civil Engineering, Indian Institute of Technology Guwahati, for the award of the degree of Doctor of Philosophy, is a record of an original research work carried out by him under my supervision and guidance. The thesis has fulfilled all requirements as per the regulations of the institute and in my opinion, has reached the standard needed for submission. The results presented in this thesis have not been submitted to any other university or institute for the award of any degree or diploma.

Dr. T.V. Bharat
Associate Professor
Geotechnical Division
Civil Engineering Department
IIT Guwahati

Acknowledgement

I would like to express my sincere gratitude and thanks to my supervisor Dr. T.V. Bharat for his enormous help and valuable guidance during my entire PhD work. I particularly thank him for imparting interest towards the field of academic research and training me continuously towards it. I strongly believe without his valuable inputs, suggestions, and guidance, this work would not have shaped the way it has.

I would like to reserve special thanks for my Doctoral Committee (DC) chairman, Dr. Rajan Choudhury, and all the DC members, Dr. Anil Kr Mishra and Dr. S.K. Majumder for their immense help and valuable advice in improving the quality of the work. I extend my heartfelt gratitude to my previous DC members, Dr. Sangamesh Deepak and Late Dr. Narayan Reddy for their word of appreciation and valuable support in enhancing the work quality.

My sincere thanks to all the faculty members of the Geotechnical Division, Department of Civil Engineering, IIT Guwahati for providing me with the opportunity to credit various courses during my PhD period in which they introduced various concepts and provided critical insights in the subject of Geotechnical engineering. I shall also like to thank the staff members of the Geotechnical Engineering lab for being warm and cordial with me throughout my stay and providing me with all the necessary help to carry out my experiments.

I would like to convey special thanks to the other group members in my Supervisors' lab, namely, Mr. Dhanesh Sing Das, Mr. Himanshu Yadav, Mr. Ankti Srivastava for all the productive discussions pertaining to my research. I extend my humble thanks to the staff of Central Instruments Facility (IITG), Center of Environment, IITG, Environmental Engineering (Civil Department, IITG) for allowing me to carry out various sample analysis as and when required. I also would like to reserve special thanks for another research scholar, Mr. Chandra Bhanu Gupt for providing help in getting the EDX results at various times during my research work. I extend my thanks and gratitude to Dr. Rajesh Kumar Upadhayay, former faculty of Chemical Engineering Department, IIT Guwahati, and Mr. Trilokpati Tribedi, Research Scholar, Chemical Engineering Department for all the assistance they provided me in performing the pore-fraction analysis experiments. I shall like to thank the Ministry of Human Resource and Development, India, for providing financial assistance and the Indian Institute of Technology, Guwahati, for all the necessary facilities for the successful completion of this work.

I also take this opportunity to thank my parents Mr. Bibek Das and Mrs. Mandira Das and my sister Miss Barnali Das for the love, care, and faith they bestowed upon me during my PhD period. I shall like to thank my spiritual Guru Prabhupad Shree Nataraj Kishore Goswami for his love and guidance which helped me immensely in my life. My Gurudev motivated me to aim high and his advice is always a blessing for me. I also reserve special thanks for my maternal uncle Dr. Narayan Chakraborty for his untiring and sustained mental support during various phases of my life. Finally, I want to whole-heartedly thank my dearest Lord Krishna (Radhaballabh/ Laddu Gopal) for HIS blessings and love.

Abstract

The bottom liner facilities comprising of bentonites are popularly used in municipal solid waste (MSW) landfills to impede the flow of generated leachates. Owing to various virtues such as low saturated hydraulic conductivity ($k_s < 10^{-9}$ *m/s*), and very high sorption potential the bentonites are preferred as hydraulic barriers. Diffusion is thus, the predominant mechanism for the leachate flow through such impermeable barriers in the absence of advection. Several available studies reveal the degradation of the bentonite performance and the consequent increase in the hydraulic conductivity of the compacted bentonites due to their longer exposure to salt leachates. Under such conditions, the effective flow path for the diffusing species through the barrier system might get altered, which in turn could influence the mass transport parameters, viz., effective diffusion coefficient (D_e), and retardation factor (R_d). The long-term influence of the aggressive salt solutions on the diffusion behaviour of the salt-laden liner is essential for the long-term performance of the bentonite-based barrier systems.

The self-sealing ability of the granulated bentonite barriers is another virtue owing to which the dominant transport mechanism in geosynthetic clay liners (GCLS) is diffusion, The existing studies indicate that the osmotic potential of the granular bentonites decreases in the presence of salt solutions. However, the studies related to the sealing and swelling ability of granular bentonite under high ionic strength salt solutions are scarce. Moreover, the granular bentonites in geosynthetic clay liners are mostly exposed to aggressive salt leachates under the overburden waste load in the un-hydrated state. Therefore, the sealing and swelling ability of the granular bentonite in the un-hydrated state under chemo-mechanical loading remains to be understood.

In the present study, the diffusion characteristics of compacted powdered and granular bentonite were studied extensively in the presence of various salt concentrations. The influence of the sorption potential on the diffusion rates of various salt cations was also presented. Further, the sealing and swelling potential of compacted granular bentonite in the presence of various salt solutions and under the overburden stresses induced by the waste in municipal solid waste landfills was presented in this work. It was shown in this present study that the design parameters viz., effective diffusion coefficient, and retardation factor were significantly influenced by the type of permeating fluid. In the presence of high ionic strength salt solutions, the diffusion rates were significantly higher through both powder and granular bentonite. Further, the present study reveals for the first time that the sealing ability of the GB was completely lost upon permeation with high salt concentrations and under low overburden stresses. The inter-aggregate voids present in the granular bentonite remained intact and the condition is favourable for easy mobility of different contaminants, including viruses and pathogens, into the environment. The applicability of the granular bentonites in the form of geosynthetic clay liners as a bottom liner facility in a higher saline environment, therefore, remains a serious concern.

In order to address this problem, a protective layer consisting of kaolin was proposed in this work. The effectiveness of the kaolin-bentonite layered system in high saline conditions was presented for the first time. The proposed barrier system was found to perform satisfactorily even in the presence of high ionic strength salt solutions for both powdered and granular bentonite in terms of the diffusion rates of the salts. The microstructural and the elemental

compositional analysis revealed that the addition of kaolin allowed the underlying granular bentonite layer to disintegrate into smaller particles and seal the inter-aggregate voids. The study also provides a qualitative assessment of the applicability of the clay-based barrier systems in attenuating various viral pathogens.

Keywords: Powder bentonite, granular bentonite, salt-leachate, effective diffusion coefficient, retardation factor, sealing ability, kaolin-bentonite layer

Table of contents

List of Figures

List of Tables

Abbreviations

GCL	Geosynthetic clay liners
MSW	Municipal solid waste
BMW	Bio-medical waste
PB	Powdered bentonite
GB	Granular bentonite
CEC	Cation exchange capacity
SSA	Specific surface area
EGME	Ethylene glycol mono-ethyl ether
ESV	Equilibrium sediment volume
CONTRADIS	Contaminant Transport due to Diffusion in Soils
DDL	Diffused double layer
EDX	Energy-Dispersive X-ray
FESEM	Field Emission Scanning Electron Microscope
ST	Sealing time
CoV	Coronavirus

Nomenclature

D_e	Effective diffusion coefficient (m^2/s)
H_s	Equivalent height of the contaminant in the source reservoir (cm)
H_c	Equivalent height of the contaminant in the collector reservoir (cm)
H_r	Equivalent height of the contaminant in the source and collector reservoir (cm)
K_s	Saturated hydraulic conductivity (cm/s)
R_d	Retardation factor
n	Porosity
c	Concentration of the solute (mg/l)
c_0	Initial concentration of the solute (mg/l)
x	Spatial distance
ρ_d	Dry density (Mg/m^3)
c/c_0	Normalized relative concentration of the solute
α_j	Roots of transcendental equation
D_0	Free solution diffusion coefficient (m^t/s)
τ	Tortuosity
V_{eq}	Final sediment colume (cm^3/g)
I	Measured intensity of any medium (cps)
I_0	Initial intensity in air (cps)
μ_{eff}	Effective attenuation coefficient (cm^{-1})
μ_s	Soil attenuation coefficient in air-dry state (cm^{-1})
μ_w	Attenuation coefficient of water (cm^{-1})

ε_{ssat}	Volume fraction of the soil solids in the saturated state
ε_s	Volume fraction of the soil solids in the air-dry state
k_f, $1/n$	Freundlich isotherm parameters
β	Contact angle
v_s	Volume of the suspension (ml)
w	Mass of the adsorbent material (mg)
q_e	Amount of solute adsorbed per mass
φ	Electrostatic potential
v	Valence of the ion
e'	Elementary charge
ε	Dielectric constant
k_BT	Thermal energy per ion

Chapter 1

Introduction

1.1 General

Rapid industrialization and the enormous increase in population density has contributed immensely to the increase in domestic and industrial waste. In order to address this huge waste disposal need of a particular city or a region, landfill becomes inevitable. Landfills are the engineered waste containment facilities that allow the disposal of waste in a safe and effective manner. In the earlier times, the landfills were devoid of any bottom liner facilities to restrict the migration of the generated leachate. However, the need for the bottom hydraulic barriers was realized to eliminate the adverse effects of the landfill leachate on the surrounding land and groundwater (Daniel, 1993; Bouazza and Impe, 1998; Rushbrooh, 1999; Kong et al., 2017). In the municipal solid waste landfills, a single bottom liner system is used to reduce the exposure of the generated leachate within the landfills to the surrounding environment. A leachate collection system of porous material is placed above the bottom liners to reduce the amount of generated leachate reaching the liners (Rushbrook and Pugh, 1999; Blight, 1996; Bouazza and Impe, 1998; Du et al., 2009). The guidelines provided by the environmental protection agencies of various countries advocate the use of soils as bottom liners that has hydraulic conductivity lower than $1x10^{-9}$ m/s (Manassero, 1997; CJJ113, 2007; EPA, 2015). The successful performance of the landfill is governed by the effective design of such bottom liner systems. Compacted clay liners (CCLs) comprising of highly plastic clays viz., powdered bentonite were initially used to achieve the required hydraulic conductivity and the thickness of the CCLs varies from ~0.75-1 m (Daniel, 1993; Ahsford and Husain 1996; Al-yaqout and Townsend, 2003; Safari et al., 2012; Jingjing, 2014).

The thick CCLs allowed minimal leachate flux to the surrounding land and water table. However, since the last two decades, geosynthetic clay liners (GCLs) have gained more popularity. The GCLs comprise of a thin layer of granulated bentonite (~5-7 mm) sandwiched between two geotextile layers. The various virtues, viz., ease of handling and installation, easy availability, lesser thickness, and resistance to environmental degradation

makes the GCLs a suitable alternative over the conventional compacted clay liners (Mazzieri and Pasqualini, 2000; Bouazza, 2002; Bradshaw and Benson, 2014; Darde et al., 2020; Yan et al., 2020). Although the GCLs have emerged as the most preferable barrier material due to the aforementioned virtues, the attenuation of the leachate flux, in the long run, is minimal in comparison to CCLs. Thus the CCLs are still one of the desired hydraulic barriers in landfills in some regions (Giroud et al., 2015; Xie et al., 2015. Shu et al., 2017).

Apart from maintaining the saturated hydraulic conductivity lower than the limiting value ($k_s \leq 10^{-9}$ cm/sec), the bentonite-based barrier systems have very high retention capacity for cations (Benson et al., 1994; Kau et al., 1998; Rowe and Lake, 2000; Katsumi et al., 2007; Bharat, 2013; Bohnhoff and Shackelford, 2014; Chen et al., 2016). Owing to such low hydraulic conductivity of the bentonites, the slow diffusion process augmented by high sorption potential is the sole predominant mechanism in the landfills. The advection transport is, therefore, absent in these leachate containment facilities as the barriers are nearly impermeable to the migration of salts under the hydraulic gradients.

Commonly, the MSW landfills comprise of leachates of high salinity that include an array of inorganic cations, viz., Lithium (Li^+), sodium (Na^+), potassium (K^+), and calcium (Ca^{2+}) due to salt-laden solid waste from the rubber industry (Ozgunar et al., 2007; Boopathy et al., 2013); as coal combustion waste from the coal-fired plants (Salihoglu et al., 2016; Tian et al., 2019; Chen et al., 2019; Zainab and Chen, 2020); as construction and demolition waste from the construction industries (Weber et al. 2002; Yeheyis et al., 2013; Turkyilmaz et al., 2019); and as stabilized inorganic hazardous waste produced due to stabilization of the waste from the electroplating industries (Conner and Hoefner, 1998; Wang et al., 2019). Due to the frequent and increased disposal of waste from such industries, the bentonite-based liners are eventually exposed to the high ionic strength salt leachates. Several available studies reveal that the plasticity of the bentonite decreases with the salt concentrations (Sridharan and 1986; Di Maio et al., 2004; Mishra et al., 2009; Sridharan, 2014) which consequently increases the hydraulic conductivity (Rao and Mathews, 1995; Shan et al., 2002; Kolstad et al., 2004; Jo et al., 2005; Bradshaw and Benson, 2013; Setz et al., 2017). Owing to such changes in the hydraulic conductivity of the bentonite, the effective flow path for the contaminants through the bentonite gets altered which in turn has the potential to affect the

diffusion characteristics of the bentonite. For an efficacious design of the liner systems, accurate estimation of the diffusion parameters, viz., effective diffusion coefficient (D_e), and retardation factor (R_d) in the presence of salts, thus, becomes vital. The influence of various salt cations and synthetic leachate on the mass transport parameters (D_e, R_d) of the compacted bentonite-based barrier systems is scarce.

The self-sealing ability is another important virtue that makes the bentonite-based barriers (GCLs in particular) preferable for the waste containment facilities. The granular bentonite (GB) in the GCLs contains large inter-granular voids and these voids are sealed upon hydration with water. The self-sealing ability of the GB is due to its unique swelling property when hydrated with water (Babu et al., 2001; Parastar et al., 2017; Salemi et al., 2018; Li and Rowe, 2020). In the hydrated state, the granules of the bentonite disintegrate and swell into the inter-granular space to maintain a very low hydraulic conductivity. Further, the deployed GCLs in the field are subjected to serious damages including puncture and loss of bentonite during the placement (Mazzieri and Pasqualini, 2000; Rowe and Li, 2020; Rowe and Abdelrazek, 2020). Such technological gaps are also sealed by the hydrating GB in the GCL. The GCLs, therefore, can perform satisfactorily in terms of their sealing and swelling ability only upon complete hydration with water. However, GCLs consisting of the GB in the landfills are usually in the air-dry condition and might not get fully hydrated from the sub-surface moisture. The GCLs thus are directly exposed to different landfill salt leachates in the un-hydrated state (Jo et al., 2001; Scalia and Benson, 2010; Williams, 2018).

Some laboratory studies showed a reduction in the osmotic potential of the GB in the presence of different salts (Lee and Shackelford, 2005; Setz et al., 2017). However, the sealing and swelling ability of GB under high ionic strength salt solutions are not studied. Moreover, GBs are exposed to inorganic salts in the un-hydrated state under different overburden stresses due to waste load. These overburden stresses vary from low (initial phase of waste disposal) to high (when the landfill is full) during the service life of the landfill (Peirce et al., 1986; Lake and Rowe, 2000, Wang et al., 2019). The overall mechanical stability of the landfill is influenced by the volume change behaviour of the liner during the leachate migration and under overburden stresses. Therefore, an elaborate study on the sealing and swelling ability of the air-dry granular bentonites under the salt

environment and different mechanical stress conditions is vital for evaluating the applicability of such materials for attenuating various contaminants in the landfills. Further, such a study is also important as the MSW landfills comprise of biomedical waste (BMW) that are possibly contaminated with various pathogens due to the current practice of BMW disposal in the existing landfills (WHO, 2014; CPCB, 2020; Haque et al., 2020; IGES, 2020) apart from the salt-laden solid waste. The effectiveness of the GCLs in attenuating the contagious viruses and pathogens depends on the GB behaviour in the salt leachate environment. But the applicability of compacted GB in attenuating the viral pathogens is not available yet.

Further, in order to address the problems associated with the degradation of the performance of the bentonite-based liner facilities upon permeation with various pore-fluids, an alternate liner system for the long-term satisfactory performance is vital. Some of the recently available studies reveal that kaolin soil behaves in a strikingly opposite manner in comparison to the bentonites. Due to the presence of unique termination sites in kaolin (Polomino and Santamarina 2005; Wang and Siu, 2006), the plasticity of kaolin increases, and the hydraulic conductivity of kaolin is also found to decrease in the pore-fluid environment (Sridharan et al., 1986; Sridharan, 2014; Li et al., 2013). The volume change behaviour of kaolin is also found to be opposite in comparison to bentonite upon permeation with various pore-fluids (Choudhury and Bharat, 2018). Moreover, kaolin exhibits very high sorption potential for various chemical species and viral pathogens (Clark et al., 1998; Choy et al., 2007; Vascencelos et al., 2007; Park et al., 2014; Li et al., 2015; Doi et al., 2020). Therefore, the addition of kaolin as a protective layer above the bentonite-based barrier facilities is expected to allow the bentonite layer to retain its virtues even upon longer exposure to different pore-fluids. However, such a study of the kaolin-bentonite layered system is not available.

1.2 Objective of the research work

Based on the aforementioned discussion few objectives for the present work are listed as follows:

- To study the ionic characteristics of inorganic salt solutions on the diffusion characteristics of the compacted powder and granulated bentonite.
- To study the effect of various synthetic leachates on the diffusion characteristics of compacted bentonite.
- To study the volume change behaviour and sealing ability of compacted granular bentonites in the presence of salt solution and under the possible stresses induced by the landfill-waste.
- To assess the effectiveness of the compacted clay-based barriers in attenuating the viral pathogens that are present in the MSW landfills from the virus-contaminated bio-medical wastes.
- To study the applicability of an alternate barrier system comprising of the kaolin-bentonite layer for the satisfactory performance of such systems in the presence of high ionic strength salt solutions.
- To study the chemo-mechanical and diffusion behaviour of the kaolin-bentonite layered system in the presence of the expected salt solutions in the MSW landfills.

1.3 Organisation of the thesis

Having identified the objectives, the thesis is divided into nine chapters including five contributing chapters. **Chapter 1** presents the introduction to the problem, the motivation behind the research work, and the objectives of the present work. A detailed review of the available literature relating to the effect of pore fluid on various engineering properties of the powder and granulated bentonite was presented in **Chapter 2**. The critical appraisal of the available related work leading to the objective of the present study was also presented in this chapter. **Chapter 3** provides information on the various soil and salt solutions used in the study. The laboratory experimental methodology for estimating the mass transport parameters of the studied soils from the transient through diffusion test was presented in this chapter. The adopted procedure for estimating the sealing potential of granular bentonite under the influence of various salt concentrations was discussed in this chapter. The pore-fraction, micro-structural and elemental compositional analysis for the studied bentonite

samples after equilibration with various salt solutions was also presented in this chapter. Results and discussion from the study are presented in chapters 4 - 8. **Chapter 4** presents the effect of the size, valence, and concentration of the salt cations on the diffusion behavior of both compacted powder and granulated bentonite. The application of a Java-based inverse analysis suit in estimating the model parameters from the experimental data for analyzing diffusion behaviour was presented. **Chapter 5** presents the influence of various synthetic salt leachates on the diffusion characteristics of powder bentonite under different compaction densities. A detailed discussion on the elemental adsorption by the compacted bentonite post equilibration with different salt solutions was presented and supported with EDX results. The long-term diffusion behavior of the compacted powdered bentonite was presented in this chapter. The change in the accessible porosity during the salt migration through the compacted bentonite augmented by pore-fraction analysis was also presented in this chapter. **Chapter 6** presents the volume change behaviour and sealing ability of the compacted granular bentonite under the influence of various salt solutions. The effect of loading condition and the concentration of the permeating fluid on the sealing behaviour of the granulated bentonite was also presented. The sealing potential and the volume change behaviour of an alternate barrier system (kaolin-bentonite layered system) was then discussed in **Chapter 7**. The influence of various salt type and salt concentrations on the diffusion behaviour of the kaolin-bentonite layered system was also discussed in this chapter. **Chapter 8** provides the qualitative assessment of the clay-based barrier systems in attenuating the virus-contaminated bio-medical waste from the available limited sorption data**.** The effectiveness of the kaolin-bentonite layered system in attenuating the viral pathogens was also discussed in this chapter. Important conclusions and scope for future work were discussed in **Chapter 9** based on the detailed investigation of the results and gaps in the present work.

Chapter 2

Background and Literature Review

2.1 General

Landfills are the unparalleled engineered containment facilities for addressing the ever-growing waste disposable problems. Before the modern-day landfills, very few engineering control measures were adopted and the generated daily waste was mostly disposed of in open dumpsites or incinerated. However, post the 1950s, significant attention was given to get rid of the negative environmental impact of open dumping and incineration resulting in the development of landfills (Bagchi, 1990; Daniel, 1993, Worrell and Vessilend, 2012). The landfill construction is carried out in numerous phases to accommodate the daily waste of a particular locality in various cells (Fig.2.1). The generated leachate from the disposed waste in the cells is encapsulated by bentonite-based liners to reduce its exposure to the surrounding environment. A leachate collection system of porous material is placed above the bottom liners to reduce the amount of generated leachate reaching the liners (Rushbrook and Pugh, 1999; Blight, 1996; Bouazza and Impe, 1998; Du et al., 2009).

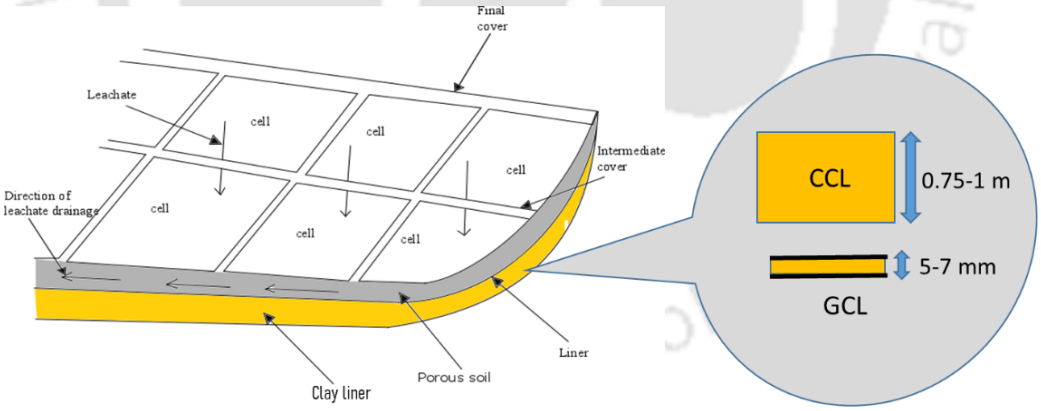

Figure 2.1: Illustration of a landfill with bottom liner facility (after, Rushbrook and Pugh, 1999)

The successful performance of a landfill is dependent on the efficacious design of the bottom liner systems. A low permeable soil having hydraulic conductivity less than $1x10^{-9}$ m/s is deemed suitable for use as a liner material. Traditionally, thick compacted clay liners (CCLs)

of fine bentonite powder or bentonite amended soil were used to achieve the limiting value of hydraulic conductivity. The powdered bentonite in the CCLs allowed very negligible contaminant flux to the bottom of the liner system and thus was effective in the complete attenuation of the leachates (Al-yaqout and Townsend, 2003; Safari et al., 2012; Jingjing, 2014). However, in recent times, geo-synthetic clay liners (GCLs) comprising of a thin granular bentonite layer (~5-7 mm thickness) is used as a suitable alternative to the conventional CCLs. Apart from being highly impermeable material, the GCLs require less labor in installation and handling, it is dust-free and provides excellent resistance to the wet and dry cycles in comparison to the traditional CCLs which makes it a preferable liner (Mitchell, 1993, Bouazza, 2002; Di Maio, 2004; Darde et al., 2020). Notwithstanding the additional virtues of the GCLs, the thick CCLs in the form of powdered bentonite still find their application in the modern-day landfills as it provides more attenuation ability in comparison to the recent GCLs (Jingjing, 2014; Xie et al., 2015; Shu et al., 2017). Thus, the CCLs/GCLs are the common types of bentonite-based liners that are used as the bottom liner facility depending on the requirement of the leachate attenuation ability (Fig. 2.1).

The powdered bentonite and granulated bentonite used in the CCLs and GCLs are obtained by the processing of the bentonite solids. The quarrying of the bentonite deposits and the subsequent processing can provide the required gradation of bentonite (powdered/granulated form). The bentonite exploited by quarrying is initially in solid form with a very moisture level (~30%). The processing is carried out after drying of the bentonite solids to the desired level. Post drying the bentonite solids are crushed and sliced and subjected to further drying in rotary kilns (EPA, 2005; Kutlic et al., 2012; Wyoming Mining Association). The crushed bentonites are then grounded at very high speed in the roller mills. The milling at high speed allows the pulverization of the bentonites into a fine powder of particle size less than 0.037 mm and the granulated bentonite can be obtained by simple sieving of the crushed bentonite post drying. If the grounded bentonite is calcium dominant, it is activated with soda-ash to obtain the desired properties (Fig.2.2).

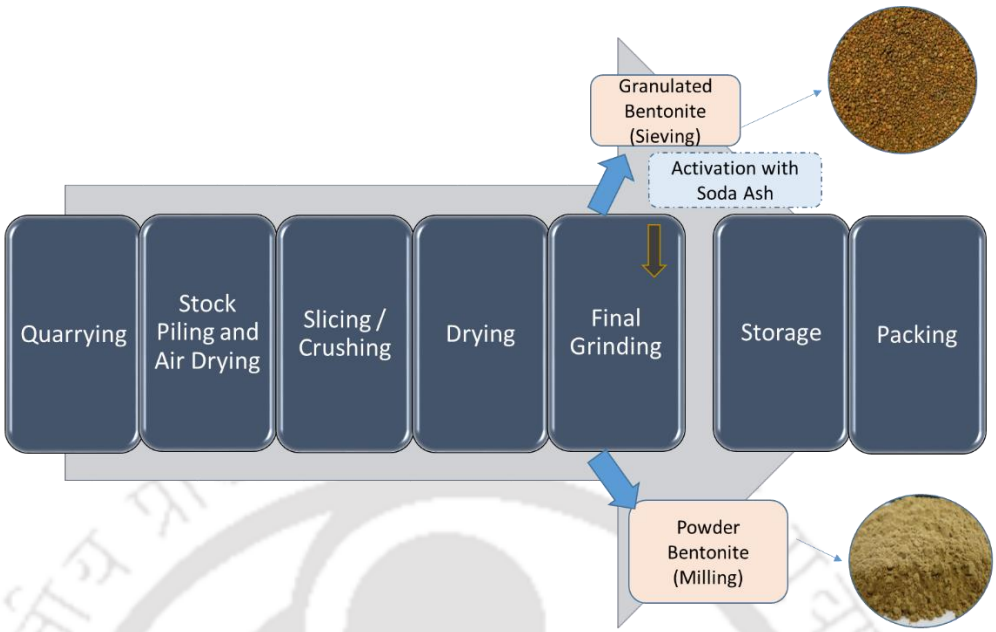

Figure 2.2: Processing of the bentonite

The powder/granular bentonite used in the bottom liner systems is rich in montmorillonite mineral. Montmorillonite is a 2:1 mineral, wherein an octahedral sheet is sandwiched between two sheets of tetrahedral. The octahedral sheets consist of trivalent aluminium (Al^{3+}) with hydroxyl ion (OH^{-}) at the vertices, and the tetrahedral sheet consists of tetravalent silicon (Si^{4+}) with oxygen atoms (0^{2-}) at the vertices. The individual 2:1 association of the unit layers of the minerals are bonded by hydrogen bonding and the successive unit layers are bonded by weak van der Waals forces (Velde, 1995; Lyklema, 1995; Mitchell and Soga, 2005). Due to the weak bonding between the interlayers, water or other polar molecules can easily penetrate between the layers and increase the basal spacing resulting in the swelling of the minerals. Bentonites are characterized by high specific surface area (SSA) and cation exchange capacity (CEC).

Further, montmorillonite-rich bentonite surface carries net negative charge due to isomorphous substitution which involves the replacement of the structural cation by lower valence cation in the crystal lattice. A diffuse double layer (DDL) is formed around the platelets in the presence of water (Mitchell, 1993) that allows the bentonites to maintain very low hydraulic conductivity. The surface properties such as specific surface area and cation

exchange capacity influence the formation of the DDLs. The variation of the hydraulic conductivity and other surface properties of the bentonites in the presence of any pore-fluid is due to the change in the DDL thickness (Muhunthan, 1991; Dolinar et al., 2007; Khorshidi and Lu, 2016).

2.2 Diffused double layer theory

In the presence of pore-fluid, the counter-ions are electrostatically attracted by the negatively-charged clay surface but are forced to diffuse away towards the bulk solution due to the concentration gradient (van Olphen, 1963). At equilibrium, cations accumulate around the clay platelets as a diffuse layer with a concentration of cations decreasing from the surface to the bulk solution. The counter-ion (i.e., cation) distribution as a function of distance from the particle surface is given by (van Olphen, 1963; Sparks, 1999; Bharat et al., 2013; Bharat and Sridharan, 2015):

$$y = 2\ln\left(\frac{\exp(\kappa x)+\tanh(z)}{\exp(\kappa x)+\tanh(z)}\right) \tag{2.1}$$

where y is the scaled potential ($y = ve'\varphi/k_BT$) at any distance, x, from the clay surface, z is the scaled surface potential ($z = ve'\varphi_0/k_BT$), $1/k$ is the equation constant, e' is the elementary electric charge, v is the valence of the cations, k_BT is the thermal energy per ion, and φ is the electrostatic potential. The equation constant (DDL thickness) can be expressed as (van Olphen, 1963)

$$1/\kappa = \sqrt{\frac{\varepsilon k_B T}{8\pi e'^2 v^2 n}} \tag{2.2}$$

where ε is the dielectric constant, n is ion concentration in the bulk solution (ions/cm^3), e' is the elementary electric charge, v is the valence of the cations, and k_BT is the thermal energy per ion.

The thickness of the DDL controls the engineering behavior of bentonite clays. The DDL thickness changes with the change in electrolyte concentration; cation properties; dielectric constant; and cation complexion between the surface cations and the cations in the pore-fluid

(Mitchell, 1993; Rao and Mathew, 1995; Sridharan and Prakash, 1999; Bharat and Sridharan, 2015a,b; Bharat and Das, 2017). For landfill applications, bentonites in the powdered and granulated form are used depending on the design requirement and availability of the processed soil. Apart from being highly impermeable and an excellent adsorbent, the bentonites exhibits high sealing ability in the presence of water due to the formation of the DDLs. However, in the presence of the electrolyte solutions (salts) the surface and engineering properties get altered for both powdered and granulated bentonites due to the change in the DDL thickness.

Available studies relating to the effect of the electrolyte concentration on the engineering and various index properties of bentonites are discussed below.

2.3 Effect of salt solutions on the long-term hydraulic behavior of bentonites

Bentonites are preferred as the barrier material as they can restrain the leachate flow considerably because of their impervious nature and high adsorbing capacity. The compacted bentonite-based barrier system is expected to maintain the hydraulic conductivity lower than 10^{-9} m/s for effectively minimizing the rate of contaminant migration through liners (Benson et al., 1994; Petrov and Rowe, 1997; Lake and Rowe, 2000; Lee and Shackelford, 2005). The hydraulic conductivity, however, increases with the permeation of inorganic salts due to the suppression of diffuse double layers (DDLs) between the clay platelets and improves the formation of the platelet clusters (Shackelford and Lee 2003).

Enormous studies relating to the variation of the hydraulic conductivity with time under the influence of salt permeation are available. The effect of salt type and concentration on the long-term hydraulic conductivity of the powder and granular bentonites are studied since the 1990s. The available studies reveal that the increase in salt concentration and salt cation valence increases the hydraulic conductivity significantly (Edil et al. 1991; Imamura et al., 1996; Gleason et al., 1997; Petrov and Rowe 1997; Stern and Shackelford, 1998; Lin and Benson 2000; Egloffstein, 2001; Rao and Mathew, 2005; Shackelford et al., 2000; Jo et al., 2001; Lee et al., 2005). An increase in the concentration leads to a greater exchange of surface cations by the cations present in the bulk solution rendering the DDL to alter considerably and as a result the affecting hydraulic conductivity with time. The effect of

cation valence on the hydraulic conductivity of clay-bentonite (powder bentonite) mix was studied by Sharaiatmadari et al. (2011). The findings from this study revealed that the increase in the hydraulic conductivity of the soil was 25% more in the presence of $CaCl_2$ in comparison to that of NaCl. The findings were consistent with that of Shackelford et al. (2000) and Jo et al. (2001). However, the effect of the valence of the salt cation is found to be significant only at low concentrations, whereas at a higher concentration no significant difference in the conductivity was found with the increase in the cation valence as studied by Mishra et al. (2009).

For the monovalent cations, an increase in the hydrated cationic radius of the adsorbed cations results in lower hydraulic conductivity (Rao and Mathew, 1995; Jo et al., 2001; Shackelford et al., 2000; Thammathiwat and Chimoye, 2010). The changes in the DDL thickness is, therefore, found to be inversely proportional to the hydraulic conductivity of the powdered bentonite soil. When the powder bentonite is permeated with higher valence salt cation and high concentration salts, the DDL thickness is suppressed leading to Vander Waals attraction between the clay particles and thus forming a flocculated structure.

For the granular bentonites, the effect of pre-saturation on the hydraulic behavior was studied by Ruhl and Daniel (1997). The study showed that the pre-saturated GCL showed low hydraulic conductivity in comparison to the case where the GCL was directly permeated with any pore-fluid. Similar results were also obtained by Wang et al. (2019), where it was seen that for a given condition the soil pre-saturated with water showed lower hydraulic conductivity in comparison to the soil which was directly permeated with a salt solution. The effect of pre-hydration of GCL was also studied Jo et al. (2005), where it was found that permeation with 0.1M KCl and NaCl increased the hydraulic conductivity by two orders of magnitude, and at a similar concentration of $CaCl_2$, the hydraulic conductivity increased by more than three orders of magnitude in comparison to the case when permeated with water.

The effect of pore-fluid on the bentonite quality of different GCLs was also studied by Lee et al. (2005), under the influence of different concentrations of $CaCl_2$. The GCL with the higher quality bentonite (HQB) is characterized by a greater content of sodium montmorillonite, higher plasticity index, and higher cation exchange capacity relative to the GCL with the lower quality bentonite (LQB). When the GCL was permeated first permeated

with DW and then inundated with $CaCl_2$ solution, the hydraulic conductivity was lower than the case where the GCL was permeated directly with the calcium chloride salts. The observation was consistent for both the qualities of bentonite, however, the degradation was more for HQB, in terms of final hydraulic conductivity. The hydraulic conductivity was of the order 10^{-5} cm/sec for 500 mM concentration of $CaCl_2$ for HQB. It was observed that non-prehydrated soil undergoes severe degradation and in the field, the bentonite liner is usually placed in the air-dried condition. The effect of bentonite content, compaction density, and type of bonds between the geotextiles on the hydraulic conductivity of the granular bentonite was studied by Parastar et al. (2017). It was observed that the GCL performed better in terms of its hydraulic conductivity at higher compaction density and with higher bentonite content. Further, the increase in the density of the needle-punching resulted in better hydraulic performance for the GCLs. Although a significant amount of studies are available on the loss of osmotic potential and the consequent increase in the hydraulic conductivity of the granular bentonites in the presence of salt solutions, the sealing and swelling ability of the granular bentonite in non-prehydrated conditions under the expected waste needs to be thoroughly studied.

2.4 Effect of pore-fluid on the sediment volume of bentonites

Laboratory index tests such as sediment volume tests are routinely performed to assess the hydraulic behavior of the soil under various electrolyte concentrations for its use as liner material for landfills (Lin and Benson, 2000; Lee and Shackelford, 2005). The sediment volume test gives a qualitative understanding of the long-term hydraulic behaviour of the bentonites. A direct relationship between the sediment volume and the hydraulic conductivity of kaolin clay was established by Bowders et al. (1986). For granular bentonites, a strong relationship was obtained between hydraulic conductivity and sediment volume (Jo et al., 2001; Kolstad et al., 2004). Similar to the hydraulic conductivity results, sediment volume studies on bentonite suggest that an increase in the concentration of the pore-fluid results in a lower sediment volume (Mishra et al., 2009; Lee and Shackelford, 2005). The decrease in sediment volume with the increase in concentration is due to the decrease in the DDL thickness (Jo et al., 2001).

The effect of cation valence on the free swell index of granular bentonite was studied by Thammathiwat and Chimoye (2010), and it was found that for a particular concentration, the swell volume was smaller with divalent and trivalent cations in comparison to the monovalent cations. This was attributed to the lower DDL thickness of the clay platelets in the presence of higher valence salt cation. Moreover, with the increase in the hydrated cationic radius of the pore-fluid, the sediment volume was found to increase (Sridharan et al., 1986). This was due to the increase in the DDL thickness with the hydrated cationic size in the same group of the periodic table. The swell volume of the soil is dependent on the quality of the bentonite where a higher quality of bentonite is subjected to greater degradation in the presence of high concentration pore-fluids (Lee and Shackelford, 2005). In the case of GCLs or granular bentonites, at higher concentrations, significant compression of the adsorbed layer of cations takes place resulting in the formation of particle flocs which settles more quickly and thus gives lesser sediment volume. As the waste leachate in the landfill consist of a wide variation of salts, the sediment volume study for both granular and powder bentonites is importnat. A comparison of the sediment volume behaviour of different bentonites used as liner materials in the presence of various pore-fluid will provide knowledge of the long-term behavior of such liner materials.

2.5 Effect of pore fluid on the liquid limit of bentonite

The water content at which the shearing resistance of a soil approaches to that of a liquid is understood to be the liquid limit of a soil (Sridharan and Prakash 2000). The engineering properties of the bentonites are primarily associated with the plasticity behaviour. The available literature on the effect of pore-fluid concentration indicates that the liquid limit for bentonite soil decreases with the increase in the pore-fluid concentration. In other words, the liquid limit is inversely proportional to the hydraulic conductivity when the concentration and valence of the electrolytes are varied (Mishra et al., 2005; Arasan and Yetimuglu, 2008). The findings on GCLs are qualitatively in good agreement with the observations on expansive clays based on the diffuse double layer theory (Mesri and Olson 1971; Achari et al. 1999; Sridharan and Choudhury 2008). The suppression of DDLs of the clay platelets due to the influence of pore-fluid concentration, dielectric constant, and valence results a decrease in both sediment volume (Sridharan and Prakash 1999) and the liquid limit water

content (Sridharan et al., 1986); but increase in the hydraulic conductivity (Kolstad et al., 2004). This depression in the DDL thickness decreases the amount of moisture required to bring the minimum shearing resistance between the clay platelets, thus decreasing the liquid limit with the increase in concentration.

From the available literature study, it was understood that the hydraulic conductivity of the powder and granulated bentonite changes with the change in electrolyte concentration; cation properties; and cation complexion between the surface cations and the cations in the pore-fluid (Mitchell, 1993; Rao and Mathew, 1995; Sridharan and Prakash, 1999; Bharat and Sridharan, 2015; Bharat and Das, 2017). As diffusion is the dominant mechanism for the leachate flow through the bentonites, the change in the hydraulic conductivity of the soil is also expected to affect the diffusion characteristics. The effective design of the bentonite-based bottom liners involves accurate estimation of the model parameters, viz., effective diffusion coefficient, and retardation factor. Therefore, the studies relating to the influence of salt-cation type and concentrations on the model parameters is essential. Some of the available studies on the influence of pore-fluid on the diffusion behaviour of compacted bentonite soils were discussed sec. 2.7. and the diffusion theory was presented sec. 2.6.

Moreover, the osmotic potential of the granular bentonites is found to be lost in the presence of salt solutions. The granular bentonites which are placed in the air-dry condition in the GCLs are expected to be exposed to the aggressive salt leachates in the un-hydrated state and under the overburden waste load. The sealing ability of the granular bentonites under such chemo-mechanical loading remains to be understood.

2.6 Diffusion Theory

Salt diffusion is defined by its movement from a region of higher concentration to a low concentration due to the concentration gradient. The diffusive flux given by Fick's first law is (Shackelford, 1991; Barone et al., 1992; Bharat et al., 2009):

$$F_d = -D_0 \frac{\partial C}{\partial x} \tag{2.3}$$

where F_d is the Flux or amount of solute that would flow through a unit area during a unit time interval, c is the concentration of the salt ion in the liquid phase, x is the direction of transport, D_0 is the free solution diffusion coefficient.

Due to the tortuous pathway, the diffusion through the soil is expected to be much lesser in comparison to the aqueous solution (Shackelford, 1989). The tortuous pathway in the soil is accounted in the EQ. 2.3 with a tortuosity factor, τ. The ratio of the straight line microscopic distance (x) to the actual flow path (x') is defined as the tortuosity of the soil which is given as $\tau = x/x'$, (Shackelford, 1989). Hence the diffusive flux when the flow takes place through the soil is modified as:

$$F_d = -D_e n \frac{\partial C}{\partial x} \tag{2.4}$$

D_e is the effective diffusion coefficient which is given by the equation:

$$D_e = D_o \tau$$

where τ is the tortuosity coefficient

The Eq. 2.4 defines the steady-state diffusive flux given by Fick's first law and the transient state diffusive flux describing the one-dimensional governing diffusion equation for saturated soils is given by

$$\frac{\partial c}{\partial t} = \frac{D_e}{R_d} \frac{\partial^2 c}{\partial x^2} \tag{2.5}$$

where c is the salt concentration in the soil pores, t is the diffusing time, D_e is the effective diffusion coefficient, n is the porosity, x is the distance from the source, and R_d is the retardation factor which describes the sorption potential of a soil. The retardation factor for linear sorption case is expressed as

$$R_d = 1 + \frac{\rho K_d}{n} \tag{2.6}$$

where K_d is the distribution coefficient, ρ is the dry bulk density and n is the porosity of the clay plug.

Several laboratory diffusion studies are used to estimate the design parameters based on the solution to the Eq. 2.5 and the respective initial and boundary conditions. Laboratory techniques such as through-diffusion or double-reservoir technique (Barone et al., 1992; Kau et al., 1998; Badv and Abdolalizadeh, 2004; Rowe and Booker, 1985; Rowe et al., 1988), in-diffusion or single-reservoir technique (Shackelford et al.,1989; Shackelford and Daniel 1991a, 1991b; Meiszkowski, 2003), out-diffusion (Van Loon and Jakob, 2005; Sardini et al., 2003), and half-cell techniques (Gilham et al. 1984; Robin et al., 1987) are routinely used to estimate the temporal and spatial changes of contaminant concentration estimate the model parameters (D_e, R_d) The effect of the various pore-fluid on the diffusion characteristics of compacted clayey soils was discussed in the next section.

2.7 Pore-fluid effect on the diffusion behavior of bentonites

For the effective design of the bentonite-based barriers, proper knowledge of the diffusion mechanism is essential. Notwithstanding the barrier being impermeable to the flow of contaminants due to the absence of advection, the contaminants can migrate due to diffusion (Gilaham et al. 1984; Rowe et al., 1988; Shackelford et al., 1991; Johnson et al., 1999). Many studies have been conducted to understand the diffusion behaviour of such low permeable liners.

Barone et al. (1992) estimated the diffusion coefficient of volatile organic compounds, viz., chloroform, toluene, aniline, and 1,4-dioaxane through naturally available clayey soil adopting the double-reservoir technique. The migration rate of the soluble species (acetone and 1,4-dioxane) was faster in comparison to the which were hydrophobic in nature (chloroform and toluene). Owing to the high tendency of the hydrophobic species to adsorb on the soil organic matter. Thus the diffusion coefficient of the soil varied significantly for various diffusing contaminants. The sorption potential of the soil was also significantly different.

The effect of chloride migration through a compacted bentonite liner was studied by King et al. (1993) by the single-reservoir technique. The saturated hydraulic conductivity of the soil was nearly of the order of 10^{-10} m/s, however, after 4 years chloride was already present at 0.4 meters for the total 1.2 meters thick liner system. This indicates that even in the absence

of advection the diffusion rates for a particular ion can be enormous and significant. The thickness of the liner is governed by the diffusion coefficient of the contaminant species through the clay liner (Shackelford, 1991). Thus for the design of the liners accurate estimate of the design parameters is essential for restricting the migration of the contaminants over a long period.

Transient in-diffusion test conducted on powder bentonite with different chloride salts shows that the anion diffusion rate for different salts was similar and resulted in the same diffusion coefficient (Rowe et al., 1988). However, a significant variation in cation diffusion was observed (Rowe et al., 1988). Kau et al. (1999) performed through-diffusion tests on commercial kaolin and bentonite clays for various anions and metals. The Fluoride diffusion coefficient was significantly higher for kaolinite in comparison to the montmorillonite mineral indicating montmorillonite to be a better adsorbent for fluoride.

Based on the study of Lake and Rowe (2000), the diffusion coefficient for the GCLs obtained from the in-diffusion technique depends on a number of factors viz., hydrating liquid, GCL bonding type, and contaminant concentration. In the presence of water, the diffusion coefficient for the GCL was found to be lower in comparison to the diffusion coefficient obtained for the GCL in the presence a salt solution. At lower concentrations of NaCl ($n<1M$) the diffusion coefficients were sensitive to change in concentrations for both Na^+ and Cl^-, but at higher concentrations ($n>1M$) the diffusion parameters were insensitive to the change in the concentration. The diffusion of anionic tracer ($^{36}Cl^-$) and neutral water (HTO) was performed through compacted bentonite by the through-diffusion technique (Garcia-Gutieirrez et al., 2004). The effective diffusion coefficient was found to be dependent on the accessible porosity through the soil. The accessible porosity for HTO was equal to the total porosity of the soil and thereby exhibiting a higher diffusion coefficient. On the other hand, the accessible porosity for $^{36}Cl^-$ was only a fraction of the total porosity and the corresponding diffusion coefficient was higher.

Diffusion studies through GCL for various hazardous waste indicate high sorption of hazardous material by the geotextile component of the GCL (Lake and Rowe, 2004; Rowe et al., 2005). The sorption test performed by Ganne et al. (2018) on geotextiles from two GCLs revealed that the sorption coefficient was high for all geotextiles indicating high

sorption by geotextile of GCL Heavy metal diffusion studies through clays showed no significant variation of the diffusion coefficients for different metals (Shackelford and Daniel, 1991; Lange et al., 2009). Lorenzetti et al. (2005) conducted a laboratory diffusion test on organo-bentonite and conventional sodium bentonite. The sorption of organic contaminant by organo-bentonite amended was higher, resulting in very low solute transport through the amended material.

Thus the diffusion coefficient for different migrating ions was found to be different. The concentration and type of the pore-fluid have the potential to modify the microstructure of the bentonite soil which in turn affects the migration rate through the soil. The diffusion coefficient gets altered due to the pore-fluid effect and hence the liner thickness needs to be designed considering such changes (Bouazza, 2002; Shackelford, 1991). Moreover, due to the smaller thickness of the GCLs, they have a shorter diffusive path compared to CCL and the comparison for the migration rate of a particular ion under similar conditions is not available. Most of the previous studies on granular and powder bentonite were confined to volatile organics and heavy metal migration. However, studies relating to the salt migration through the compacted powder and granular bentonite under a wide variation of salt concentration and synthetic salt leachate and under different compaction density is scarce. Moreover, a proper laboratory experimental method is essential to accurately measure the model parameters as different existing methodologies have their own advantages and disadvantages (Shackelford and Daniel, 1989; Barone et al., 1992). Appropriate diffusion cell must be used for determining the diffusion parameters, as adsorption by the cell may result in an unrealistic high diffusion coefficient (Barone et al., 1992).

The transient through-diffusion technique is more advantageous compared to other techniques due to its non-destructive nature and simplicity in the experimental measurements although all the methods lead to the same design parameters (Bharat et al., 2008; Bharat, 2009). The measured concentration data is analyzed using the mathematical formulation based on Fick's diffusion equation (Shackelford, 1991). Finite mass boundary conditions are employed in the mathematical model to represent the boundary conditions in the through-diffusion technique (Rowe and Booker, 1985). Several past studies developed numerical and semi-analytical solutions to the transient through-diffusion problem with linear sorption

assumption (Rowe et al., 1988; Moridis, 1999; Itakura et al. 2003; Garcia-Gutierrez et al., 2005; Bharat et al., 2009; Bharat et al., 2012). A closed-form analytical solution was developed for the through-diffusion problem by Bharat (2013) which is computationally robust. The model parameters are accurately estimated using optimization techniques that minimize the error between the measured and theoretically obtained concentration data (Bharat et al., 2009).

2.8 Experimental and theoretical Background for through-diffusion

In the through-diffusion technique, the intact plug of barrier material (clay) is placed within the diffusion cell. A source and a collector reservoir is connected to the clay plug as shown in Fig. 2.3. Before the commencement of the diffusion test both the reservoir is filled with distilled water to saturate the clay plug. After saturation is ensured, the source solution is replaced with the contaminating species/salt solutions (Barone et al., 1992, Rowe et al., 1988; Shackelford, 1991, Shackelford et al., 1989; Garcia-Gutierrez et al., 2004), while the collector reservoir is filled with fresh distilled water. After the introduction of the salt solution in the source reservoir mass transport of the chemical constituents takes place by molecular diffusion due to concentration gradient (Shackelford et al., 1989). This method is easy to perform and it simulates the field condition of flow through the liner however the time taken can be high.

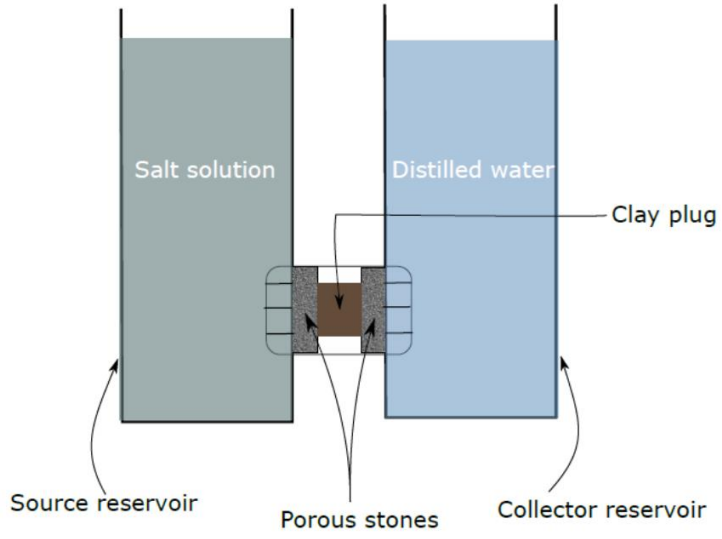

Figure 2.3: Illustration of through-diffusion set-up (after Bharat et al., 2012)

The initial condition of the diffusion experiment was given by

$$c(0 < x < L, t = 0) = 0 \tag{2.7}$$

where L is the length of the clay plug. The initial condition reflects that the clay is free of the contaminant at the beginning of the experiment, $t = 0$

The boundary conditions at the source and collector reservoirs, respectively, are given Rowe and Booker. (1985); Barone et al. (1992); Rowe at al. (1988); Bharat, (2009); Bharat et al. (2012)

$$c(x = 0, t) = c_0 + \frac{nD_e}{H_s}\int_0^t \left(\frac{\partial c}{\partial x}\right)_{x=0} dt \tag{2.8}$$

$$c(x = L, t) = -\frac{nD_e}{H_c}\int_0^t \left(\frac{\partial c}{\partial x}\right)_{x=L} dt \tag{2.9}$$

where c_0 is the initial concentration of the contaminant species at time $t = 0$; H_s and H_c are the equivalent heights of source and collector reservoirs, respectively. The boundary conditions in the through-diffusion experiment are analogous to the field conditions. The equations (2.5 – 2.9) are solved either using numerical or semi-analytical techniques to obtain theoretical contaminant concentration distribution with spatial distance and time (Rowe and Booker, 1985; Moridis, 1998; Bell et al., 2002; Samper et al., 2006; Bharat et al., 2009; Chen et al., 2012). Due to the nature of the theoretical solution, the design parameter estimation using inverse analysis is computationally inefficient (Bharat, 2013). A closed-form analytical solution for transient through-diffusion problem was developed by Bharat (2009; 2013) using the method of Laplace transformation and integral theorem. The solution at the boundaries is given by

$$\frac{c(x = 0, t)}{c_0} = \frac{1}{2 + K} + 2K\sum_{j=1}^{\infty} \frac{(\alpha_j{}^2 + K^2)e^{-\alpha_j{}^2 T}}{4\alpha_j{}^2(K + 1) - (2K - (\alpha_j{}^2 - K^2))(\alpha_j{}^2 - K^2)} \tag{2.10}$$

$$\frac{c(x = L, t)}{c_0} = \frac{1}{2 + K} - 2K\sum_{j=1}^{\infty} \frac{(\alpha_j{}^2 + K^2)e^{-\alpha_j{}^2 T}}{4\alpha_j{}^2(K + 1) - (2K - (\alpha_j{}^2 - K^2))(\alpha_j{}^2 - K^2)} \tag{2.11}$$

where $K = \frac{nR_d}{H_r}$, $T = \frac{tD_e}{R_d L^2}$, H_r is the equivalent height of the source and collect reservoirs,

α_j are the eigenvalues of the following transcendental equation

$$\tan \alpha_j = \frac{2K\alpha_j}{\alpha_j^2 - K^2} \tag{2.12}$$

where α_j are the roots of the aforementioned equation. The eigenvalues of the eq. (2.12) were obtained using a discontinuous, multimodal optimization algorithm using the Glowworm swarm optimization technique (Bharat, 2008). The closed-form solutions in Eq. (2.10) – Eq. (2.11) were evaluated using the first 20 numbers of roots using the optimization technique (Bharat, 2013).

From the aforementioned review of literature, it was understood that in the presence of various salt solutions the engineering and index properties of the bentonite-based barriers are significantly altered. The osmotic potential of the bentonites is lost due to the long-term exposure to the saline medium. The change in the hydraulic conductivity due to the microstructural changes in the bentonite is expected to bring changes in the migration rate of the diffusing salt ions. However, the effect of the varied salt type concentrations and synthetic salt leachate on the estimation of the mass transport parameters of different bentonite-based barriers is scarce. Moreover, the through-diffusion technique in the estimation of the mass transport parameters was understood to be more advantageous over the other existing techniques. As the performance of the bentonite-based barriers deteriorates in terms of the increasing hydraulic conductivity during the long-term to the salt exposure, an alternative liner material for satisfactory performance was realized.

2.9 Potential use of kaolin as a barrier material

Kaolinite is a two-layer mineral where the silica tetrahedral sheet is associated with the alumina octahedral sheet in a 1:1 ratio. In contrast to montmorillonite, strong hydrogen bonding binds the unit layer of kaolinite and as a result, it does not undergo swelling. Although kaolinite carries a net negative charge due to isomorphous substitution, the structural charge on the basal surface is negligible due to small CEC (Ma and Agleton. 1999; Choudhury and Bharat, 2018). However, kaolinite mineral is characterized by pH-dependent charges on the edge and alumina basal surface due to the presence of reactive termination sites. The alteration in the edge charges of kaolinite is dependent on the iso-electric point (IEP) of the edge. In the presence of acidic solutions, when the pH of the solution is less than

the IEP- edge, positive charges are induced in the edges (Polomino and Santamarina, 2005, Wang and Siu, 2006). On the other hand, in the presence of a highly alkaline bulk solution where the pH is more than the IEP-edge and IEP-surface, the charges on the edge and surface become negative. Moreover, in comparison to montmorillonite, the total positively charged edge area of kaolinite is much higher. The type of clay mineral would influence the amount of adsorption for a particular charged particle. For montmorillonite, the basal surface would contribute significantly to the adsorption of a particular ion, whereas for kaolinite it is the edge charges which dictate the adsorption capacity. Further, some of the available literature suggests that kaolin exhibit strikingly contrasting behaviour in comparison to the bentonite due to interaction with different pore-fluids. The plasticity of kaolin increase (Sridharan et al., 1986; Sridharan, 2014) with increased salt concentration, which consequently decreases the hydraulic conductivity (Li et al., 2013) due to the sorption ability of the termination sites. Moreover, the volume change behaviour of the kaolin in the presence of pore-fluids is found to be opposite in comparison to the bentonite (Choudhury and Bharat, 2018). The kaolinite mineral due to its unique termination sites also exhibits a very high adsorption affinity for salt cations (Jorgen. 2002; Vascencelos et al., 2007; Li et al., 2015; Matlok et al., 2015; Doi et al., 2020). Based on the available literature information which describes the contrasting behaviour of kaolin in comparison to bentonites in the presence of pore-fluids, kaolin along with the bentonite is expected to perform satisfactorily with time. However, an extensive study on the potential use of kaolin as an additional/protective barrier layer is not explored yet.

2.10 Problems associated with the bio-medical waste (BMW)

Apart from the salt leachates, the MSW landfills also comprise of biomedical waste (BMW) that are possibly contaminated with various pathogens due to the current practice of BMW disposal in the existing landfills. The excessive generation of the virus-contaminated biomedical waste (BMW) during pandemic/epidemic times, can cause serious hindrance to the safe disposal and containment of the passive transmission of the virus from such wastes. The waste generated while treating an infected patient, including the cotton swabs, samples, sharps, unused/expired vaccines, diapers, any hospital derived infectious materials and all the inputs essential for the medical diagnosis are classified as BMW (WHO, 2004;

Wanyoike, 2017; Sharma et al., 2020; Wang and Su 2020). The current recommendations of preventing the secondary transmission of virus-contaminated BMW and single-use medical gear relies on open dumping or landfilling without any pre-treatment (Ahmed, 2020; Reddy, 2020). Such unregulated disposal practice has the potential to deter the cessation of virus transmission if it gets direct exposure to the environment due to the improper liner facilities in the landfills. Moreover, the attenuation capacity of the bentonite-based liner systems for any viral pathogen is not known. As pathogens like SARS-CoV, poliovirus, and several other human viral pathogen can enter the landfills in the form of BMW, encapsulation of the BMW is of utmost importance for prevention of the passive transmission of these pathogens and avoiding any future outbreak.

Several past studies reveal that clay minerals like montmorillonite and kaolinite are very effective in adsorbing various human viral pathogens and bacteriophages (Goyal and Gerba, 1979; Vilker and Burge 1980; Clark et al., 1998; Choy et al., 2007; Park et al., 2014). Due to the unique surface and edge characteristics of the clay minerals, several viruses are found to exhibit a strong adsorption affinity towards such clays. The possible mechanism of the virus-clay interaction absorbed on the available literature was provided in sec. 2.11.

2.11 Virus-clay mineral interaction

Both montmorillonite and kaolinite mineral exhibit contact angle (β) hysteresis wherein the clay minerals are hydrophilic in nature in an aqueous environment having β=0° (wetting) and hydrophobic when β>65° (drying). The contact angle increases significantly during the water exclusion from the clay surface and it exhibits hydrophobic characteristics (Chrysikopoulos and Syngouna, 2012). Although the siloxane layer in the clay mineral is hydrophobic at β>65°, the surface is wetting for the formation of the diffused double layer in the presence of water. Such characteristics of the clay minerals govern their interaction with other hydrophilic and hydrophobic biological entities (Stotzky, 1985; Yu et al., 2013).

The interaction between the clay minerals and the virus surface is governed by various factors like the type of clay mineral, clay mineral characteristics under virus environment, the pH and IEP of the virus, and the hydrophobicity of the protein coat which encapsulates

the nucleic acid. Three different mechanisms are understood to be responsible for the clay-virus interaction to sorb the studied pathogens on the clay mineral surface.

Electrostatic interaction and cation bridging: when the pH of virus suspension is less than the IEP of the virus, the amino acids of the protein coat are positively charged. Under such conditions, the positively charged protein molecules are adsorbed on the negatively charged surface of montmorillonite by electrostatic interaction (Fig. 2.4a). However, when the protein of the virus is net negatively charged i.e., pH >IEP, the adsorption of the virus is stronger when divalent cations are present on the montmorillonite surface (Dashman and Stotzky, 1983). The presence of divalent cations on the clay surface can act as bridges between the negatively charged clay and the virus surface resulting in the binding of the two surfaces (Fig. 2.4 b) (Stotzky, 1985; Franchi et al., 1999; Beall et al., 2009). In contrast to montmorillonite, the negatively charged virus binds on the positively charged edges of the kaolinite. This is due to the presence of a relatively higher surface area on the edges of kaolinite (Park et al., 2015; Syngouna and Chrysikopoulos, 2010).

Hydrogen bonding: This interaction is dominant where the IEP of the clay mineral, kaolinite in particular, is lesser than the bulk solution pH. The clay mineral in the acidic environment results in proton transfer from the clay surface to the virus thus adding positive charge to the interacting protein coat (Fig. 2.4 c). Such an interaction by hydrogen bonding is followed by the electrostatic interaction between the newly acquired positive charge by the virus surface and the negatively charged alumina basal surface (Carlson et al., 1968; Schaub and Sagik, 1975; Chottapadhyay and Puls, 1999). Hydrogen bonding is also possible between the hydroxyl group at the broken edge of the clay mineral surface with the C, N functional group present in the amino group of virus protein coat. Further, under the pore-fluid environment, when the exchangeable cations in the clay surface are in the hydrated state, water bridging due to H-bonds between the anionic group of the protein and the hydrated cations results in interaction between the two surfaces (Stotzky, 1981).

Hydrophobic interaction: Different pathogens have a different extent of hydrophobicity in the non-polar amino acid chain of the outer protein coat. When the virus approaches the clay mineral surface due to hydrogen bonding and electrostatic interactions, the water molecules

near the clay surface might drain out, resulting in the increase of the contact angle (β>65°). Under such a condition the siloxane surface of the clay mineral exhibit hydrophobic characteristics and owing to which a strong interaction results between the hydrophobic groups of the virus and the clay mineral surface (Fig. 2.4 d). The nature and extent of the hydrophobicity determine the interaction of the virus with the clay mineral (Gerba et al., 1984; (Bales et al., 1991; Chattopadhyay and Puls, 1999; Yu et al., 2013; Armanious, 2020). Such interactions between the hydrophobic groups is understood to be the dominant mechanism of a negatively charged virus on the negatively charged montmorillonite surface in addition to hydrogen bonding.

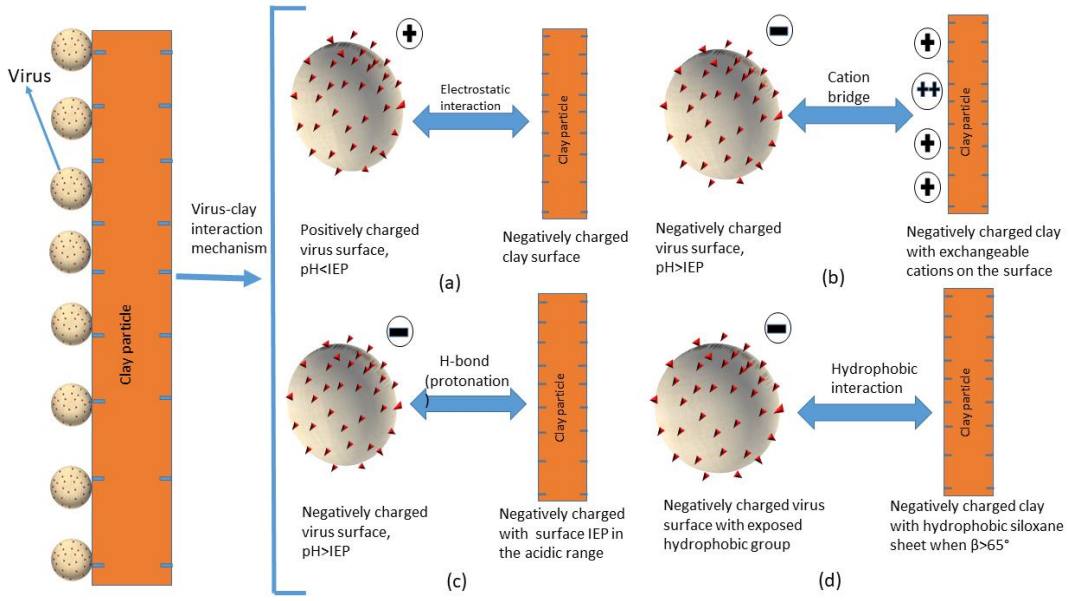

Figure 2.4: Virus-clay interaction mechanism (a) electrostatic interaction, (b) cation bridging, (c) hydrogen bonding, (d) hydrophobic interaction

From the above discussion, it was understood that the adsorption mechanism of virus onto clay is different for different viruses. However, the applicability of the clay minerals in the containment of various virus-contaminated BMW remains to be understood. In the clay-based barrier systems, the virus flow will be governed by the diffusion mechanism due to the low saturated hydraulic conductivity of the clay minerals. The estimation of the diffusion rate of various viral pathogens through clay-based barriers remains to be studied.

2.12 Motivation of the research work

Based on the aforementioned discussion, the gaps in the available research forming the motivation of the present work are listed as below:

- A Majority of the past studies reveal that the bentonite interacts strongly with the leachates and most importantly with the salt leachates, leading to degradation in its various properties with time like swell potential, liquid limit and saturated hydraulic conductivity. As the flow of leachate through the impermeable barrier systems is governed by the diffusion mechanism, therefore, changes in the plasticity and hydraulic conductivity is expected to influence the diffusion characteristics of the bentonites. Hence, an extensive diffusion study for both powder and granular bentonite in the presence of various salts is essential. Such a study was carried out in this work and discussed in Chapter 4.
- Moreover, the liners in the landfills are subjected to salt leachates of various concentrations and also as a combination of various salts. The study on the diffusion characteristics of bentonites under synthetic salt leachates of high ionic strength is not available elsewhere. Further, the study on the long-term diffusion behaviour of the bentonite-based barrier systems which are devoid of the sorption potential due to the continuous leachate flow in the landfill sites remains to be studied. Therefore, the influence of the various synthetic salt leachates on the diffusion behaviour of compacted powdered bentonite was extensively studied and discussed in Chapter 5. The long-term diffusion behaviour of compacted powdered bentonite was also studied for the first time and presented in Chapter 5.
- In recent times, the granulated bentonite in the GCLs have gained more popularity in comparison to the powder bentonite in restricting the generated leachate from the landfill facilities due to its unique sealing ability upon hydration. However, studies suggest a significant loss of osmotic potential of granular bentonite when it interacts with salt leachates, if not pre-hydrated with water. In the field conditions, the granular bentonites get exposed to salt leachates in the un-hydrated state and subjected to overburden stresses from the dumped waste. The sealing ability and swelling behaviour of the un-hydrated

granulated bentonite under such chemo-mechanical loading is not known. Therefore, the sealing ability and volume change behaviour of the compacted granulated bentonite in the presence of various pore-fluid under different overburden stresses was studied and the results were discussed in Chapter 6.

- An alternate liner material in order to address the problem associated with the degradation of the bentonite performance in terms of its hydraulic conductivity during its exposure to salt leachates is a need of the hour. As the kaolin performs in a completely contrasting manner in comparison to bentonite under the pore-fluid environment, the applicability of a kaolin layer as a protective layer to the bentonite could be explored for the first time. The sealing ability, volume change behaviour and diffusion characteristics of the compacted kaolin-granulated bentonite was, thus, studied and the results were discussed in Chapter 7.
- The increased rate of disposal of bio-medical waste (BMW) on the MSW landfills has the potential to pose a serious threat to the environment if the compacted clay-based materials do not perform satisfactorily. The performance assessment of the clay-based barriers in attenuating the viral pathogens, in the long run, is not available elsewhere. Therefore, a qualitative assessment of the montmorillonite/kaolinite based barrier systems in attenuating various human viral pathogens that has the potential to enter the landfills in the form of BMW, was performed for the first time and presented in Chapter 8.

Chapter 3

Materials and Methods

3.1 Materials

High-quality powder bentonite (PB) procured from the Barmer district of Rajasthan, India, was used in the present study. The granular bentonite (GB) used in the present study was exhumed from the commercial GCL (Maccaferri, India) manufactured for landfill applications. The GB mass per unit area was 3.96 Kg/m^2 having a thickness of ~5 mm. The PB and GB utilized for the present work were considered to be one of the most suitable liner materials for MSW landfills based on the index and surface properties that were presented in Table 1. The specific gravity of the GB was determined by the density bottle method as per IS-2720 (Part-III). The liquid limit and the plastic limit of the GB were determined as per the standard IS-2720 (Part-V) and the shrinkage limit was obtained by following the procedure as per IS-2720 (Part-VI). The total cation exchange capacity (CEC) was estimated based on the standard procedure as described by Chapman (1965) and the specific surface area (SSA) was determined using the ethylene glycol mono-ethyl ether (EGME) procedure on four duplicate samples (Cerato and Lutenegger, 2002). Further, a commercially available kaolin clay without any pre-treatment was also used in the present study to assess the applicability of the kaolin as a protective layer to GCL in the presence of high ionic strength inorganic salt solutions. A detailed characterization of the kaolin based on the recent study by Choudhury and Bharat (2018) was reproduced in Table 3.1.

Distilled water and chloride salt solutions comprising of lithium, sodium, potassium, and calcium were used as pore-fluids to understand the diffusion, swelling, and hydraulic behaviour of PB, GB, and the kaolin-GB layered system. The analytical grade chemicals corresponding to a purity of 99% were procured from Merck (Germany) or Spectrochem (India), and supplied by a local vendor. The pore-fluids were considered to represent the salt leachates in the municipal solid waste landfills in the form of salt-laden solid waste from the rubber industry, as coal combustion products from coal-fired industries, and as inorganic waste from various construction and electroplating industries (Ozgunar et al., 2007;

Boopathy et al., 2013; Yeheyis et al., 2013; Turkyilmaz et al., 2019; Tian et al., 2019; Wang et al., 2019). Further, the laboratory experiments were performed for individual salt concentration ranging from 0.01-1 M, by dissolving the salt of the required mass in distilled water at solubility temperature. The molecular weight, hydrated size, and valence of the individual salt cation was presented in table 3.2

Table 3.1: Index and surface properties of studied soils

Property	Granular Bentonite (GB)	Powder Bentonite (PB)	Commercial Kaolin (Choudhury and Bharat, 2018)
Specific Gravity	2.75	2.77	2.62
Liquid Limit	458	393	40
Plastic Limit	56	50	32
Shrinkage Limit	15	18	28
Total CEC (meq/100g)	97.9	71.7	5
Specific surface area (m^2/g)	505*	495*	12**

* By EGME technique

** By BET technique

Table 3.2: Properties of the salts solutions used

Salts	Molecular weight (g/mol)*	Hydrated radius (Å)*	Valence
Lithium chloride	42.394	7.3-10.3	1
Sodium chloride	58.44	5.6-7.9	1
Potassium chloride	74.55	3.8-5.32	1
Calcium Chloride	110.98	9.6	2

*Sridharan and Prakash (1999)

3.2 Laboratory methods

3.2.1 Equilibrium sediment volume test

The equilibrium sediment volume (ESV) test is a commonly adapted test to assess the swelling behaviour of soils and evaluating its subsequent engineering applications. Equilibrium sediment volume tests were conducted using 100 ml graduated measuring glass jars. A 2 g of oven-dried (at 105^0 C) clay soil was thoroughly mixed with a predetermined salt solution using a mechanical stirrer. The mixing was continued for about 20 min. The suspension, after thorough mixing, was transferred into the measuring jars and an additional solution was added to fill up to the 100 ml mark. The suspension was allowed to settle until the equilibrium was reached. The equilibrium time with different electrolyte solutions was observed to be less than 24 hrs. The tests were conducted at room temperature which varied from 28^0 to 32^0C, during the testing time. The final sediment volume was visually recorded to an accuracy of 0.5 ml. Three independent tests were conducted in each case for the reproducibility with an accuracy of ±0.5 ml. Finally, the equilibrium sediment volume was expressed as the ratio of final sediment volume to the initial dry mass of the clay (Sridharan and Prakash, 2004). The final sediment volume was taken as an average value from three independent tests. The schematic of the equilibrium sediment volume test was shown in Fig. 3.1.

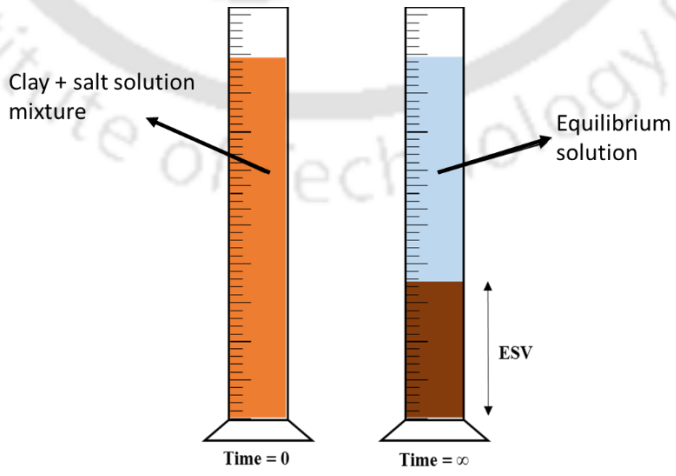

Figure 3.1: Schematic of Equilibrium sediment volume test

3.2.2 Permeation test under chemo-mechanical loading

The experimental setup for evaluating the volume change and sealing behaviour of the compacted GB under pore-fluid permeation was shown in Fig. 3.2. A 54 mm diameter, permeation cell was fabricated from a solid perspex tube to accommodate 10 mm thick GB with two movable porous stones on either end. The placement density of the GB within the GCL utilized for the present study was found to be ~1.17 Mg/m^3, which falls in the estimated range of placement density in many GCLs (ρ_d*=1.0-1.3 Mg/m*^{3}), (Lake and Rowe, 1999; Alonso et al., 2011; Seiphoori et al., 2016). The GB was, therefore, compacted in the cell at a dry density of 1.1 Mg/m^3. Filter papers were placed between the porous stone and GB on either end, to prevent any clogging of the porous stones during the permeation. After compaction and placement of the porous stones at the two ends of the GB, the cell was carefully positioned on the loading assembly. The cell was then connected to a graduated burette with a valve on one end, which facilitates the permeation of pore-fluid through the compacted GB. Before the commencement of the test, the burette was filled with the desired pore-fluid of a particular concentration with the valve closed. A strain-gauge having a precision of 0.001 mm was fixed firmly on the top of the sample to record the vertical displacement of the compacted soil sample as shown in Fig. 3.2. The test was initiated by maintaining the desired mechanical stress on the sample and, consequently, the permeation of the fluid was allowed from the bottom of the cell by opening the valve of the burette. All the tests were performed at two mechanical stresses, viz., 50 kPa and 100 kPa, to understand the swelling/collapse and sealing potential of the GB under different ionic strength fluids that are expected in the field. The fluid permeation rate was estimated by the falling head technique (ASTM D5856 2015), whilst the compacted soil was permeated with the desired pore-fluid under the applied stresses. The fluid permeation rate is similar to the hydraulic conductivity of the soil in saturated conditions. The test was continued until the fluid permeation rate was constant over a period of 24 hours. The vertical displacement reading (expressed as normalized thickness, h/h_0) from the strain-gauge and the fluid permeation rate (expressed in *m/s*) provided the swelling potential and sealing potential of the soil, respectively.

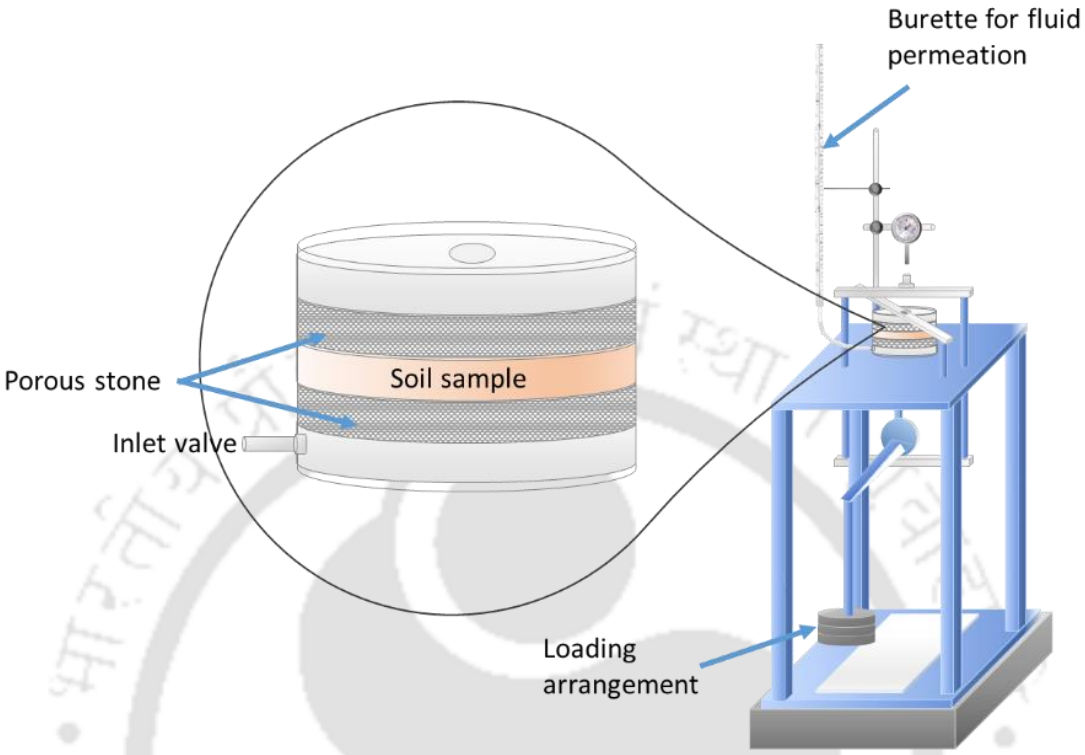

Figure 3.2: Experimental set-up for evaluating the sealing ability of the GB under chemo-mechanical loading

The compacted GB was assumed to have achieved complete sealing by closing all the inter-granular and inter-aggregate voids when an equilibrium permeation rate of $1x10^{-9}$ m/s was achieved. Thus, the sealing time for the GB under the influence of different pore-fluids was established based on the permeation rate of the fluid for its use a liner material. The volume change behaviour and sealing potential of the kaolin-GB layered system (described in Chapter 7) was also established by following the same procedure as adapted for the GB layer alone. The only difference being a kaolin layer of 5 mm thickness was compacted at the dry density of 1.6 Mg/m^3 and placed below the compacted 5 mm thick GB layer in such a way that the pore-fluid was made to permeate through the compacted kaolin layer first as the permeation of different salt solutions was allowed from the bottom of the cell. As the sealing ability of the GB is not influenced by its thickness, the thickness of the GB layer in the kaolin-GB layered system was reduced to 5 mm. An overall 10 mm thick kaolin-GB layer was maintained in the permeation cell.

3.2.3 Through-diffusion test

To understand the diffusion characteristics of the compacted PB and GB under salt environment, through-diffusion testing was used, in this study, as this technique is non-destructive and the concentration profile along the soil depth is not required. The testing is faster, further, the sample dimension does not influence the accuracy of model parameter estimation. A 10 mm thick and 24 mm diameter diffusion cell was, therefore, used in this study. The diffusion cell was fabricated from solid plexiglass tubes to accommodate the clay plug and 5 mm thick porous stones as illustrated in Fig. 3.3a. A detailed drawing of the diffusion cell was provided in Fig. 3.3b. The bentonite samples (PB/GB) in the dry state were statically compacted in diffusion cells at the desired densities, and the porous discs were placed on either side of the bentonite plug. The cell was then attached to the reservoirs on either side by capping on the outer thread of the cell. A rubber gasket was used around the outer threading to prevent leakage. The reservoirs were then filled with distilled water for saturation from both the sides.

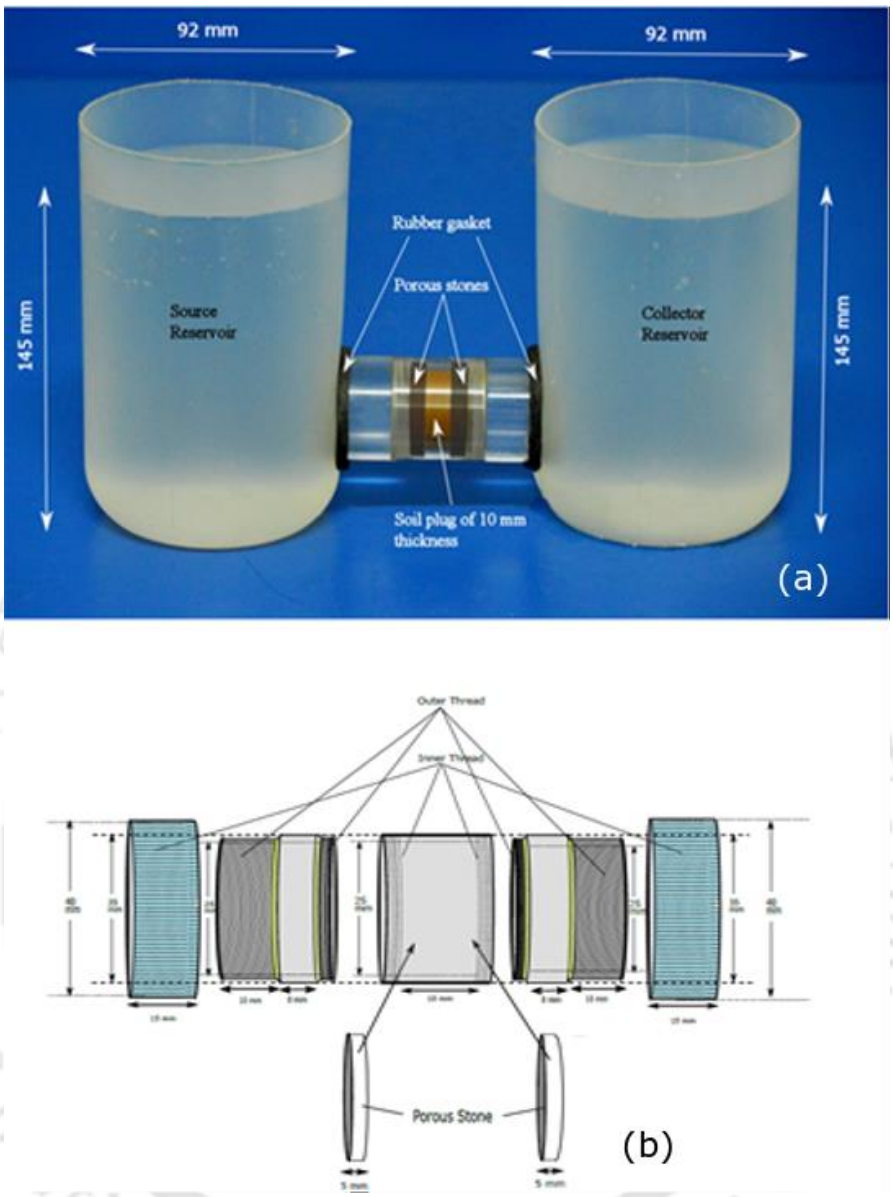

Figure 3.3: (a) Fabricated through-diffusion testing set-up, (b) details of the diffusion cell

The saturation took nearly 30 days which was assessed by weighing the diffusion cell at regular intervals. The diffusion experiment was commenced soon after the saturation of the bentonite by replacing the source reservoir with known salt concentration. The water in the collector reservoir was also replaced with distilled water to avoid the influence of any excess salt deposition from the clay plug on diffusion. The electrolytes in the reservoirs were regularly stirred to maintain the uniform concentration through the reservoir at any given time. A ~5 *ml* samples were collected from the reservoirs at frequent intervals of time for

determining the concentration. The concentration of a given cation was measured using a flame photometer (®Systronics India, Type – 128) after required dilution by following the test method (Munns et al., 2010). The measured concentration with time in both source and collector reservoirs were used for the diffusion analysis. The concentration of both the reservoirs showed a nearly constant reading after 60 days for most of the considered salt concentrations. Therefore, the mass transport parameter of the studied soils in the presence of different salts was estimated from the measured data of 60 days. The through-diffusion tests for the compacted PB under the pore-fluid environment were conducted at two different dry-densities (ρ_d) of 1.1 Mg/m^3 and 1.3 Mg/m^3. For the comparison of diffusion characteristics through the PB and GB, the diffusion test through the GB was also conducted at ρ_d = 1.3 Mg/m^3.

The thickness of the sample was maintained at 10 mm for salt diffusion through the individual PB/GB layer. However, for the kaolin-GB layered system, a 5 mm thick kaolin sample compacted at the dry density of 1.6 Mg/m^3 was placed along with the compacted GB layer of 5 mm thickness. The layered system was so positioned that the flow of solute was allowed through the kaolin layer first.

3.2.4 Long-term through-diffusion test

The long-term diffusion test was conducted to understand the behavior of the compacted bentonite devoid of the sorption potential after the complete cessation of the exchange process. The long-term diffusion test was a two-stage process where the first step comprised of permeating the compacted bentonite with the desired salt solution post hydration with the distilled water. In the second stage, the through-diffusion test was performed on the same compacted soil sample post permeation (Fig. 3.4 a-b).

The soil was first compacted at the dry density of 1.3 Mg/m^3 in the diffusion cell having a diameter of 24 mm diameter thickness of 10 mm and then fixed on either end by caps. One end of the cap was connected to a water burette from a height of 8.75 meters to saturate the soil sample. After saturation was ensured, water in the burette was replaced by the pore-fluids. A series of such tests were conducted with inorganic salt solutions consisting of LiCl, NaCl, and KCl of viz., 0.01, 0.1, 0.5, and 1 M concentrations. After the complete permeation

of a particular fluid was ascertained, the tests were terminated, and the cell was dismantled. The compacted bentonite plug saturated with a particular pore-fluid was then introduced to the through-diffusion set-up carefully with minimal disturbance. The source reservoir contained the same pore-fluid having a similar concentration with which the bentonite was permeated in the first stage. The through-diffusion process was the same as explained in section 3.2.3.

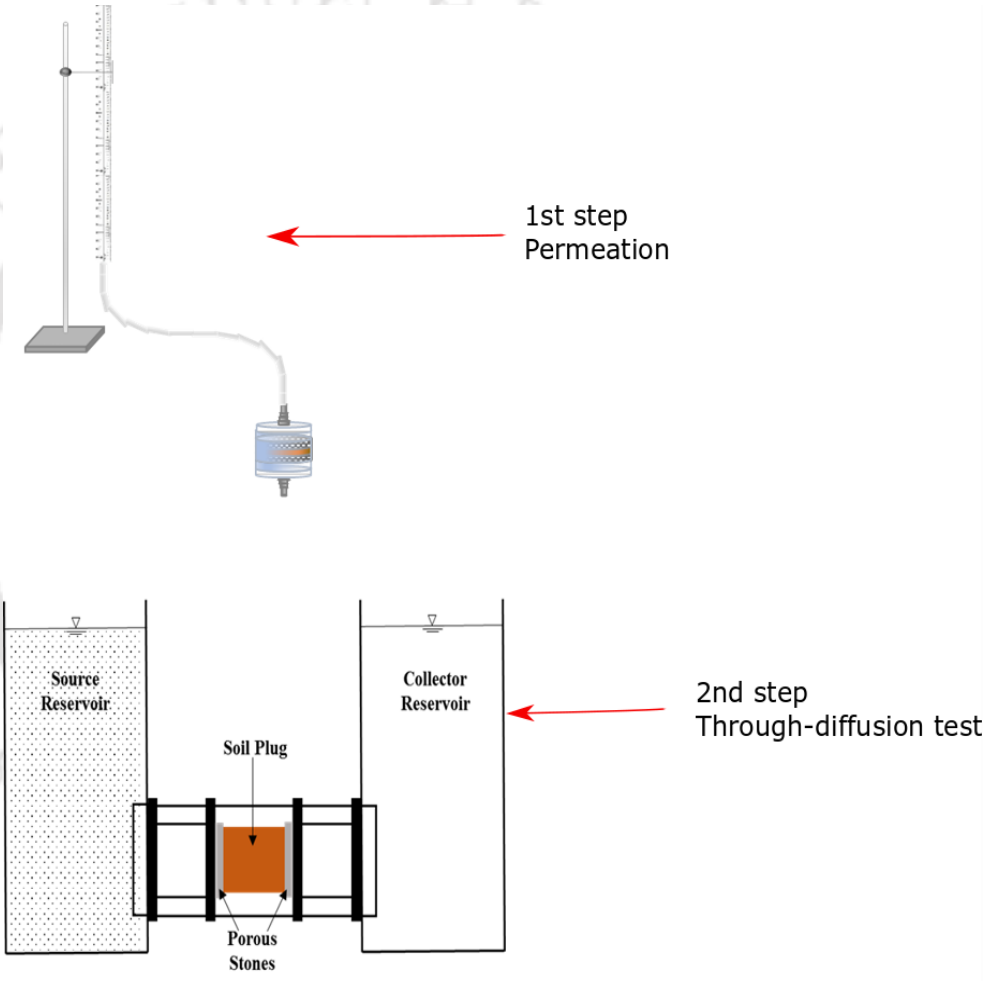

Figure 3.4: Long-term through diffusion (a) 1st step of permeation through the permeameter, (b) 2nd step through-diffusion test same as Fig. 3.3a

3.2.5 Elemental compositional and Micro-structural analyses

For quantification of the amount of salt-ions adsorbed on the surface of PB after the long-term diffusion test, elemental compositional analysis by two different methods was adapted.

In both methods, the PB clay plug after the termination of the diffusion experiment for the studied salt mixtures was analyzed. The first method was similar to the CEC estimation. It comprised of taking a known amount of clay from the diffusion test after termination and mixing it with a known volume of 1 M ammonium acetate solution in a beaker. The soil-solution was thoroughly mixed for a sufficient time allowing all the surface cations to be replaced by the ammonium ions. The clay mixture was then centrifuged to obtain a clear supernatant at the top. The supernatant was filtered and then analyzed for different inorganic salt cations using a flame photometer.

The second method comprised of estimating the elemental compositions (including the surface cations) on the surface of the PB clay plug due to diffusion of the salt mixture by Energy-Dispersive X-ray (EDX) spectroscopy. The representative specimens for the EDX analysis were obtained using the freeze-drying technique in Lyophilizer (FreezeDry System, LabconcoFreeZone®) at −60 °c. The EDX enabled identifying the elemental composition in a selected spectrum of the lyophilized sample.

To understand the adsorption affinity of the soils for the salt cations, the elemental compositional analysis was also performed on the GB and kaolin samples of the kaolin-GB layered system by EDX post permeation with various salt solutions. Further, the microstructural analysis was performed using Field Emission Scanning Electron Microscope (FESEM) to understand the sealing behaviour of the GB upon permeation different pore-fluids. The representative specimens for the FESEM analysis were obtained using freeze-drying technique in Lyophilizer.

3.2.6 Pore-fraction analysis

The pore-fraction analysis of the PB at the end of the long-term diffusion test was performed using Gamma-ray attenuation (GRA). GRA is one of the most common methods to obtain the void fraction in a two-phase system (Thiyagarajan et al., 1990; Pires and Pereira, 2013; Sarifzadeh et al., 2017). In the present study, GRA was utilized to obtain the void fraction in the PB based on its attenuation capacity. The narrow mono-energetic gamma-ray (Cs^{137}) was passed through the compacted PB placed inside the diffusion cell (Fig. 3.5a). The pathlength of the gamma-ray was established such that it matches the thickness and diameter of the PB

sample in the D1 and D2 direction, respectively (Fig. 3.5b). The sodium iodide (NaI) scintillation was used as the detector unit. Lead collimators were used in the setup to ensure the narrow beam was passed in a straight-line path through the soil sample to reach the detector unit. The intensity counts based on the attenuation ability of the PB was detected by the NaI scintillation. The attenuated intensity of the beam is given by the Lambert-Beer exponential law (Petrick and Swanson, 1958)

$$I = I_0 e^{-\mu_{eff}\Delta x} \tag{3.1}$$

where I is the measured intensity in count per sec (cps) after the beam is passed through a sample and I_0 is the initial intensity in cps and Δx is the pathlength in cm. μ_{eff} is the effective attenuation coefficient (cm^{-1}) and is unique for the material. For a two-phase system, μ_{eff} is the sum of the linear attenuation coefficient of the individual phases. The void-fraction can be estimated based on the μ_{eff} value,

In order to estimate the void fraction of the PB samples in the presence of various salts, the attenuation capacity of the compacted soil (μ_s) was first evaluated by knowing the energy counts after passing the gamma-ray through the empty diffusion cell and then through the compacted PB within the cell (Fig. 3.5c). The μ_s of the soil is given by:

$$\mu_s = \frac{\mu_{eff}}{\varepsilon_s} \tag{3.2}$$

where μ_{eff} is obtained based on Eq. 3.1 and the ε_s (solid fraction) in the soil mass were obtained knowing the initial density of the PB (ρ_d=1.3 Mg/m^3).

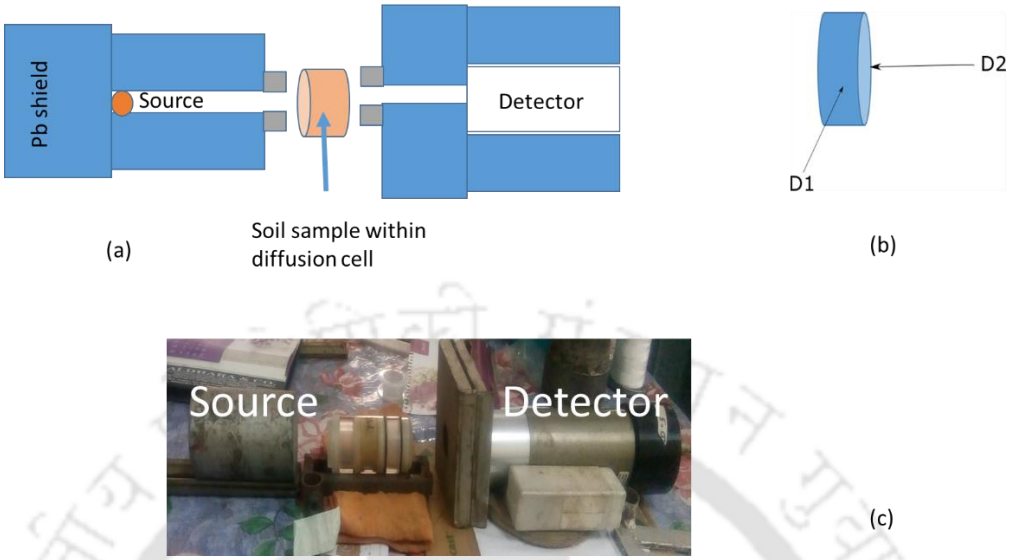

Figure 3.5: (a) Illustration of the set-up for GRA (b) Projection of gamma rays along the D1 and D2 direction through the soil sample, (c) laboratory set-up of densitometry

The μ_s for the PB which is a material constant was then utilized to measure the void fraction of the water-saturated soil. The energy counts were measured by passing the gamma-ray through the water-saturated PB and the corresponding μ_{eff} was calculated (Eq. 3.1). The void fraction for the PB is given by the equation:

$$\mu_{eff} = \mu_s \varepsilon_{ssat} + \mu_w \varepsilon_w \tag{3.3}$$

where μ_w is the attenuation coefficient of water which was estimated following the similar procedure adopted for obtaining the μ_s, ε_{ssat} is the volume fraction of soil solids in the saturated condition. The void-fraction of the initially saturated soil (before the commencement of the diffusion test) was evaluated knowing ε_{ssat}. The void fractions for all the samples after the completion of the diffusion test were then evaluated by following the above procedure in the D1 and D2 directions.

Chapter 4

Diffusion characteristics of compacted powder and granulated bentonite under inorganic salt environment

4.1 General

Salt diffusion studies through compacted bentonites are important for designing the waste disposal facilities and assessment of the existing facilities. As the behavior of plastic clays is governed by physical chemistry, the effect of physicochemical parameters on diffusion rates of the bentonites is required to be studied. In this chapter, the result of the transient through diffusion tests with different salts that contain different monovalent cations and divalent cations were presented. The influence of concentration, hydrated size, and valence of the salt cations on the contaminant migration through PB was studied experimentally. Further, the diffusion characteristic of PB and GB were compared for the same control parameters under similar compaction density (ρ_d=1.3 Mg/m^3). The development of an inverse analysis suite was described in section 4.2. The Java-based inverse analysis suite was utilized for estimating the mass transport parameters from the observations made from the through-diffusion experiments.

The effect of concentration, hydrated size, and valence of the cations on the mass transport parameters of the compacted PB and GB was analyzed and discussed based on the physico-chemical response of bentonite under pore-fluid environment.

4.2 Development of CONTRADIS

The name CONTRADIS stands for "**CON**taminant **TRA**nsport due to **DI**ffusion in **S**oils". POLLUTE is the only one software package available until now that is widely used by Geo-environmental engineers for contaminant migration analysis. It is being used in the industry for more than fifteen years now. But the drawbacks of this commercially available software include non-availability of the option for performing inverse analysis and higher cost involved. The present software CONTRADIS, is built for overcoming the limitations of

POLLUTE. The software suite is based on Java and can run in various operating systems, viz., Linux, Windows 8, and later. The software can perform both forward and inverse analysis for the through-diffusion problem.

4.2.1 Forward and inverse analyses

The forward analysis of the diffusion problems involves estimating the temporal variation of the concentration in the source and collector reservoir for a known value of the model parameters and vice versa in the inverse analysis problem. However, in order to achieve this, the convergence of the closed-form analytical solutions (Eq. 2.10-2.11) by finding the first positive non-zero roots of the transcendental equation (Eq. 2.12) is required. The eigen solutions (roots) for the transcendental equation were obtained by using a discontinuous, multimodal optimization algorithm using the glow-worm swarm optimization technique (Bharat, 2013). The closed-form solutions in Eqs. (2.10)–(2.11) were then evaluated using the first 20 numbers of roots using the optimization technique (ref).

The inverse problem of determining the diffusion coefficient and linear retardation factor was solved by minimizing the error between theoretical and measured concentration data in the source and collector reservoirs at different time intervals. The minimization was accomplished by particle swarm optimization technique (Bharat et al, 2008; 2012; 2013). Code for the aforementioned forward and inverse analyses were written (Bharat, 2013) and implemented in the main program to develop the non-commercial software suite which was named CONTRADIS. The software was verified on the synthetic data obtained from calculated concentration values as input data taken from the available literature (Fig. 4.1 a-b). The source and collector reservoir data (Fig. 4.1a) for the diffusion of acetone and aniline (Barone et al., 1992) and HTO (Garcia-Giteirrez et al., 2004) through the compacted bentonite soil was utilized to estimate the model parameters (D_e, R_d) by inverse analysis through CONTRADIS. The theoretical plot generated by the developed software fits well with the literature experimental data. Moreover, the theoretical plot generated by the POLLUTE was in good agreement with the CONTRADIS. The estimated model parameters by CONTRADIS was presented in Fig. 4.1b. As the estimated model parameters was in good agreement with the literature data, the CONTRADIS was utilized to estimate the model parameters from the measured data of the present study.

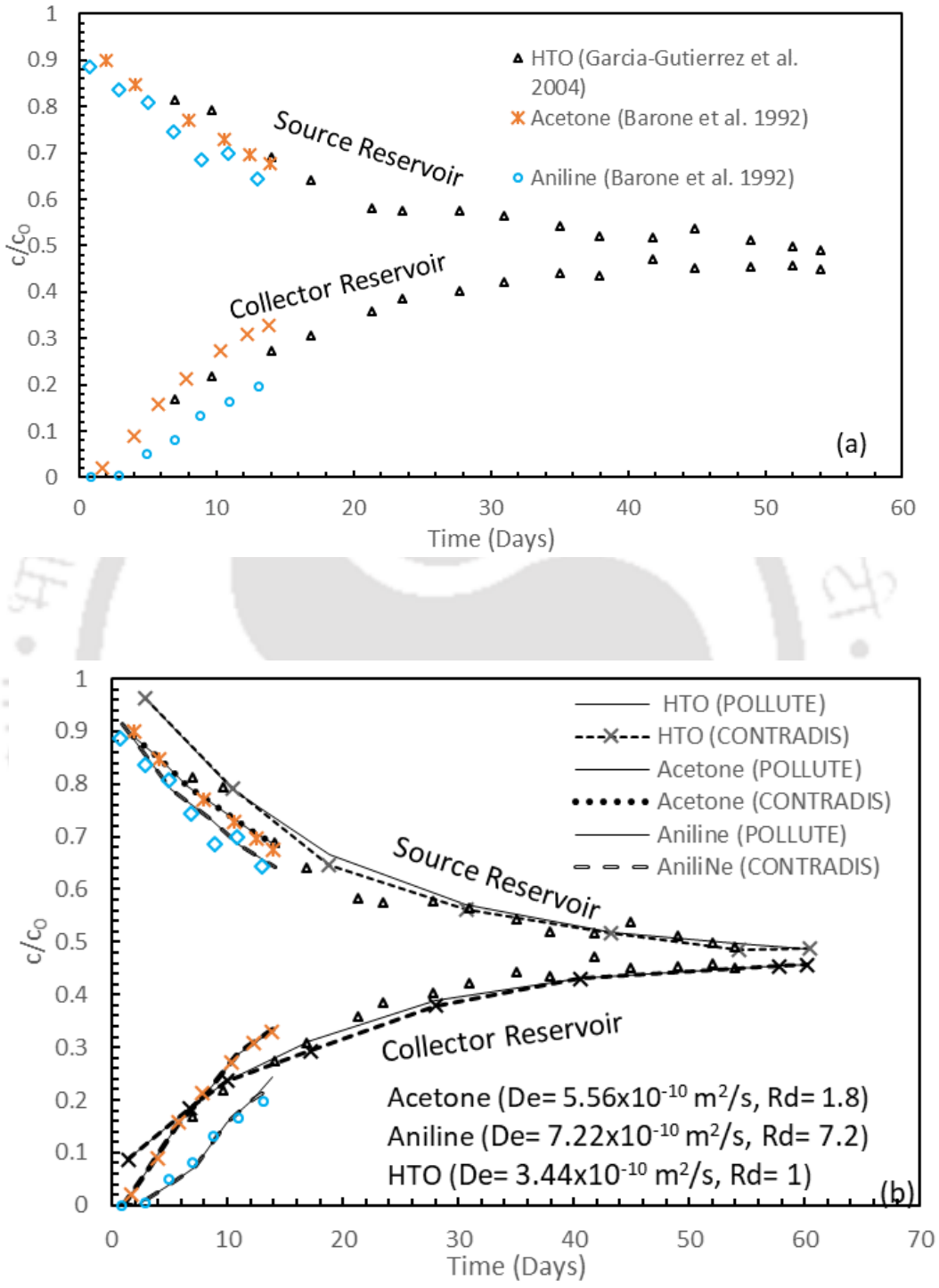

Figure 4.1: (a) Experimental concentration data (synthetic data) for the diffusion of acetone, aniline, and HTO through compacted bentonite, (b) estimation of the model parameters from the experimental data by POLLUTE and CONTRADIS

4.3 Results and Discussion

4.3.1 Effect of cation concentration

The measured concentration data with time from the through-diffusion experiments in the source and collector reservoirs for various pore-fluids through PB at the same compaction density (ρ_d=1.3 Mg/m^3) was shown in Fig. 4.2a- 4.2c. The measured data were presented as relative concentrations, c/c_0, by normalizing the measured concentration, c, with initial concentration, c_0. The salt-cation concentration in the source reservoir decreased with time and the concentration increased with time in the collector reservoir, for all the studied pore-fluids.

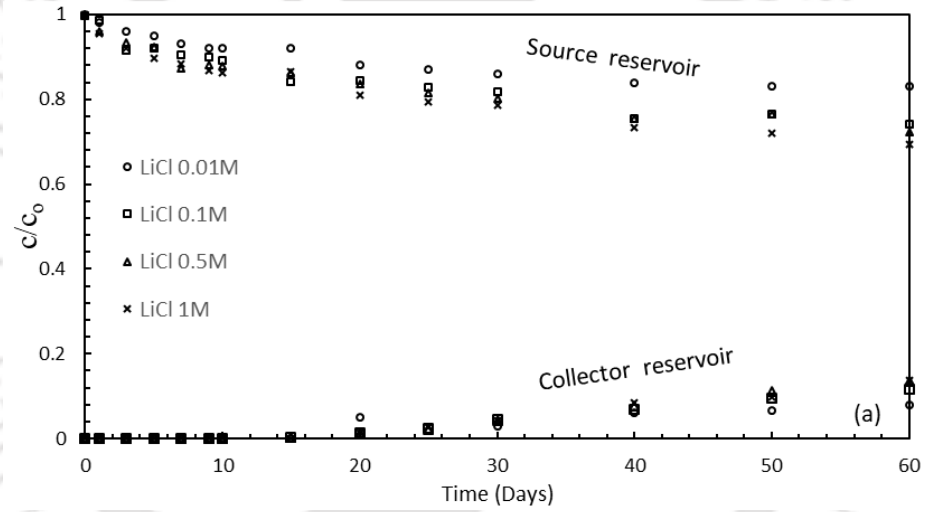

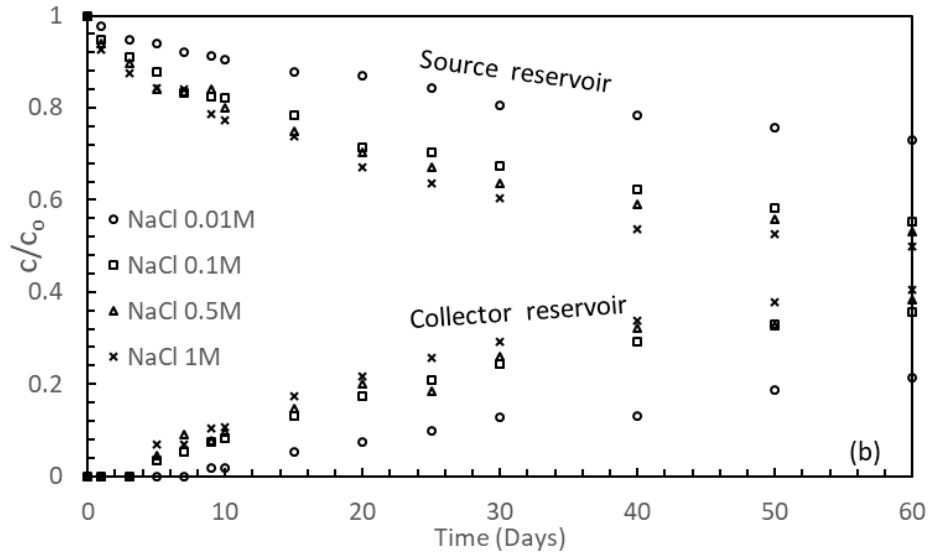

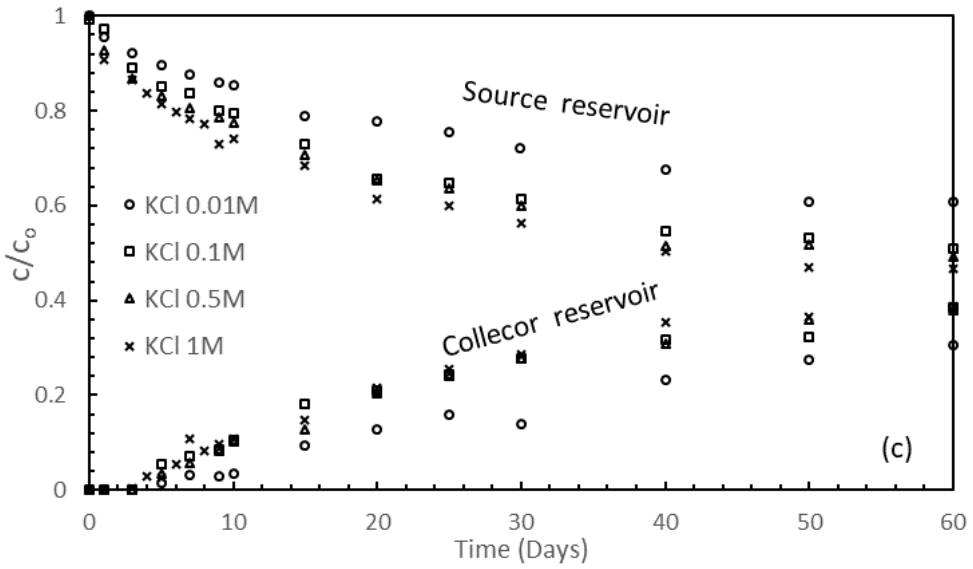

Figure 4.2: Temporal data of measured salt concentration in source and collector reservoirs for (a) LiCl, (b) NaCl and (c) KCl

The reservoir concentration data indicated that the diffusion rate of lithium ions through the compacted PB increased slightly with the increase in the salt concentration. When a concentration gradient of 0.01M LiCl was maintained, the relative concentration (c/c_0) of lithium ion in th source reservoir after 60 days was 0.84, which reduced to only 0.78 at 1M LiCl. The lithium ion was absent in the collector reservoir for the first 15 days for all the studied concentrations indicating strong adsorption of lithium ion by the mineral surface of the PB (Fig. 4.2a). On the other hand, a significant increase in the diffusion rate through the PB was observed with the increase in the concentration of NaCl and more prominently for KCl. After two months of the diffusion test, the c/c_0 of the sodium ion in the source reservoir was ~0.8 when a concentration gradient of 0.01M NaCl was maintained, while the c/c_0 at 1M NaCl during the same time interval was 0.57. Similarly, the test performed at 0.01M KCl concentration showed that the c/c_0 of the potassium ion after 60 days in the source reservoir was ~0.65 while in the presence of 1M KCl the c/c_0 was ~0.51 (Fig. 4.2 b-c). The collector reservoir data indicated that a small amount of sodium and potassium ions were present just after 5 days of the commencement of the diffusion test in the presence of higher initial concentrations for both NaCl and KCl (n> 0.5M).

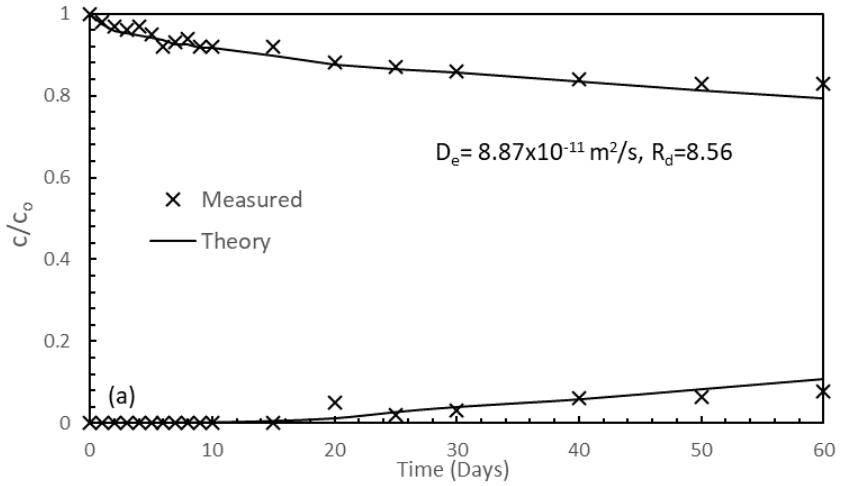

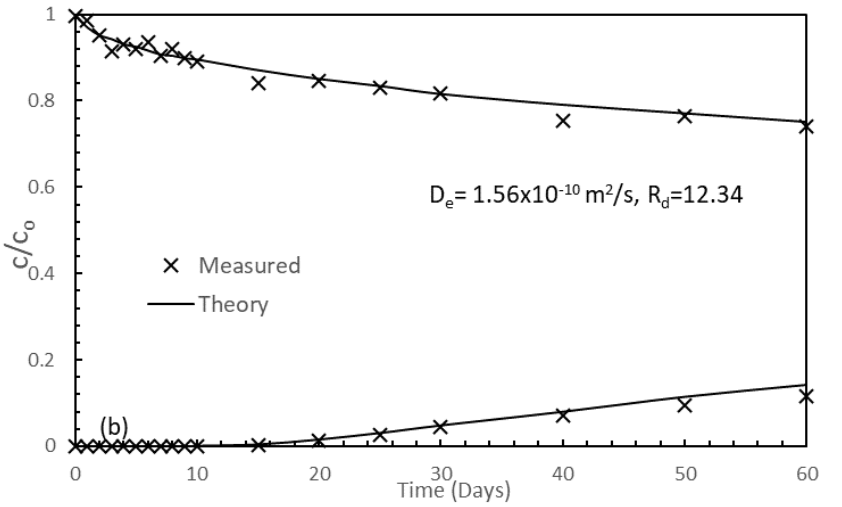

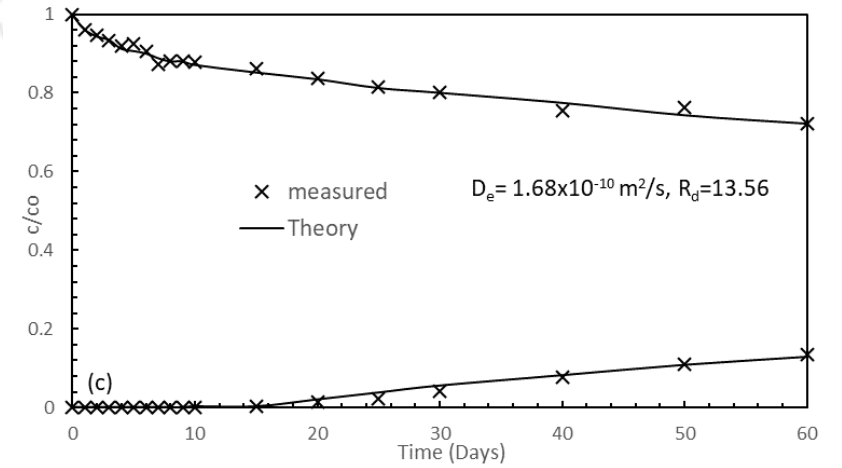

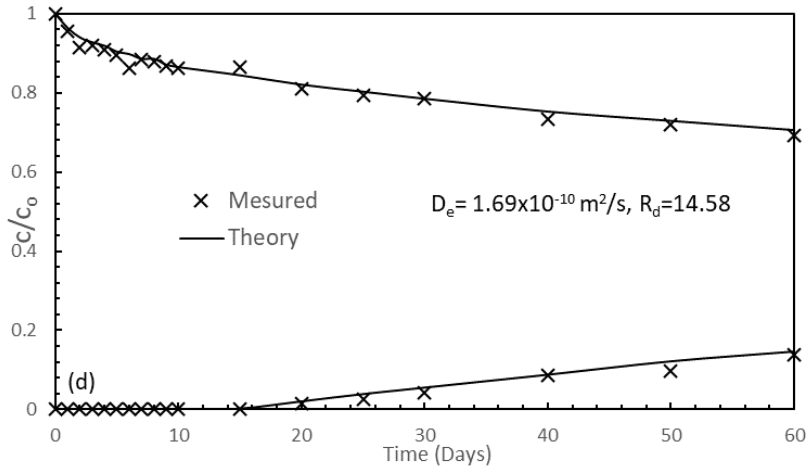

Figure 4.3: Comparison of the experimental concentration profile with the theoretical plots for (a) 0.01M LiCl, (b) 0.1M LICl, (c) 0.5M LiCl and (d) 1M LiCl

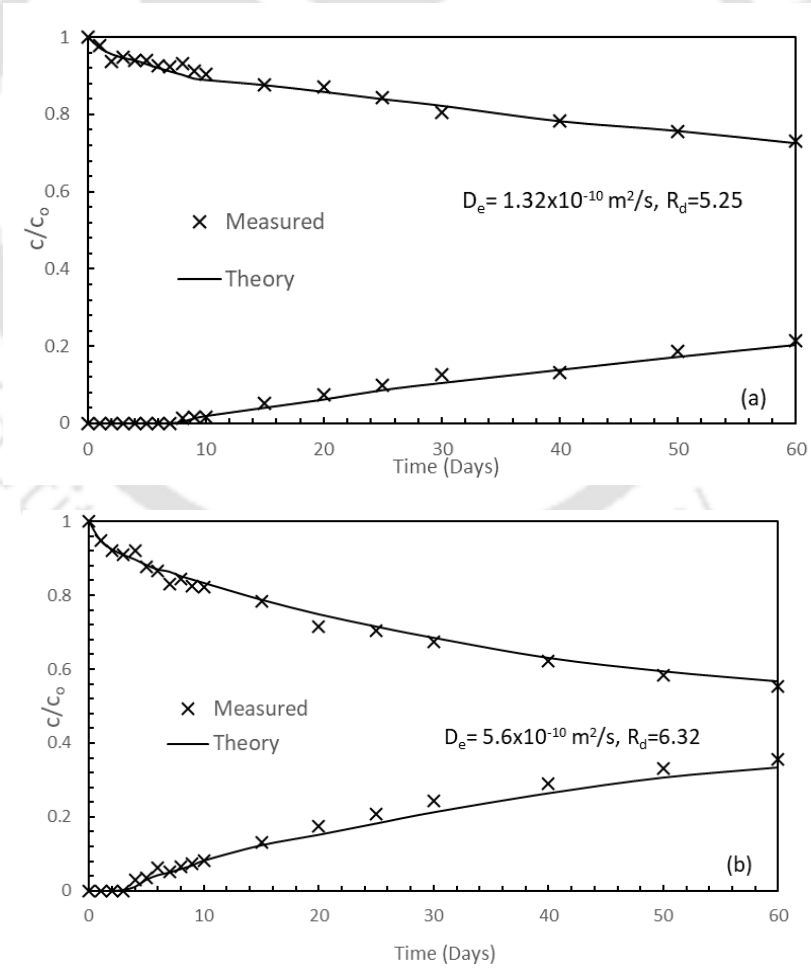

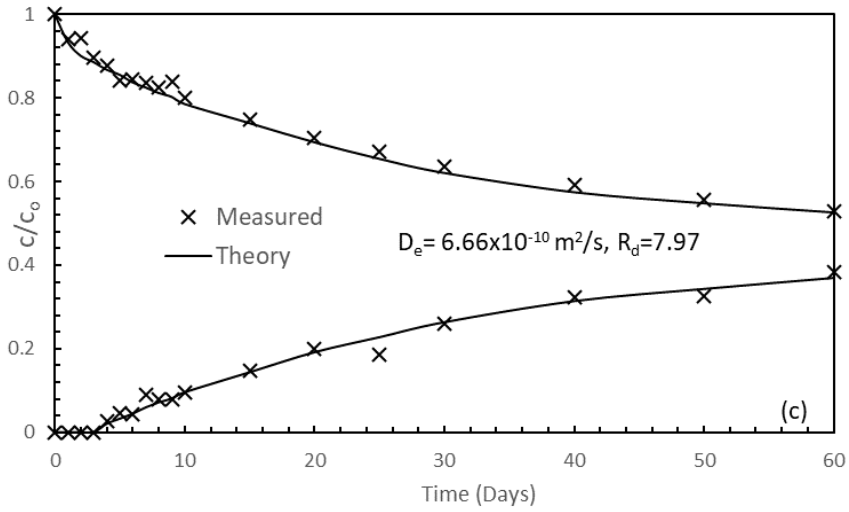

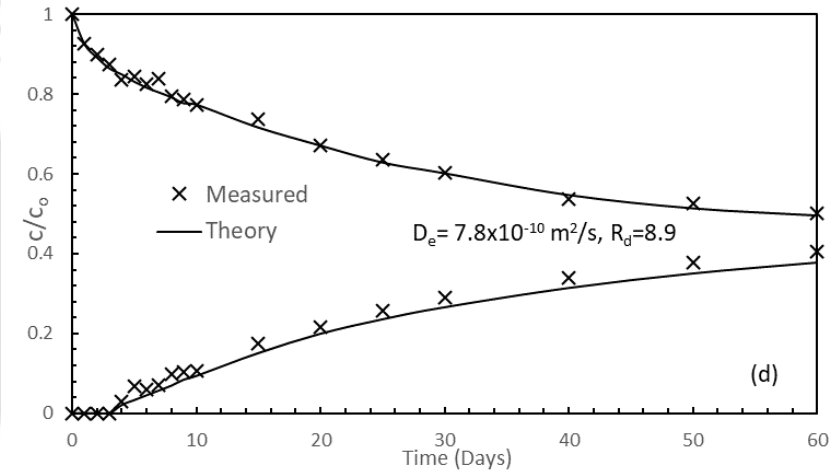

Figure 4.4: Comparison of the experimental concentration profile with the theoretical plots for (a) 0.01M NaCl, (b)0.1M NaCl, (c) 0.5M NaCl and (d) 1M NaCl

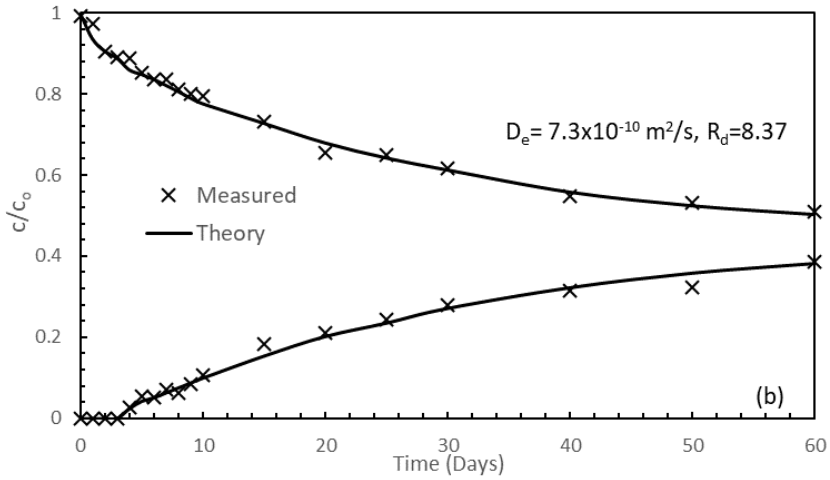

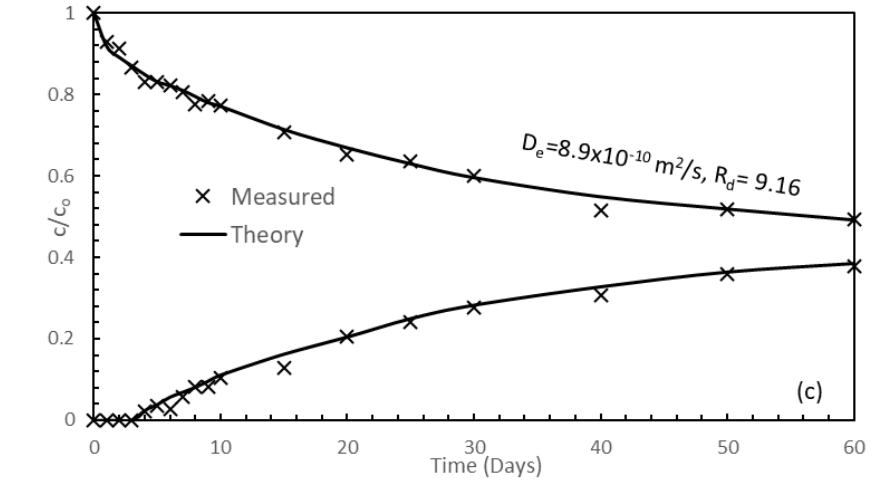

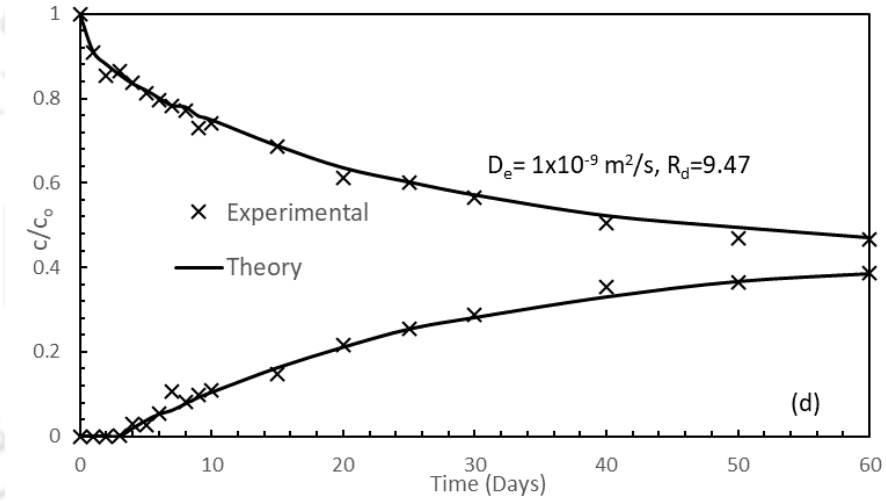

Figure 4.5: Comparison of the experimental concentration profile with the theoretical plots for (a) 0.01M KCl, (b) 0.1M KCl, (c) 0.5M KCl and (d) 1M KCl

The measured experimental data were used to determine the diffusion and linear sorption parameters by the inverse analysis using CONTRADIS. The model parameters (D_e, R_d) obtained by minimizing the error between measured data and theoretical concentration plots for different salts were presented in Table 4.1. The theoretical concentration plot using the optimized design parameters (Table 4.1) for different salts were given in Figs. 4.3-4.5. The theoretical concentration plots obtained using the optimized model parameters were in good agreement with the measured concentration data for all the studied cases were presented. The effective diffusion coefficient (D_e) of the lithium ion in the compacted PB was 8.87x10^{-11} m^2/s when a concentration gradient of 0.01M LiCl was maintained. However, the D_e

increased to $1.56x10^{-10}$ m^2/s and $1.68x10^{-10}$ m^2/s when the concentration gradients of 0.1M and 0.5M were maintained, respectively. Moreover, the D_e of the lithium ions in the PB was $1.69x10^{-10}$ m^2/s when a concentration gradient of 1M LiCl was maintained, indicating that for n>0.1M the D_e for lithium ions was nearly constant (Fig 4.3 a-d). However, the retardation factor (R_d) increased with the increase in the concentration of the LiCl solution.

The increase in the D_e with the increase in the concentration of the salt solution was more pronounced in the presence of NaCl and KCl salts. The D_e of the sodium ion through the PB at 0.01M NaCl concentration was $1.32x10^{-10}$ m^2/s, which increased to $5.6x10^{-10}$ and $6.6x10^{-10}$ m^2/s at 0.1M and 0.5M NaCl concentration, respectively. The maximum D_e for the sodium ion (D_e =$7.68x10^{-10}$ m^2/s) was observed in the presence of 1M NaCl (Fig. 4.4 a-d). Similarly, with the increase in the concentration of KCl solution the D_e increased considerably (Fig. 4.5 a-d). The D_e of the potassium ion at 0.01M KCl was $3.56x10^{-10}$ m^2/s, which increased nearly by an order of magnitude (D_e=$1.01x10^{-9}$ m^2/s) at 1M KCl. Moreover, similar to the trend observed in the presence of LiCl solution, the retardation factor (R_d) increased with the increase in the concentration of the NaCl and KCl solutions. The reported D_e was found to have a standard deviation of 3.1%, and the R_d showed a standard deviation of 3.7%.

The increase in the migration rate of a particular ion through the PB with the increase in the initial concentration of the source solutions was due to the suppression of the DDL thickness at higher concentrations (n>0.5M). As the concentration of ions in the bulk solution exposed to the mineral surface of PB increases, replacement of the surface cations by the cations present in the bulk solution occurs, which contributes to the suppression of the DDL thickness. Such changes in the adsorbed complex of the studied PB contributes to the alteration of the inter-particle forces. With the decrease in the DDL thickness, the inter-particle repulsive force reduces and the particles tend to flocculate and thereby reducing the effective flow path for the diffusing ions. Hence, the D_e was maximum for all the studied salt cations at higher ionic strength solutions due to the reduced flow path. Further, the increase in the concentration of the bulk solution results in significant cation complexion allowing more surface cations to be exchanged with the cations in the bulk solutions. This increase in the cation exchange at higher concentrations results in the increased R_d for all the studied salts.

4.3.2 Effect of cation size and valence

The diffusion rates of various salt cations having similar initial ionic strength (*n=0.2M*) was shown in Fig. 4.6 to understand the effect of cation size and valence. The hydrated size and valence of the salt cations were presented in Table 3.2. The diffusion rate of Li^+ ions through the compacted PB was observed to be very slow compared to the other cations. The relative concentration of lithium ions in the source reservoir was ~0.8 after two months of diffusion period whereas the relative concentration of potassium and Calcium ions reached ~0.55 by this time, indicating the completion of the test. The sodium concentration in the source was ~0.6 at the end of 60 days, which was between the diffusion rates of lithium and potassium ions. The diffusion rate of potassium was faster than calcium in the beginning, but with time the rate was similar for both the salts. The difference in the relative concentration and diffusion rates at any given time indicates the cation complexion on the mineral surface. The lithium ion was absent in the collector reservoir for initial 10 days indicating strong adsorption on the mineral surface due to cation exchange and slower diffusion rates through the clay plug. The relative concentration of other cations appeared in the collector nearly after 5 days.

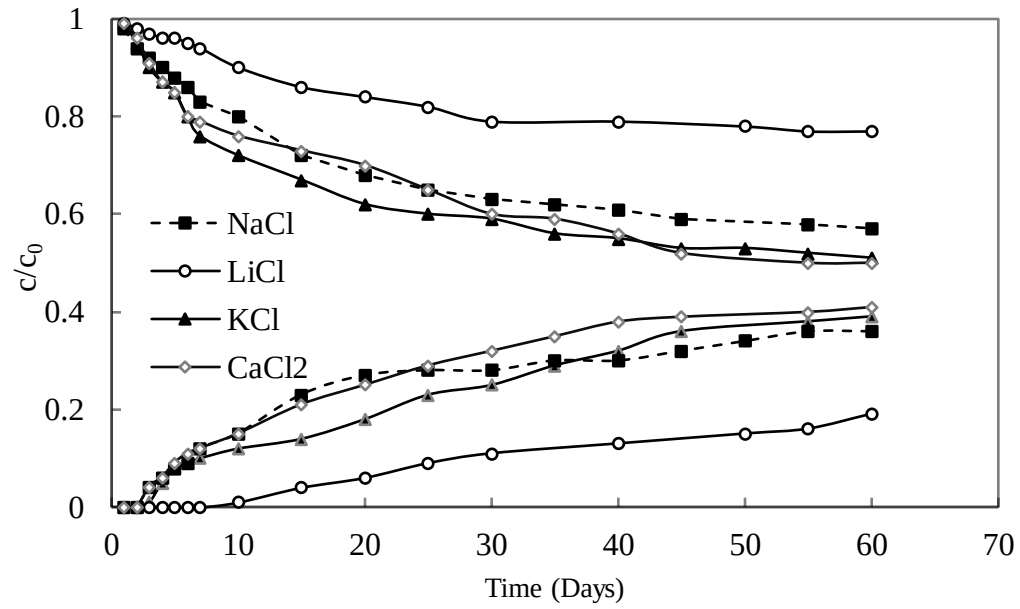

Figure 4.6: Temporal variation of the experimental concentration data with time for the monovalent and divalent salt ions at the same concentration of 0.2M

A slight deviation between the measured data and theoretical plots was noticed at the beginning of the diffusion testing ($t \leq 10$ days) for monovalent cations (Fig. 4.6 a-d). The deviation was mainly due to the cation exchange process in the initial stage of the diffusion as a significant percentage of calcium ions were present, in the exchangeable state, for the studied bentonite. The estimated diffusion coefficient and retardation factor were presented in Table 4.1.

The diffusion coefficient increased with the decrease in the hydrated cation size. The decrease in the diffusion coefficients with the increase in the radius can also be qualitatively understood from the diffuse double layer (DDL) theory. The DDL thickness increases with the increase in the cationic radius of the same group (i.e., valence) in the periodic table (Mitchell, 1993; Rao and Mathew, 1995). The increase in the DDL thickness in a compacted state, where the volume change was not allowed, reduces the mobility of the cations. The diffusion coefficient, therefore, decreased. As the retardation considers the retention mechanism along with the adsorption and absorption processes, the R_d was higher for the lithium. The diffusion coefficients of lithium and potassium differed by nearly one order magnitude (Fig. 4.7a and Fig. 4.7c). More number of free paths was available in the case of KCl due to the presence of smaller DDL thickness around the clay platelets. The diffusion coefficients of KCl and $CaCl_2$, however, were nearly the same, which was also evident from the concentration profiles in Fig. 4.7c – 4.7d. The observed trend was in agreement with the earlier observation made by Sridharan et al. (1986) on the compressibility behavior of homo-ionized bentonites, using potassium and calcium. The retardation factor for $CaCl_2$ was higher compared to KCl due to preference for higher valence cations on the mineral surface to effectively utilize the surface density (Rao and Mathew, 1995; Arsan, 2010).

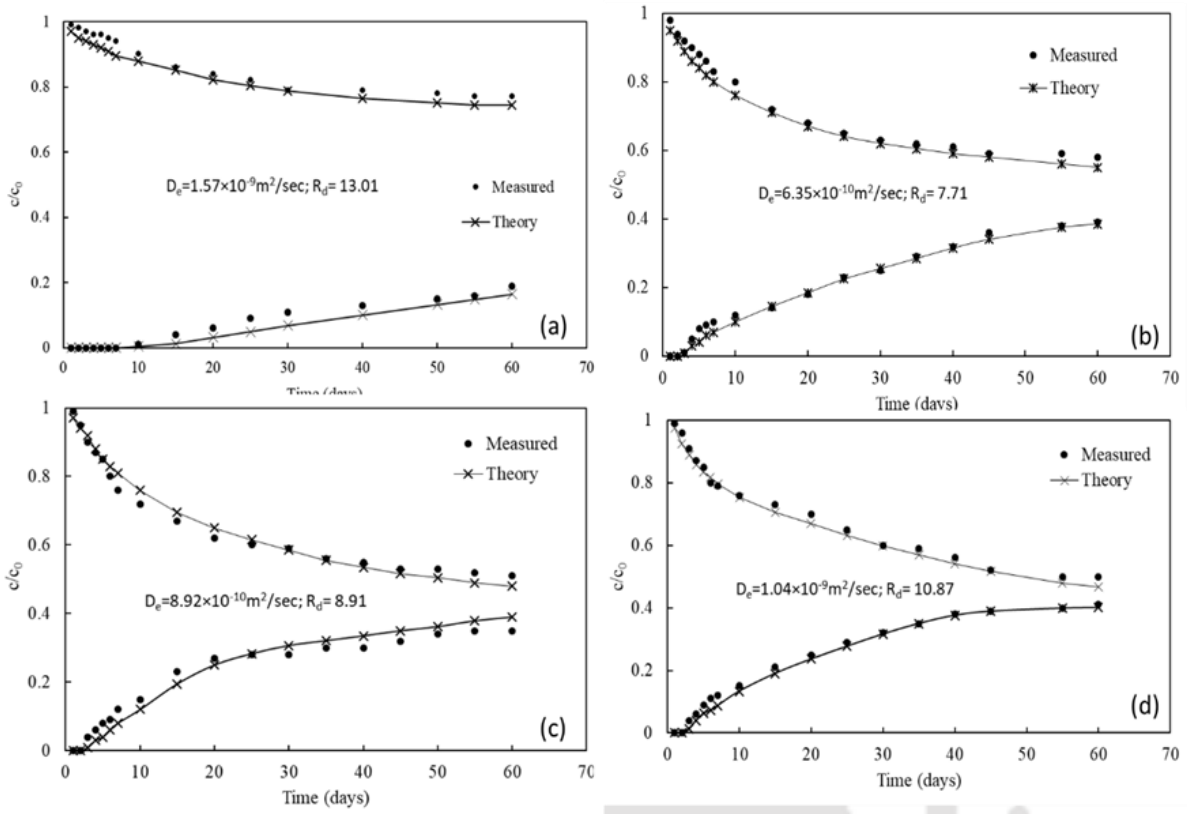

Figure 4.7: Comparison of the experimental concentration profile with the theoretical data at 0.2M concentration for (a) LiCl, (b) NaCl, (c) KCl, and (d) $CaCl_2$

4.3.3 Influence of the estimated model parameters on the liner design

The significance of the estimated mass transport parameters (Fig. 4.7 a-d) on the liner design was analyzed by considering the spatial distribution of the considered inorganic species at a given time. Theoretical data of salt concentration variation with depth after 5 years was simulated using the estimated mass transport parameters in Fig. 4.8 using the following expression (Shackelford, 1991).

$$\frac{c}{c_0} = \exp\left[\frac{nR_d x}{H_f} + \left(\frac{n}{H_f}\right)^2 D_e R_d t\right] erfc\left[\frac{x}{2\sqrt{D_e t / R_d}} + \frac{n}{H_f}\sqrt{D_e R_d t}\right] \quad 4.1$$

where all the above terms have the same meaning as described in Eq. (2.5)-(2.9).

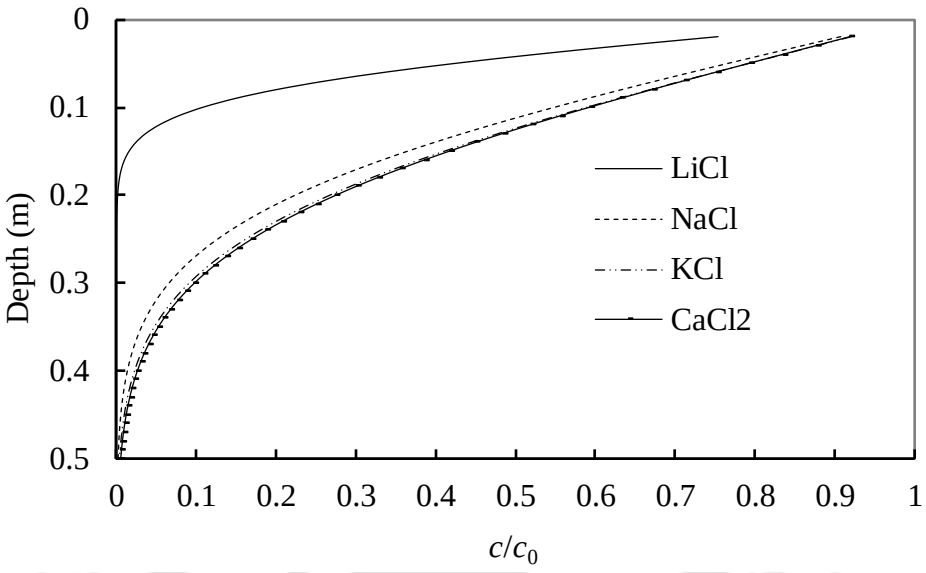

Figure 4.8: Simulated spatial variation of salt concentrations with depth through semi-infinite clay liner after 5 years by the predicted design parameters

Equation (4.1) simulates the concentration profile for the semi-infinite boundary condition at the bottom and flux boundary condition (Eq. 2.8) at the top boundary. The simulated data showed that a significant variation in the concentration data of different salts was found with depth. The LiCl salt was not reached even 0.2 m depth of the clay liner after 5 years, but a small concentration of other salts was available at 0.5 m depth at the same time. The diffusion migration of Li^+ was significantly slower than other cations due to the presence of thicker DDLs.

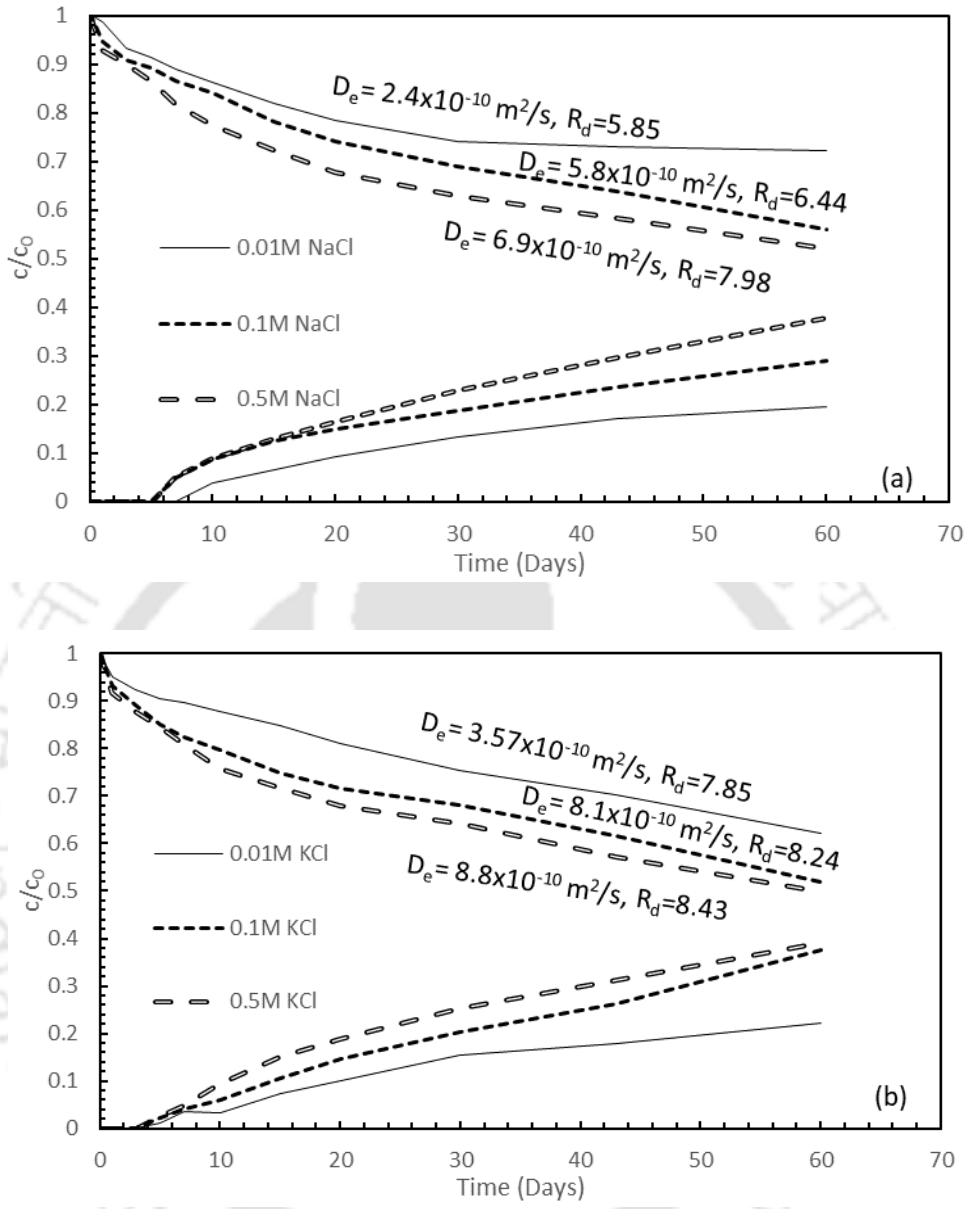

Figure 4.9: Theoretical concentration profile for different concentration of (a) NaCl, (b) KCl through GB

4.3.4 Effect of salt concentration on the diffusion characteristics of compacted GB

The effect of concentration on the migration rate of the monovalent cations through the GB was also assessed. The experimental data revealed that similar to the PB, the concentration significantly influenced the effective flow path of a particular ion through the compacted GB. The D_e for the sodium and potassium ions increased and the maximum D_e was observed for potassium ions with the increase in concentration (Fig. 4.9 a-b). The model parameters

(D_e, R_d) for both PB and GB were comparable (Table 4.1) indicating that the PB and GB behaved in a similar fashion when salt migration through the soil took place under the saturated condition. Therefore, the alteration of the pore structure of the GB due to the changes in the DDL thickness in the presence of various pore-fluid affected the flow of ions through the compacted GB. As the D_e of the lithium ions through the PB did not alter significantly at lower concentrations, the diffusion of lithium ions through GB was studied only at n=0.5M

Table 4.1: Estimated model parameters for the PB and GB under various salt concentrations

		PB		GB	
Salt	**Concentration**	D_e **(m²/s)**	R_d	D_e **(m²/s)**	R_d
LiCl	0.01M	8.87×10^{-11}	8.56	-	-
	0.1M	1.56×10^{-10}	12.34	-	-
	0.2M	1.57×10^{-10}	13.01	-	
	0.5M	1.68×10^{-10}	13.56	1.82×10^{-10}	12
	1M	1.69×10^{-10}	14.58		
NaCl	0.01M	1.32×10^{-10}	5.25	2.4×10^{-10}	5.85
	0.1M	5.6×10^{-10}	6.32	5.8×10^{-10}	6.44
	0.2M	6.3×10^{-10}	7.71	-	-
	0.5M	6.4×10^{-10}	7.97	6.9×10^{-10}	7.98
	1M	7.82×10^{-10}	8.90		
				-	-
KCl	0.01M	3.56×10^{-10}	7.96	3.57×10^{-10}	7.85
	0.1M	7.37×10^{-10}	8.37	8.1×10^{-10}	8.24
	0.2M	8.9×10^{-10}	8.92	-	-
	0.5M	8.9×10^{-10}	9.16	8.8×10^{-10}	8.43
	1M	1.01×10^{-9}	9.47	-	-
$CaCl_2$	0.2M	1.04×10^{-9}	10.87		

In the present work, the effective diffusion coefficient was compared with the equilibrium sediment volume of the compacted PB and GB in the presence of the studied salt concentrations. The past studies relate the equilibrium sediment volume with the saturated hydraulic conductivity (K_s) to understand the long-term hydraulic behaviour of compacted bentonites Bowders et al., 1986; Petrov and Rowe, 1997; Lee et al., 2005). However, the applicability of equilibrium sediment volume data to understand the diffusion behaviour of compacted PB/GB is not available.

4.4 Effect of salt type and concentration on the sediment volume of PB and GB

The measured variation of the final sediment volume (V_{eq}) from the ESV tests in the presence of the chloride salts of lithium, sodium, and potassium for both PB and GB was shown in the Fig. 4.10 a-b. Such a basic laboratory test was performed to qualitatively understand the long-term diffusion behavior of the compacted PB and GB in the presence of various salts.

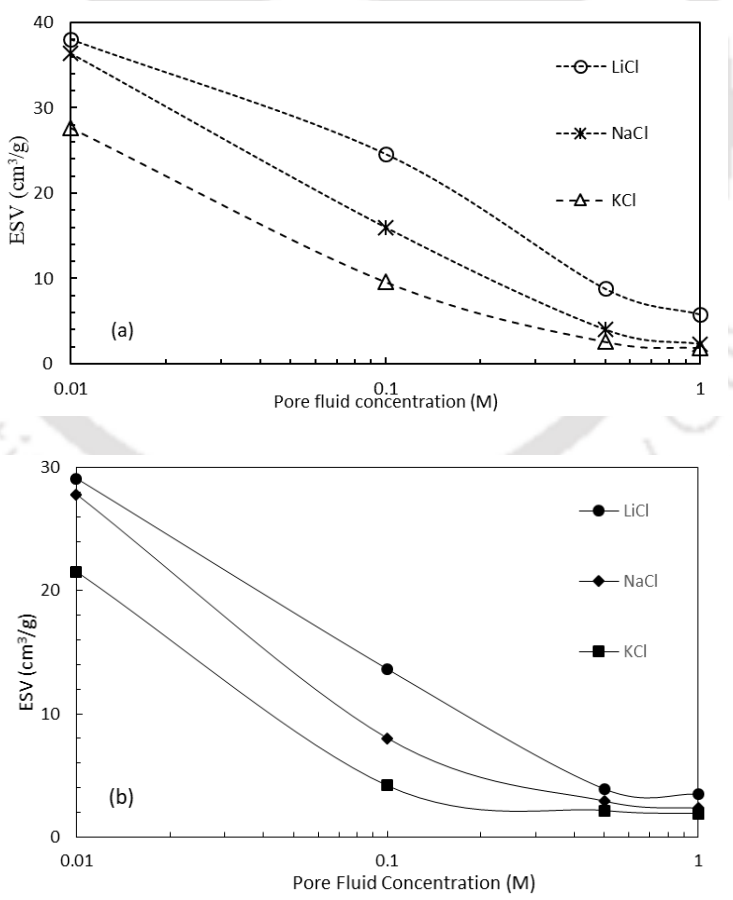

Figure 4.10: variation of the final ESV (Veq) with the pore-fluid (salt) concentration for (a) PB, (b) GB

The V_{eq} was found to decrease considerably in the presence of all the studied salt solutions for both PB and GB. For the PB the decrease in the V_{eq} with the salt concentration was due to the suppression of the DDL thickness. The decrease in the DDL thickness increases the van der Waals attraction between the clay platelets leading to the formation of a flocculated fabric and thereby the V_{eq} was low at higher concentration. On the other hand, the decrease in the V_{eq} with salt concentration for GB was primarily due to the inability of the large-sized granules to disintegrate into particles.

Moreover, a minimum V_{eq} was exhibited by both PB and GB in the presence of KCl and maximum in the presence of LiCl at all the studied concentrations. The V_{eq} in the presence of NaCl was in between the V_{eq} observed in the presence of LiCl and KCl. The hydrated size of the salt cations, therefore, played a significant role in the sediment volume of the studied bentonites. Lithium being a larger size cation, the V_{eq} was higher in comparison to the V_{eq} in the presence of sodium and potassium ions which have relatively lesser hydrated size. The behavior of the PB and GB as observed from the sediment volume test, therefore, gives a qualitative understanding of the long-term diffusion behavior of the soils in the presence of different salts. The D_e was found to be significantly high in the presence of KCl solution and least in the presence of LiCl solution. Moreover, with the increase in the concentration, the D_e increased significantly (Table 4.1). Hence, a decrease in the V_{eq} for the studied soils in the presence of a particular pore-fluid indicates a higher D_e in the presence of similar salt.

4.5 Salient Observation

- The hydrated cation size played a significant role in contaminant migration through both PB and GB
- The diffusion coefficient increased with decrease in the size of hydrated cations due to the suppression of the diffuse double layer thickness around the clay platelets.
- The effect of concentration change on the diffusion coefficient for both bentonites was more prominent in the presence of potassium ions. The diffusion coefficient of the PB and GB are nearly comparable in the presence of the studied salts.

- The pore structure of the bentonite changes with increase in the concentration gradients are thereby led to a considerable change in the effective diffusion coefficient of the ions in the compacted PB.
- The retardation factor showed an increasing trend with the increase in the concentration of a particular salt, as more amount of cations in the pore-fluid were adsorbed on the clay surface.
- The sediment volume test provided a qualitative understanding of the long-term diffusion behavior of the compacted PB and GB in the presence of various salt solutions.

Chapter 5

Diffusion characteristics of compacted PB for synthetic salt leachates

5.1 General

In the field conditions, the MSW leachate in the waste containment facilities comprises of multi-species salt solution. In the previous chapter, the diffusion characteristics of the compacted PB and GB were evaluated in the presence of a single-species salt solution. It was observed that the D_e of the diffusing ions through both PB and GB increased significantly in the higher concentration of the salts (n>0.1M). As the estimated model parameters for the PB and GB were found to be similar in the presence of single-species salt solutions, the diffusion behaviour of GB in the presence of synthetic leachate (multi-species salts) is also expected to be similar to PB. Therefore, in this chapter, the diffusion behaviour of only the compacted PB was assessed in the presence of mixed pore-fluids. Moreover, in order to understand the influence of the compaction density on the estimation of the model parameters, the through-diffusion test in the presence of synthetic leachates was performed at two different compaction densities of the PB (ρ_d=1.1 Mg/m^3 and 1.3 Mg/m^3).

Several synthetic leachate solutions were prepared by mixing the salt solutions while maintaining the individual salt concentration at 0.1M in the mixture. The synthetic leachate combinations studied were:

- LiCl-NaCl
- NaCl-KCl
- KCl-$CaCl_2$
- LiCl-NaCl-KCl-$CaCl_2$

At the end of the diffusion test, the diffusion cell was dismantled and the soil samples were lyophilized for identifying the elemental composition using the Energy-Dispersive X-ray (EDX) spectroscopy. The adsorption potential of the studied cations on the mineral surfaces

of PB was also quantified by adapting the procedure similar to the CEC for soils. The ion concentration obtained from both these methods was expressed in meq/100g.

5.2 Results and discussion

5.2.1 *Effect of synthetic salt leachate*

The samples collected from the source and collector reservoir at regular intervals were analyzed for individual cation concentration for a given salt mixture. The comparison of the temporal variation of the measured concentration in the source and collector reservoir for the studied salt mixtures through the compacted PB (ρ_d=1.1 Mg/m^3) was shown in Fig. 5.1 a-d. In the presence of the LiCl-NaCl mixture, the migration rate of sodium ion was observed to be faster than the lithium ions. Similarly, in the presence of NaCl-KCl salt mixture, the migration rate of potassium ion was found to be significantly higher than the sodium ions (Fig. 5.1a-b). Moreover, the measured concentration data suggested that the influence of a particular cation in a given mixture increases the migration rate of the companion ion. In the presence of the potassium ion in the salt mixture, the migration rate of the sodium ion was found to be higher in comparison to its rate in the LiCl-NaCl mixture. The DDL thickness in the presence of the potassium ions reduced considerably and thereby allowing an easier path for the sodium ions. It is worth noting that in the presence of the KCl-$CaCl_2$ salt mixture, the rate of decrease of concentration of calcium ion in the source reservoir was higher than the potassium ion (Fig. 5.1c). However, the calcium ions diffused at a much slower rate through the PB to reach the collector reservoir. The relative concentration of the calcium ion in the collector reservoir after two months was ~0.12, on the other hand, the relative concentration of the potassium ion in the collector reservoir was ~0.35. This was due to the significant adsorption of the divalent calcium ion on the mineral surface of PB to satisfy the charge density. The presence of the divalent calcium ions suppressed the DDL thickness, which allowed easy mobility of the companion ions. Moreover, in the presence of LiCl-NaCl-KCl-$CaCl_2$ the migration rate of sodium and lithium ion increased in comparison to its rate in the presence of other studied salt mixtures (Fig. 5.1 d). The presence of potassium and calcium ions in the salt leachate was therefore found to be detrimental in terms of the diffusion rate of other companion cations present in the leachate.

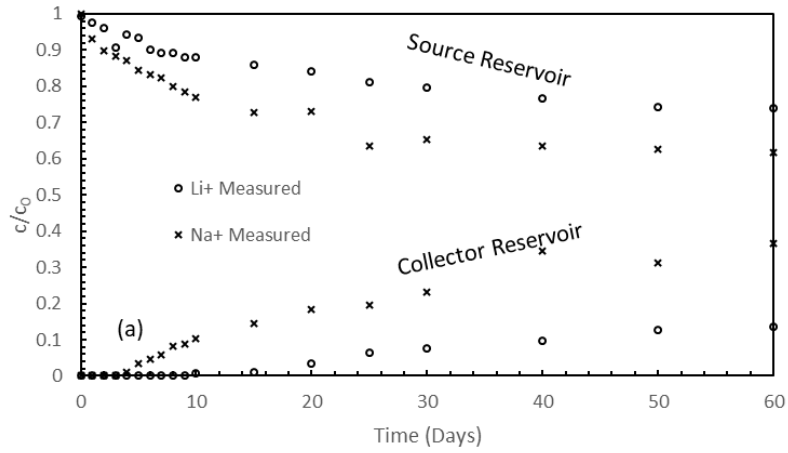

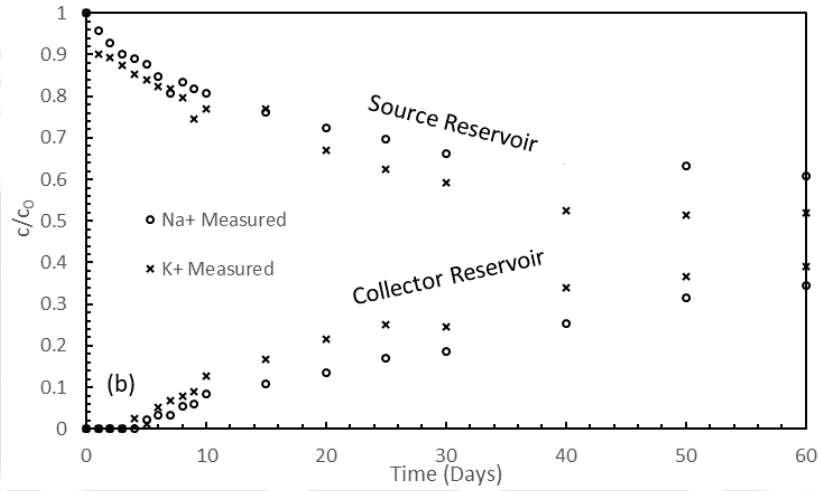

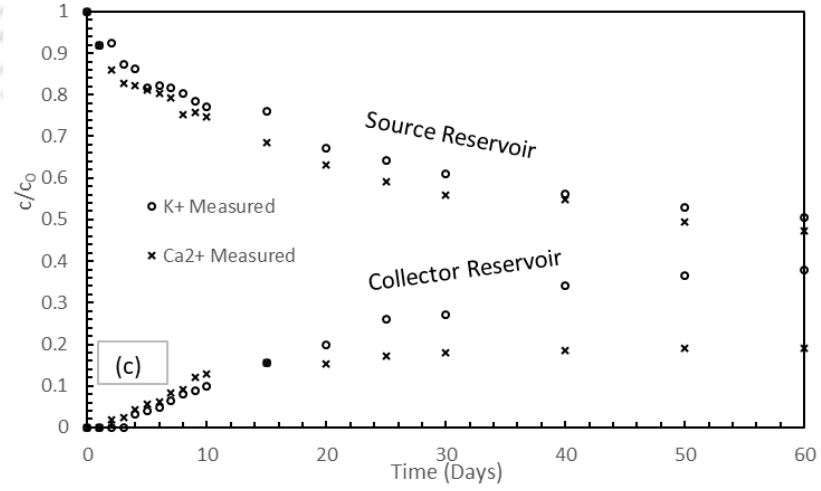

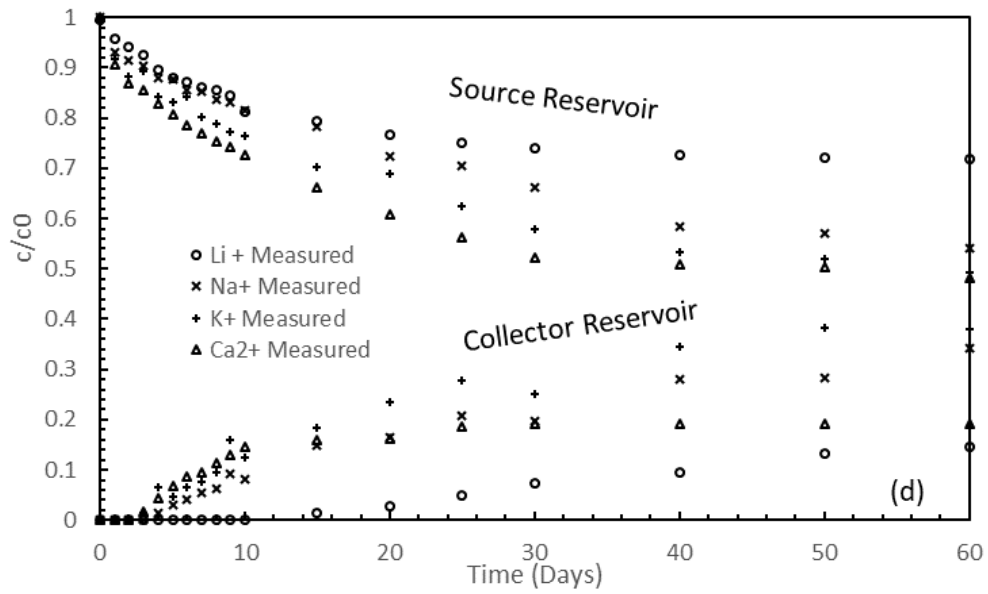

Figure 5.1: Comparison of the experimental concentration data for the individual ions present in the salt mixture of (a) LiCl-NaCl (b) NaCl-KCl, (c) KCl-$CaCl_2$ (d) LiCl-NaCl-KCl-$CaCl_2$

The measured data were used to determine the D_e, R_d of the individual ions by optimization as discussed in chapter 4. The model parameters of the diffusing ions present in the studied salt-mixtures were presented in Table 5.1. The theoretical concentration plots using the optimized design parameters (Table 5.1) for different salt mixtures were presented in Figs. 5.2 a-d, along with the measured data. A slight deviation between the theoretical concentration curve and the measured concentration data was observed during the initial times for all the cases presented and particularly for salt mixtures containing calcium ions. This was due to the sorption of the ions present in the salt leachates on the mineral surface of bentonite is complex and non-linear. The inverse analysis suit CONTRADIS was developed by assuming a linear sorption isotherm. However, due to the surface complexion in the presence of salt mixture, the theoretical plots could not accurately fit the measured data in the presence of calcium.

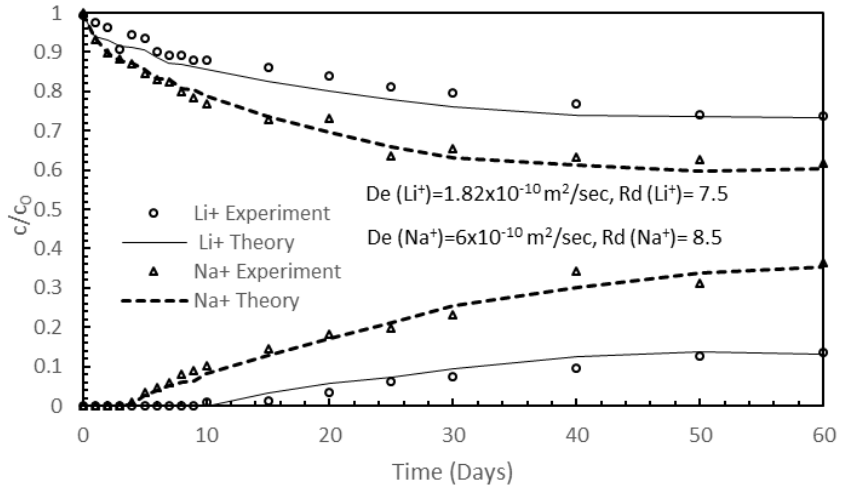

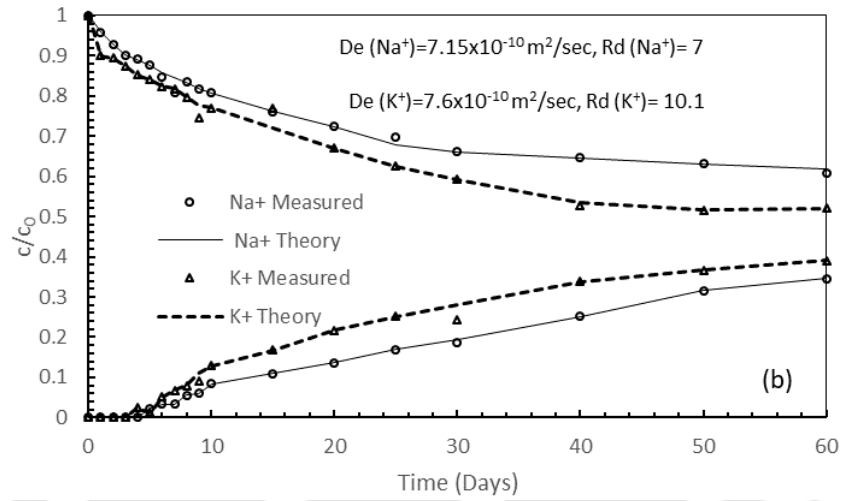

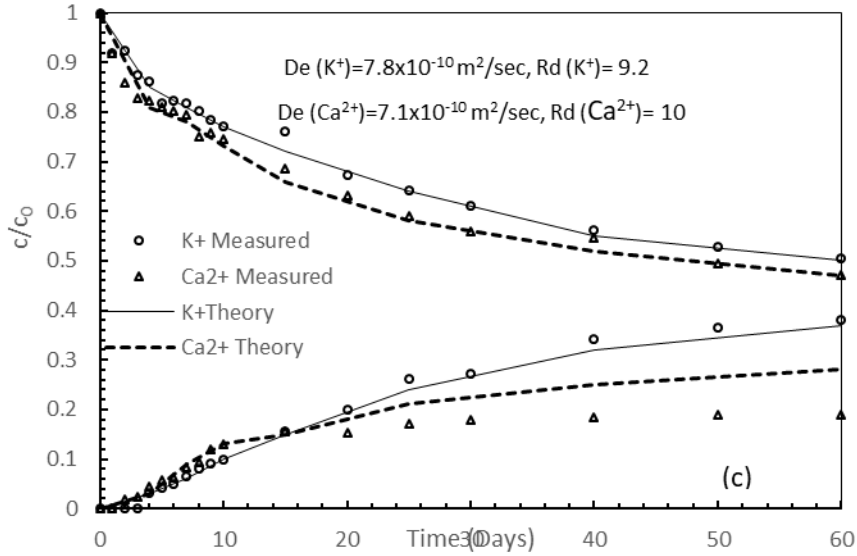

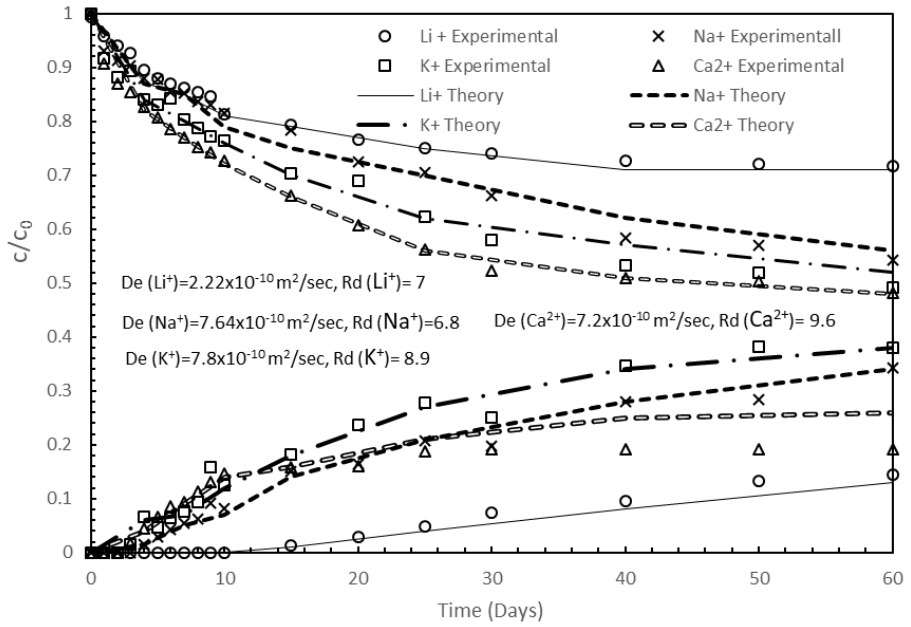

Figure 5.2: Comparison of the experimental and theoretical concentration data for the individual ions present in the salt mixture of (a) LiCl-NaCl (b) NaCl-KCl, (c) KCl-CaCl2 (d) LiCl-NaCl-KCl-CaCl2

The estimated D_e, for lithium ion in LiCl-NaCl mixture through the compacted PB was lower, however, the value increases significantly in the presence of salt mixture comprising of the smaller hydrated size cations (Fig. 5.2 a, 5.2 d). Similarly, the D_e for sodium ion in the LiCl-NaCl salt mixture was $6x10^{-10}$ m^2/s, which increased to $7.15x10^{-10}$ m^2/s in the presence of potassium ion for the NaCl-KCl salt mixture. Further, in the presence of calcium ions, the D_e for all the monovalent ions was found to be higher. Therefore, the presence of smaller sized cation and divalent cation in the salt mixture influenced the *De* for the larger sized cations in the same mixture. The presence of divalent cations primarily contributes to the DDL thinning which thereby increased the D_e for the other companion ion. It is worth noting that the D_e of the ions in the salt mixtures were higher than the corresponding D_e of the same ions when present individually (Table 4.1)

Moreover, the retardation of a particular ion was also found to be influenced by the type of companion ion present in the salt mixture. The R_d for the lithium ion was 7.5 in the LiCl-NaCl salt mixture, but, the R_d reduced to 7 due to the divalent calcium ion in the salt mixture (Fig. 5.1d). Similarly, the R_d for the sodium ion in the presence of LiCl-NaCl salt mixture was 8.5, which reduced to 7 and 6.8 in NaCl-KCl and LiCl-NaCl-KCl-$CaCl_2$ salt mixtures,

respectively. Maximum R_d was observed for the calcium and potassium ions for all the studied salt mixtures. This was due to the higher exchange of the surface cations by the potassium and calcium ions present in the bulk solutions. The higher preference of these ions on the mineral surfaces reduces the amount of sorption of lithium and sodium ions present in the salt mixture.

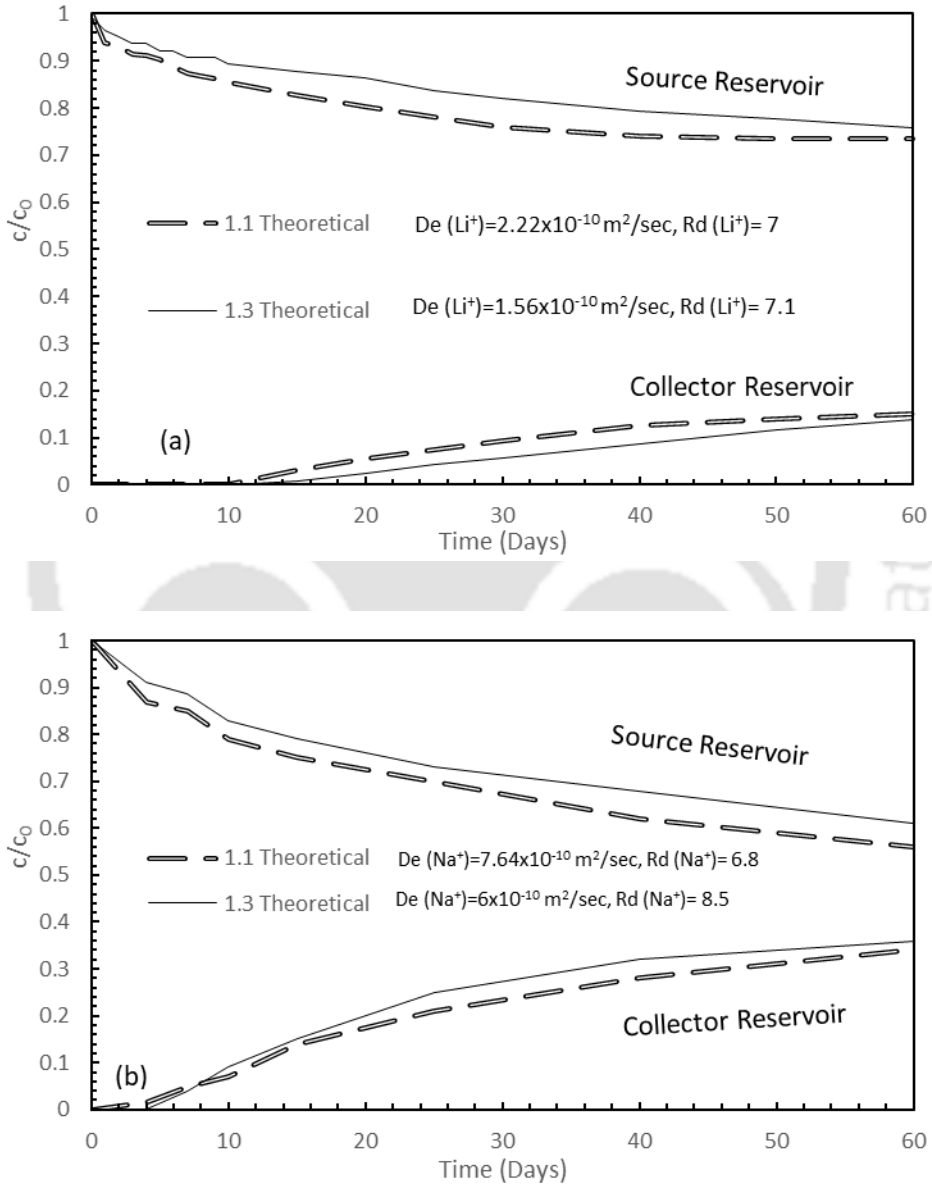

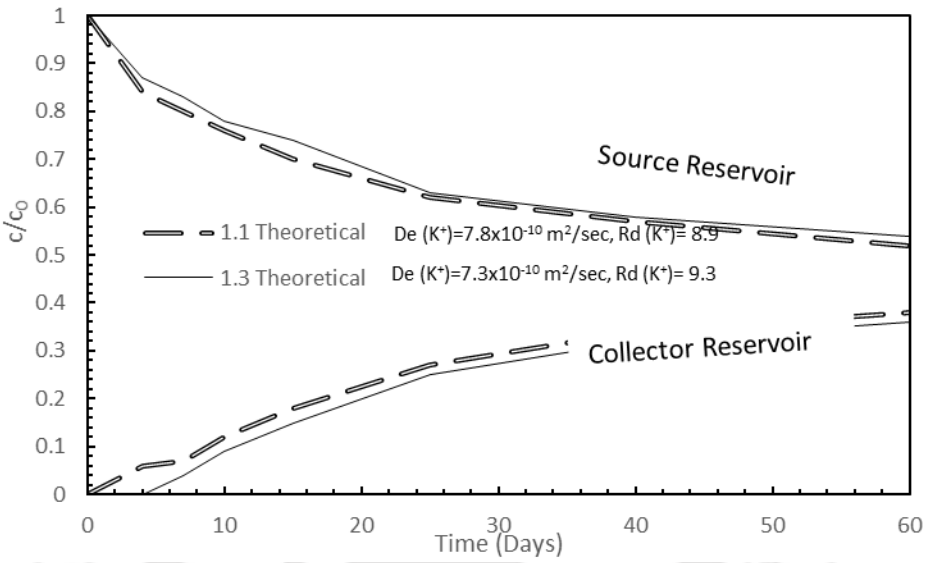

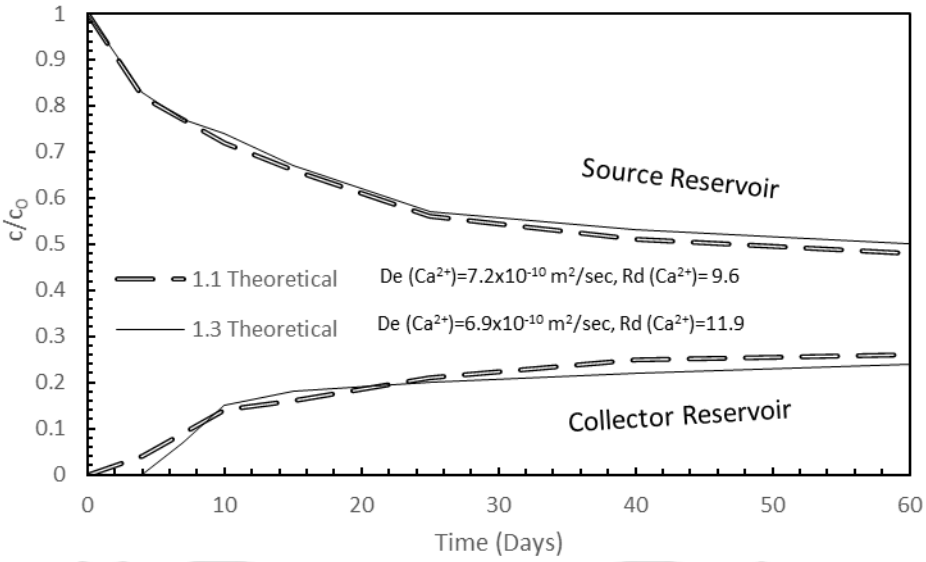

Figure 5.3: Comparison of the theoretical concentration data for the (a) lithium, (b) sodium, (c) potassium, (d) calcium ions present in the salt mixture of LiCl-NaCl-KCl-$CaCl_2$ through the PB compacted at different dry densities

Table 5.1: Model parameters obtained from the through-diffusion test

Density (Mg/m^3)	Synthetic leachate	Ions considered for analysis	D_e (m^2/sec)	R_d	*Overall* D_e (m^2/sec)	*Overall* R_d
1.1	LiCl-NaCl	Li^+	$1.82x10^{-10}$	7.5	$5.92x10^{-10}$	8.2
		Na^+	$6x10^{-10}$	8.5		
	NaCl-KCl	Na^+	$7.15x10^{-10}$	7	$7.2x10^{-10}$	9.1
		K^+	$7.6x10^{-10}$	10.1		
	$KCl-CaCl_2$	K^+	$7.8x10^{-10}$	9.2	$7.5x10^{-10}$	9.6
		Ca^+	$7.1x10^{-10}$	10		
	LiCl-NaCl-$KCl-CaCl_2$	Li^+	$2.22x10^{-10}$	7	$7.8x10^{-10}$	10.7
		Na^+	$7.64x10^{-10}$	6.8		
		K^+	$7.8x10^{-10}$	8.9		
		Ca^{2+}	$7.2x10^{-10}$	9.6		
1.3	LiCl-NaCl	Li^+	$1.2x10^{-10}$	7.8	$4.8x10^{-10}$	9.12
		Na^+	$5.6x10^{-10}$	9.2		
	NaCl-KCl	Na^+	$5.8x10^{-10}$	8.7	$6.2x10^{-10}$	9.8
		K^+	$7.2x10^{-10}$	10.2		
	$KCl-CaCl_2$	K^+	$7.8x10^{-10}$	9.4	$7.4x10^{-10}$	10.77
		Ca^+	$6.8x10^{-10}$	11		
	LiCl-NaCl-$KCl-CaCl_2$	Li^+	$1.56x10^{-10}$	7.1	$7.6x10^{-10}$	10.23
		Na^+	$6.0x10^{-10}$	8.5		
		K^+	$7.4x10^{-10}$	9.3		
		Ca^{2+}	$6.9x10^{-10}$	11.9		

5.2.2 *Effect of compaction density*

In order to understand the influence of compaction density on the migration rate and the consequent model parameters for the individual ions, the diffusion test in compacted PB at 1.3 Mg/m^3 was also performed. As the nature of the variation in the migration rates of various ions in the studied salt mixtures was similar, the theoretical concentration plot was presented only for the LiCl-NaCl-KCl-$CaCl_2$ salt-mixture (Fig. 5.4 a-d). The model parameters for all the other salt mixtures were presented in table 5.1. The increase in the compaction density of the PB decreased the D_e for the lithium and sodium ions. This was due to the increase in the tortuous pathway at higher compaction density (Fig. 5.4 a-b). However, the influence of compaction density on the D_e for the potassium and calcium ions was marginal. Further, the R_d for all the diffusing ions increased at a higher compaction density of the PB. This was primarily due to the presence of a higher amount of exchange sites present in the PB at ρ_d=1.3 Mg/m^3.

5.2.3 *Elemental compositional analysis*

For quantification of the amount of salt-ions adsorbed on the surface of PB at a compaction density of 1.1 Mg/m^3, elemental compositional analysis by two different methods were adopted (Sec. 3.2.5). The quantification enabled the understanding of the underlying mechanism in the sorption characteristics (R_d) for various diffusion tests with various salt mixtures. In both methods, the PB clay plug after the termination of the diffusion experiment for the studied salt mixtures was analyzed. The concentration of the ions present in the PB clay plug in different diffusion tests with the studied salt mixtures based on the first method (ammonium exchange method) was presented in Table 5.2. For ease of comparison, the concentration of the surface cations for water-saturated PB was also presented in the same table.

The second method comprised of estimating the elemental compositions (including the surface cations) on the surface of the PB clay plug due to diffusion of the salt mixture by EDX spectroscopy. The EDX spectra of the PB sample in the presence of different salt solutions were shown in Fig. 5.4. The spectra was characterized by distinct peaks for oxygen (O), silicon (Si), and aluminum (Al) indicating the presence of structural elements in the

basic layers. Apart from the basic elements, the EDX spectra provided the peaks for the various salt cations retarded by the PB clay plug due to diffusion of the studied salt mixtures. The corresponding weight percentage for all the tested samples was also presented in Fig. 5.4. The weight percentages expressed in the units of meq/100g are provided in Table 5.3.

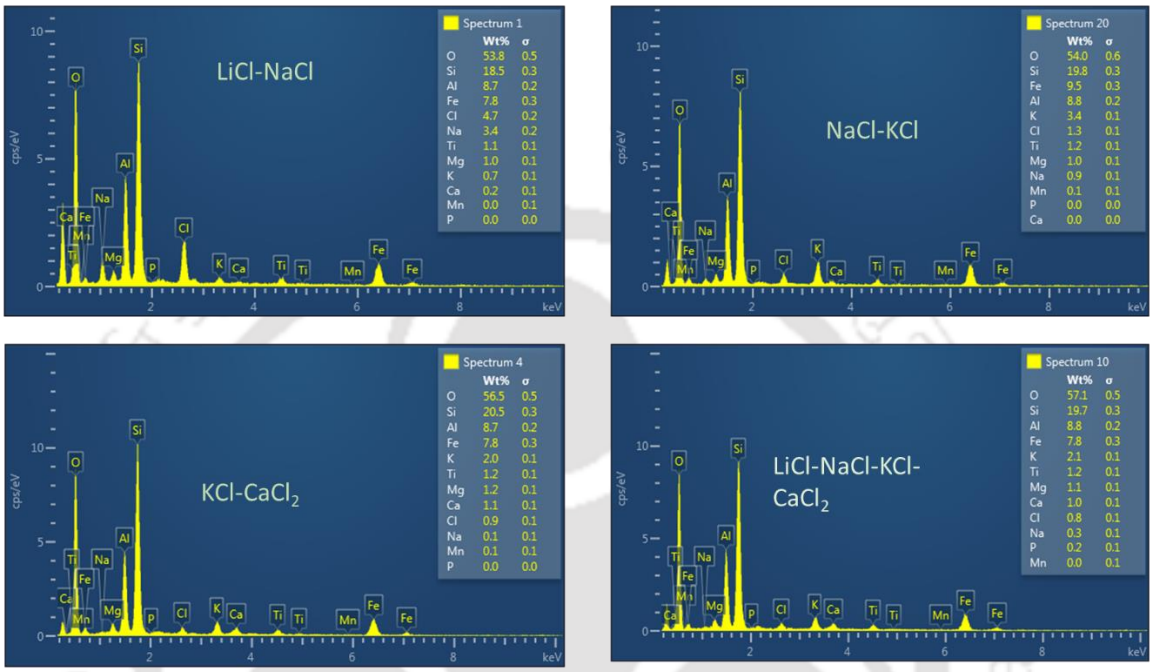

Figure 5.4: Elemental composition analysis of the PB in the presence of the studied salt mixtures

The concentration of the adsorbed ions as presented in Table 5.2-5.3, obtained by both the methods were in good agreement. The concentration of the lithium ions could not be obtained by EDX and hence not reported in the table, however, it was assumed that the sorbed lithium ion concentrations by both the methods would also be similar due to the similarity of the other ion concentration. Based on the elemental composition analysis by both the methods it was observed that in the presence of LiCl-NaCl solution, the concentration of both sodium and lithium ions was very high indicating strong sorption of these ions, while the concentration of potassium and calcium in the same mixture was negligible. However, the concentration of sorbed potassium ion was found to be significant and higher than the sodium ion due to the diffusion of NaCl-KCl solutions. Therefore, the diffusion results for the compacted PB in the presence of LiCl-NaCl salt mixture showed higher R_d for the potassium ions (Table 5.1). Moreover, the elemental compositional analysis reveals that in the salt mixture comprising of calcium ions, the concentration of calcium ion

was maximum in comparison to the other ions. The higher R_d of the calcium ion from the through-diffusion test in the presence of KCl-$CaCl_2$ and LiCl-NaCl-KCl-$CaCl_2$ confirms the observation. In the presence of KCl-$CaCl_2$ and LiCl-NaCl-KCl-$CaCl_2$ salt mixtures, the mineral surface of PB was found to have a high affinity for divalent calcium and monovalent potassium ions, which contributes to the suppression of the DDL thickness and thereby resulting in the higher diffusion coefficient of the companion ions.

Table 5.2: Elemental composition by ammonium acetate exchange method

Ions	Concentrations of the ions adsorbed on the surface of PB (meq/100g) post equilibration with ammonium acetate solution				
	Saturated with water	LiCl-NaCl	NaCl-KCl	KCl-$CaCl_2$	LiCl-NaCl-KCl -$CaCl_2$
Li^+	-	78	-	-	64
Na^+	24.4	136	34.6	2.5	11.2
K^+	16.8	13.6	85.2	50.12	52.3
Ca^{2+}	19.1	9.2	8.6	53.2	54.8

Table 5.3: Elemental composition by EDX

Ions	Concentrations of the individual ion in a salt mixture (meq/100g) from EDX			
	LiCl-NaCl	NaCl-KCl	KCl-$CaCl_2$	LiCl-NaCl-KCl -CaCl2
Li^+	-	-	-	-
Na^+	147	30.43	4.34	13.04
K^+	17.94	87.17	51.28	53.841
Ca^{2+}	10	10	55	50

The overall D_e and R_d for the various salt mixtures obtained from the temporal variation of the relative concentration of the total mass (including all the cations) of the solute in the source and collector reservoir were also presented in Table 5.1. The presence of the potassium and calcium ion in the salt mixture increased the overall D_e for the solution albeit the sorption was higher. The majority of the retardation was contributed by the potassium and calcium ions and thus the overall retardation (R_d) was high. The overall *De* was found to be the least for LiCl-NaCl salt mixture due to the presence of larger size cations like lithium and sodium. The increase in the compaction density resulted in the decrease of the overall D_e and the increase was more pronounced for the LiCl-NaCl salt mixture. The increase in the overall density does not contribute significantly to the reduction of the overall D_e for the salt mixture containing potassium and calcium ions. Therefore, the hydrated size and valence of the cations in the salt leachate dictates its overall ion migration through the compacted liner material. For the similar concentration of the salt cations, the presence of the smaller sized and divalent cations (K^+, Ca^{2+}) caused adverse effects on the flow of contaminants through the PB/GB. It was observed in the first chapter that a small increase in the D_e for a diffusing ion can increase the liner thickness for its complete encapsulation. Thus, the presence of K^+ and Ca^{2+} ions in the leachate, would result in easy mobility for the companion ions and also several other contaminants present in the leachate.

5.3 Long-term diffusion characteristics of compacted PB under salt environment

In the current times, the continuous leachate recirculation for the production of methane gas is practiced in various engineered landfills. However, continuous leachate recirculation might result in the complete cessation of the exchange process of the bottom liner system, in the long run, rendering the sorption potential of the bentonite liner systems to be negligible. In order to simulate such a field condition, long-term diffusion tests were performed on the compacted PB to understand the influence of the sorption potential of the PB clay plug on the diffusion rate of various salts. The through-diffusion test was conducted on PB samples in the presence of the same salt solution, which was used during the permeation step. The permeation of the PB was continued for a period of ~156 days. At the end of the permeation period, the exchange process is exhausted in the PB and therefore the clay surface is devoid of any sorption potential.

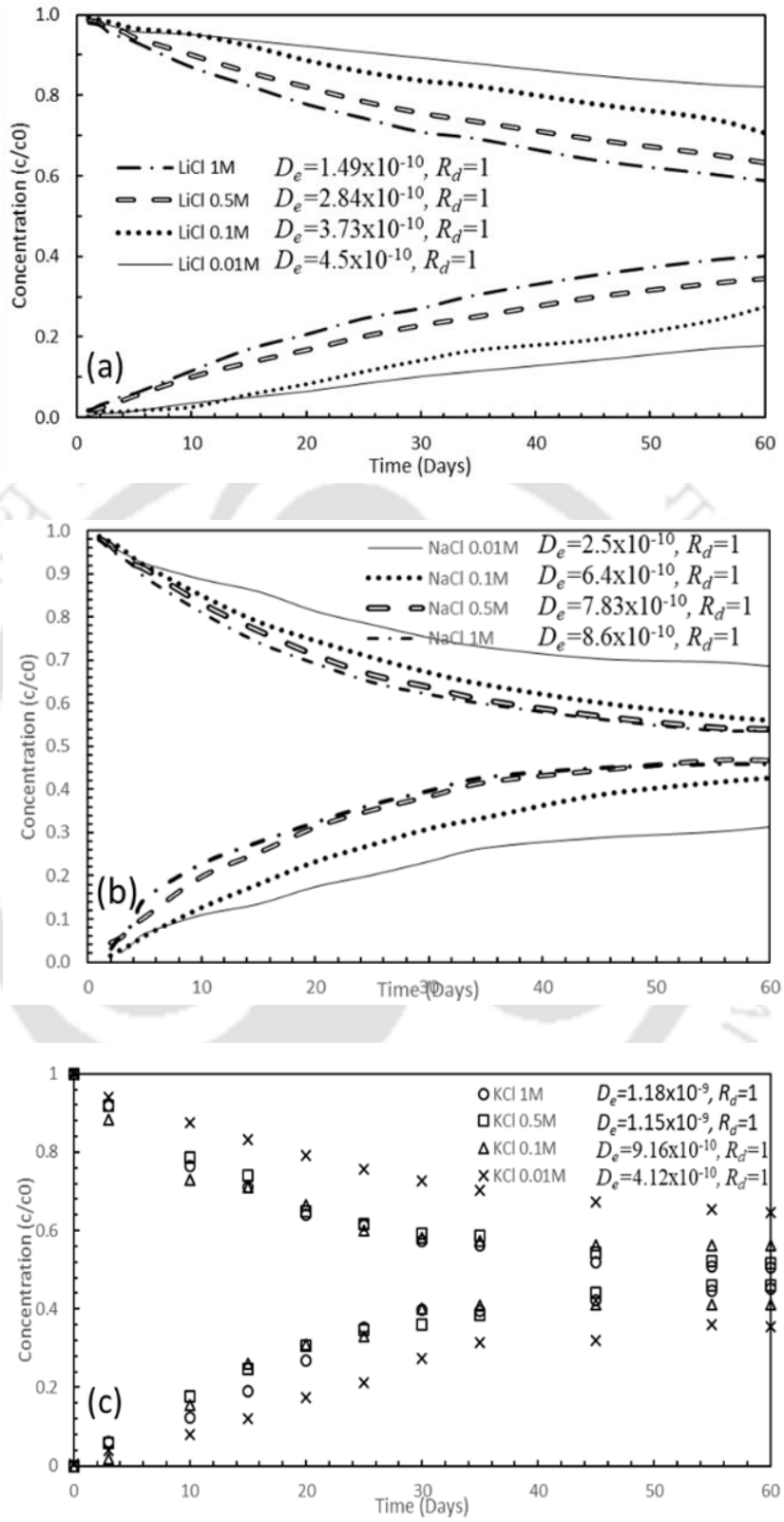

Figure 5.5: comparison of the theoretical concentration profile obtained from the long-term diffusion test for various concentration of (a) LiCl., (b) NaCl, (c) KCl

The experimental results of the long-term diffusion test through the compacted PB for 60 days post permeation was shown in Fig. 5.5 (a-c). The migration rate was found to increase with the increase in the concentration of the salt solution and more significantly in the presence of NaCl and KCl solution. It is worth noting that that the migration rate of all the studied salt cations obtained from the long-term diffusion test was considerably higher than the one obtained from the conventional through diffusion test (Chapter 4). The D_e for the lithium ions at all the studied salt concentrations showed a marginal increase. On the other hand, the *De* increased significantly in the presence of NaCl and KCl. At lower concentrations (*n=0.01M*), the D_e for all the studied salt cations were similar to the D_e obtained from the short-term diffusion test (Table 4.1). However, at higher concentrations (n>0.5M), the estimated *De* from the long-term diffusion test was much higher. This was attributed to the reduction in the sorption potential of the PB due to the cessation of the cation complexion as a result of a continuous flow of salt solution through the clay plug. Moreover, due to the significant thinning of the DDL, the accessible voids for the diffusing ions through the PB increased. The R_d was unity for all the cases to indicate that the compacted PB was devoid of the sorption in the long run. In order to quantify the accessible voids available in the PB at the time of termination of the long-term diffusion test, gamma-ray attenuation analysis was explored for the first time.

5.3.1 *Pore-fraction analysis*

In the present study, GRA was utilized to obtain the void fraction in the PB at the end of the diffusion test based on its attenuation capacity. The details of the procedure adapted was discussed in section 3.2.6. The μ_s and μ_w were estimated to be 0.1446 cm^{-1} and 0.0728 cm^{-1}, respectively. The void-fraction of the initially saturated soil (before the commencement of the diffusion test) was evaluated knowing ε_{ssat}. The void fractions for all the samples after the completion of the diffusion test were then evaluated in the D1 and D2 directions and presented in Table 5.4-5.5.

Table 5.4: Void fraction obtained from GRA along the D1 direction

Concentrations	void fraction (initial value=0.304)		
	LiCl	NaCl	KCl
0.01	0.330	0.405	0.407
0.1	0.395	0.443	0.444
0.5	0.409	0.454	0.464
1	-	0.48	0.51

Table 5.5: Void fraction obtained from GRA along the D2 direction

Concentrations	void fraction (initial value=0.32)		
	LiCl	NaCl	KCl
0.01	0.359	0.392	0.404
0.1	0.389	0.433	0.458
0.5	0.418	0.460	0.49
1	-	0.498	0.508

The void fraction along the D1 and D2 direction for the saturated PB was 0.304 and 0.32, respectively before commencing the diffusion test. However, after the completion of the diffusion test, the void fraction of the PB increased significantly along both directions. In the presence of LiCl, the increase in the void fraction at higher concentrations was 0.409 and 0.418, respectively in the D1 and D2 direction (Table 5.4-5.5). A considerable increase was observed in the presence of NaCl and KCl at higher concentrations (n>0.5M) along both directions. The void fraction for the PB in the presence of 1M NaCl and KCl was ~0.51 at the end of the diffusion test. This indicated that nearly all the pores available in the PB were accessible for the diffusing ion. The increase in the void fraction resulted in a higher D_e for

the salt cations. The cation complexion was expected to be complete during the permeation process and at higher concentration, the DDL was reduced significantly. Therefore, the migration rates were faster when the through-diffusion test was conducted in the presence of a similar salt concentration. Further, in the absence of sorption during the long-term diffusion test, an easy flow path was available for the diffusing ions resulting in higher *De*. Such a condition might prevail in the field during the stabilized phase of the landfill, where a continuous interaction of salt leachate would result in the completion of the cation complexion (exchange process) between the surface cations and the cations present in the salt leachate rendering significant reduction of the sorption potential of the soil. Such a scenario would be detrimental as the barrier would allow fast diffusion of other contaminants due to the sorption potential.

5.4 Salient observations

- The presence of smaller hydrated size companion ion in salt-mixture increased the migration rate of the larger sized cation. In the synthetic leachate containing all the four studied salts, the D_e of all the diffusing ions was higher than the corresponding value when such ions are present individually in a single salt solution.
- A detrimental effect in terms of the increase in the overall diffusion coefficient and reduction of the retardation factor was observed for the salt mixtures comprising of potassium and calcium ions.
- Elemental compositional analysis suggests that the synthetic leachate comprising of all the studied salts, a significant amount of potassium and calcium ion were adsorbed in the clay surface, resulting in the thinning of the DDL and increasing the D_e for the larger size cations
- The increase in the compaction density decreased the overall D_e of the salt mixture particularly in the presence of lithium and sodium ions. However, in the presence of potassium and calcium ions, the decrease in the overall D_e at higher compaction density was marginal.
- The long-term diffusion through the compacted PB augmented by pore-fraction analysis indicated that the D_e for all the ions increased due to the increased void fraction in the PB and reduced sorption potential due to the cessation of the cation complexion.

Chapter 6

Chemo-mechanical behavior of the compacted granular bentonite under salt environment

6.1 General

The diffusion behaviour of the saturated PB and GB was found to be similar in the presence of various salt solutions. However, in the un-hydrated state, the GBs consist of large macro-voids, and the sealing of such inter-granular voids determines the applicability of such materials as landfill liners. The GCLs consisting of the GB in the landfills are usually in the air-dry condition and might not get fully hydrated from the sub-surface moisture. The GCLs are thus directly exposed to different landfill leachates in the un-hydrated state. Commonly, the MSW landfills comprise of salt leachates due to the excessive disposal of salt-laden solid waste. The sealing and swelling ability of GB under high salt concentrations is scarce.

Moreover, GBs are exposed to the salt leachates under different overburden stresses due to waste load. These overburden stresses vary from low (initial phase of waste disposal) to high (when the landfill is full) during the service life of the landfill. The overall mechanical stability of the landfill is influenced by the volume change behaviour of the liner during the leachate migration and under overburden stresses. Therefore, an elaborate study on the sealing ability of the air-dry granular bentonites under the salt environment and different mechanical stress conditions is vital for evaluating the applicability of such materials for attenuating various contaminants in the landfills.

The sealing and swelling potential of compacted granular bentonite (GB) exhumed from GCL in the presence of various salt solutions and under the overburden stresses induced by the waste in municipal solid waste landfills were presented in this chapter. Three commonly existing chloride salt solutions in the landfill leachate, viz., sodium chloride (NaCl), potassium chloride (KCl), and calcium chloride ($CaCl_2$) were considered for the present study. Various concentrations of these salt solutions ranging from 0.01M – 0.5M were considered. The chemo-mechanical study which gives a quantitative understanding of the swelling and sealing behaviour of the compacted GB was evaluated by performing the permeation test as described in section 3.2.2 under mechanical stresses.

6.2 Results

The temporal variation of permeation rate in compacted GB by water and different concentration of NaCl under mechanical stresses of 50 kPa and 100 kPa were presented in Fig. 6.1a and Fig. 6.1b, respectively. The permeation rate of water through GB was very high for the initial 30 minutes, but the rate significantly dropped after a period of 90-100 minutes due to the sealing of the inter-granular voids in GB. On the other hand, in the presence of NaCl, the limiting value of the flow rate of $1x10^{-9}$ m/s (i.e., sealing) was achieved only at a larger time in comparison to water. Moreover, with the increase in the concentration of the NaCl solution, the sealing time (ST) for the compacted GB increased, and the larger ST was required in the presence of 0.5M NaCl (Fig. 6.1a) under the applied stress of 50 kPa. The ST for the GB was ~700 minutes in the presence of 0.01M NaCl that increased to ~2000 minutes and 4000 minutes in the presence of 0.1M and 0.5M NaCl, respectively. A similar trend was observed under 100 kPa mechanical stress (Fig. 6.1b). However, the ST of the GB improved and the limiting value of $1x10^{-9}$ m/s was achieved at a lesser time in comparison to lower mechanical stress.

The temporal variation of the normalized thickness (h/h_0) of the GB in the presence of water and different concentration of NaCl under the stress application of 50 kPa and 100 kPa was shown in Fig. 6.1c and Fig. 6.1d, respectively. The swelling potential was found to vary considerably with the type of permeant fluid. The swelling of the GB was maximum in the presence of water. On the other hand, the swelling potential of GB significantly reduced in the presence of different NaCl concentrations under both the applied stresses. With the increase in the permeation time, the swelling increased steadily after an initial collapse and reached a constant/equilibrium value. Under the applied stress of 50 kPa, the equilibrium normalized thickness of the GB layer in the presence of water was 1.21 which was reduced to 1.18 and 1.06 for NaCl of 0.01M and 0.1M, respectively (Fig. 6.1c). In the presence of 0.5M NaCl, the swelling was marginal after the initial collapse for ~1 minute and became constant after a period of 2000 minutes. A similar trend in the swelling behaviour was observed for the GB under 100 kPa stress, but the extent of swelling was slightly reduced (Fig. 6.1d).

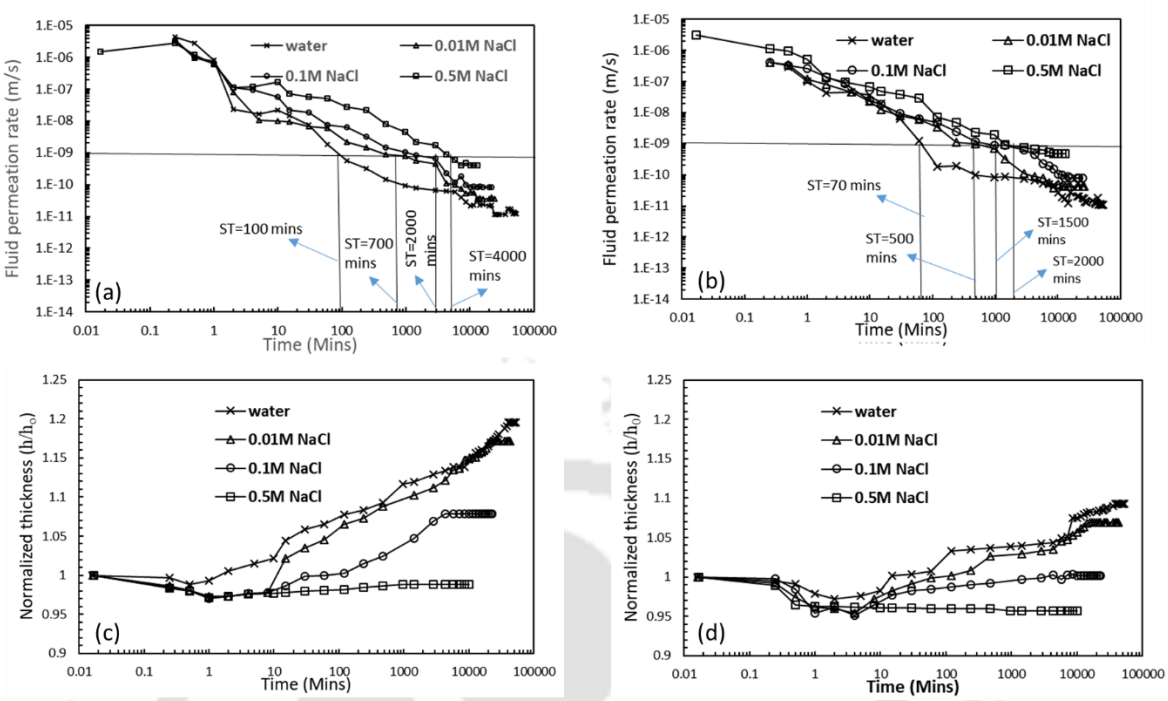

Figure 6.1: Temporal variation of the fluid permeation rate for the GB in water and various concentrations of NaCl under the stress of (a) 50 kPa (b) 100 kPa; variation of h/ho in the water and various concentrations of NaCl under the stress of (a) 50 kPa, (b) 100 kPa

The temporal variation of the permeation rate of water and KCl of varied concentrations through the compacted GB under the applied stresses of 50 and 100 kPa was presented in Fig. 6.2a and Fig. 6.2b, respectively. The estimated ST for the GB in the presence of 0.01M and 0.1M KCl under the applied stress of 50 kPa was 1500 minutes and 3600 minutes, respectively, which were significantly higher than the ST achieved in the presence of similar concentrations of NaCl. Further, a poor sealing was exhibited by the GB in the presence of 0.5M KCl at 50 kPa mechanical stress as complete sealing of inter-granular voids could not be achieved (Fig. 6.2a). On the other hand, when the tests were performed at higher mechanical stress (100 kPa), the sealing performance of the GB improved slightly in the presence of all the studied concentrations of KCl. Interestingly, under applied stress of 100 kPa, the inter-aggregate pores present in the GB got sealed in the presence of 0.5M KCl, but only after 5040 minutes (Fig. 6.2b).

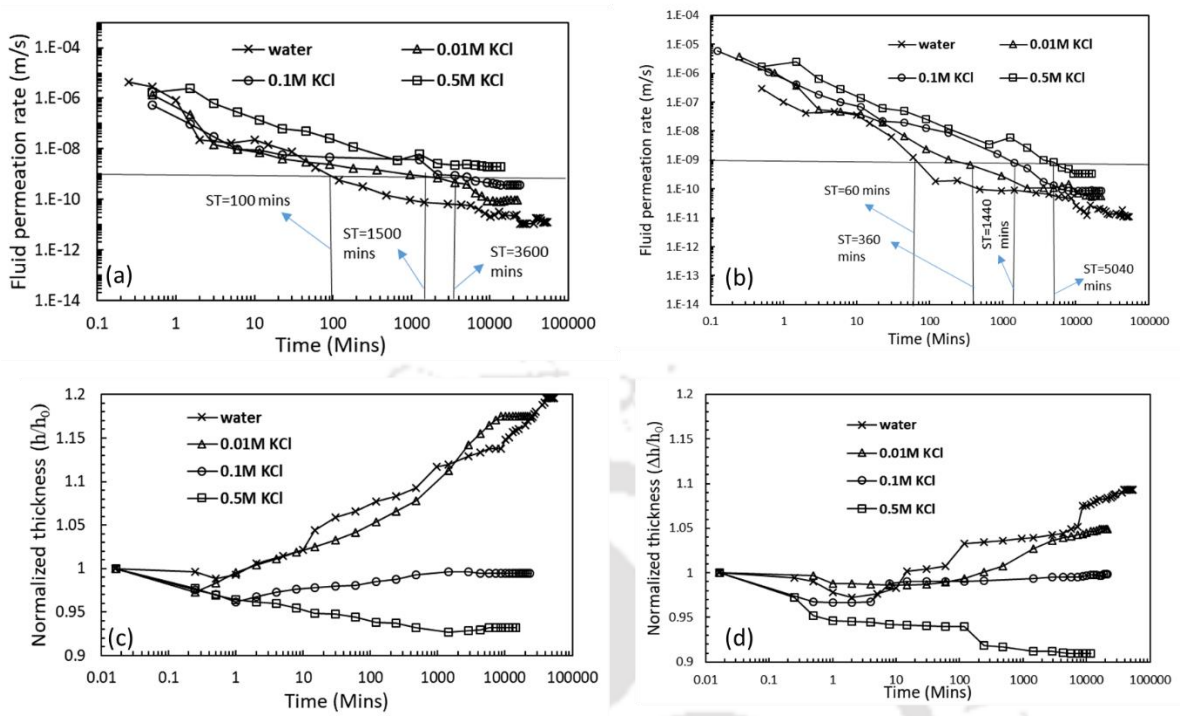

Figure 6.2: Temporal variation of the fluid permeation rate for the GB in water and various concentrations of KCl under the stress of (a) 50 kPa (b) 100 kPa; variation of h/ho in the water and various concentrations of KCl under the stress of (a) 50 kPa, (b) 100 kPa

The comparison of the temporal variation of the normalized thickness of the GB in the presence of water and different KCl concentrations under the applied stresses of 50 kPa and 100 kPa was presented in Fig. 6.2c and Fig. 6.2d, respectively. The GB swelled appreciably after the initial collapse in the presence of a lower concentration (*n=0.01M*) of KCl with an equilibrium normalized thickness of 1.17. However, the swelling was minimal in the presence of 0.1M KCl, with an equilibrium normalized thickness of ~0.99. Further, the GB in the presence of 0.5M KCl experienced considerable collapse for a large duration, and a marginal swelling was observed only after 2000 minutes. At the time of termination of the test, the normalized thickness for the GB on its exposure to 0.5M KCl was 0.95 (Fig. 6.2c). On the other hand, in the presence of 0.01M and 0.1M KCl, the amount of swelling for the GB was significantly reduced under the mechanical stress of 100 kPa in comparison to lower mechanical stress of 50 kPa. The normalized thickness for the GB in the presence of 0.01M and 0.1M KCl was ~1.05 and 1.01, respectively under 100 kPa stress. However, the normalized thickness for the GB on its exposure to 0.5M KCl under 100 kPa mechanical stress was ~0.92 indicating a collapse (Fig. 6.2d).

A detrimental effect in terms of the sealing behaviour of the GB was observed in the presence of $CaCl_2$ as the permeant fluid for the considered stresses (Fig. 6.3a-6.3b). The compacted GB in the presence of 0.1M $CaCl_2$ solution, could not seal the inter-granular voids under 50 kPa stress. However, under applied stress of 100 kPa and in the presence of 0.1M $CaCl_2$, the GB was able to seal, but only after 5000 minutes. (Fig. 6.3b). Further, in the presence of 0.5M $CaCl_2$, the larger voids present in the GB could not seal even at higher mechanical stress of 100 kPa and the permeation rate was very high (> $1x10^{-9}$ m/s). As the lower concentration of the pore-fluid does not cause a damaging influence on the GB in terms of the swell and sealing ability, the test with 0.01M $CaCl_2$ was not reported.

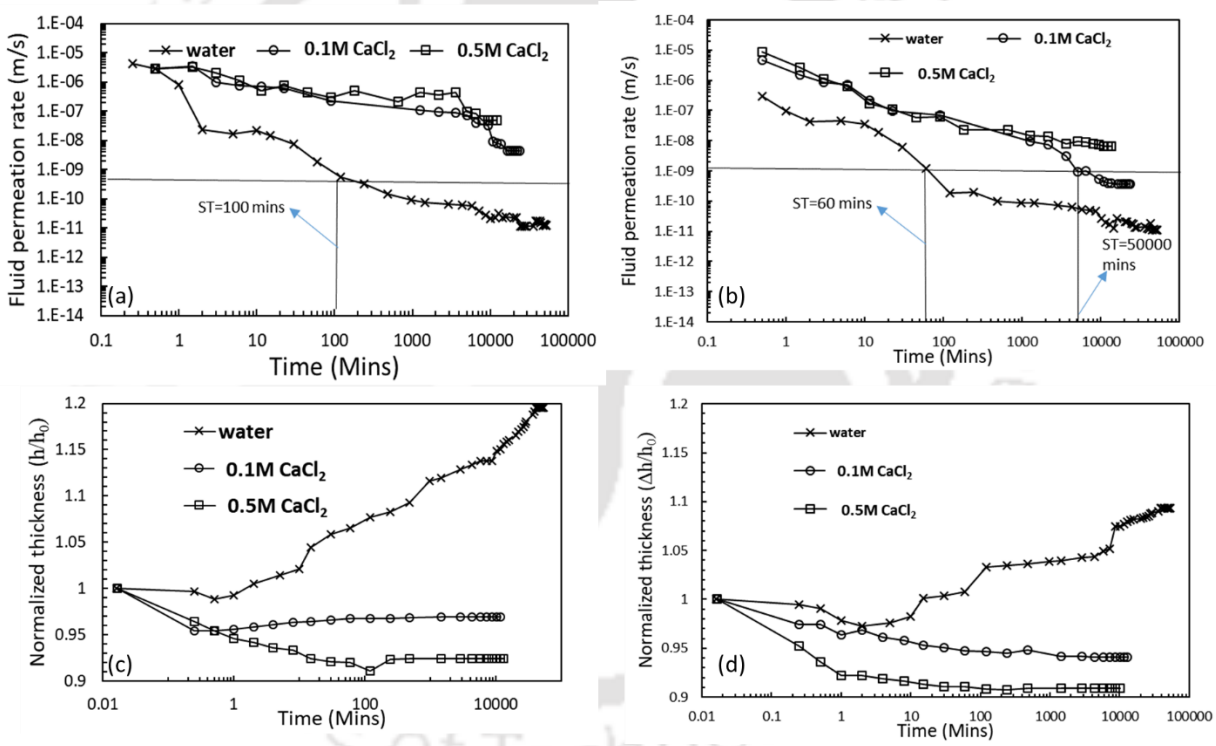

Figure 6.3: Temporal variation of the fluid permeation rate for the GB in water and various concentrations of CaCl2 under the stress of (a) 50 kPa (b) 100 kPa; variation of h/ho in the water and various concentrations of CaCl2 under the stress of (c) 50 kPa, (d) 100 kPa

The GB exhibited a negligible swelling in the presence of 0.1 M and 0.5 M $CaCl_2$, similar to the earlier case where KCl was the permeating fluid. However, the sealing could not be achieved even in the presence of 0.1M. A significant collapse was observed under 50 kPa stress (Fig. 6.3c). Although the GB could seal under 100 kPa stress, but a significant collapse

was observed in comparison to the test performed under 50 kPa stress. Similarly, the maximum collapse was observed under the applied stress of 100 kPa in the presence of 0.5M with a normalized thickness of ~0.905 (Fig. 6.3d).

6.3 Discussion

6.3.1 *Microstructural analysis*

The type and concentration of the permeating fluid played a significant role in influencing the sealing and swelling ability of the studied GB. The experimental results revealed that the individual granules were able to swell appreciably to seal the inter-granular voids in the presence of only water and low ionic strength salt solutions (*n=0.01M*). However, the ST of the GB increased and the swelling potential dropped significantly in the presence of higher salt concentrations. However, a detrimental effect was observed by the permeation of 0.5M KCl and $CaCl_2$ solutions and under the 50 kPa overburden stress. In order to understand the behaviour of the studied GB in the presence of various pore-fluids, the microstructure was studied using Field Emission Scanning Electron Microscope (FESEM). The FESEM image of the GB layer post permeation with water and 0.5M KCl under 50 kPa stress was shown in Fig. 6.4a and Fig. 6.4b, respectively. The GB in the presence of water showed (Fig. 6.4a) complete closure of pores due to fully expanded mineral sheets. On the other hand, the GB was characterized by granules of size 20-100 μm and large size inter-granular voids of size 21-31 μm in the presence of high KCl concentration (Fig. 6.4b).

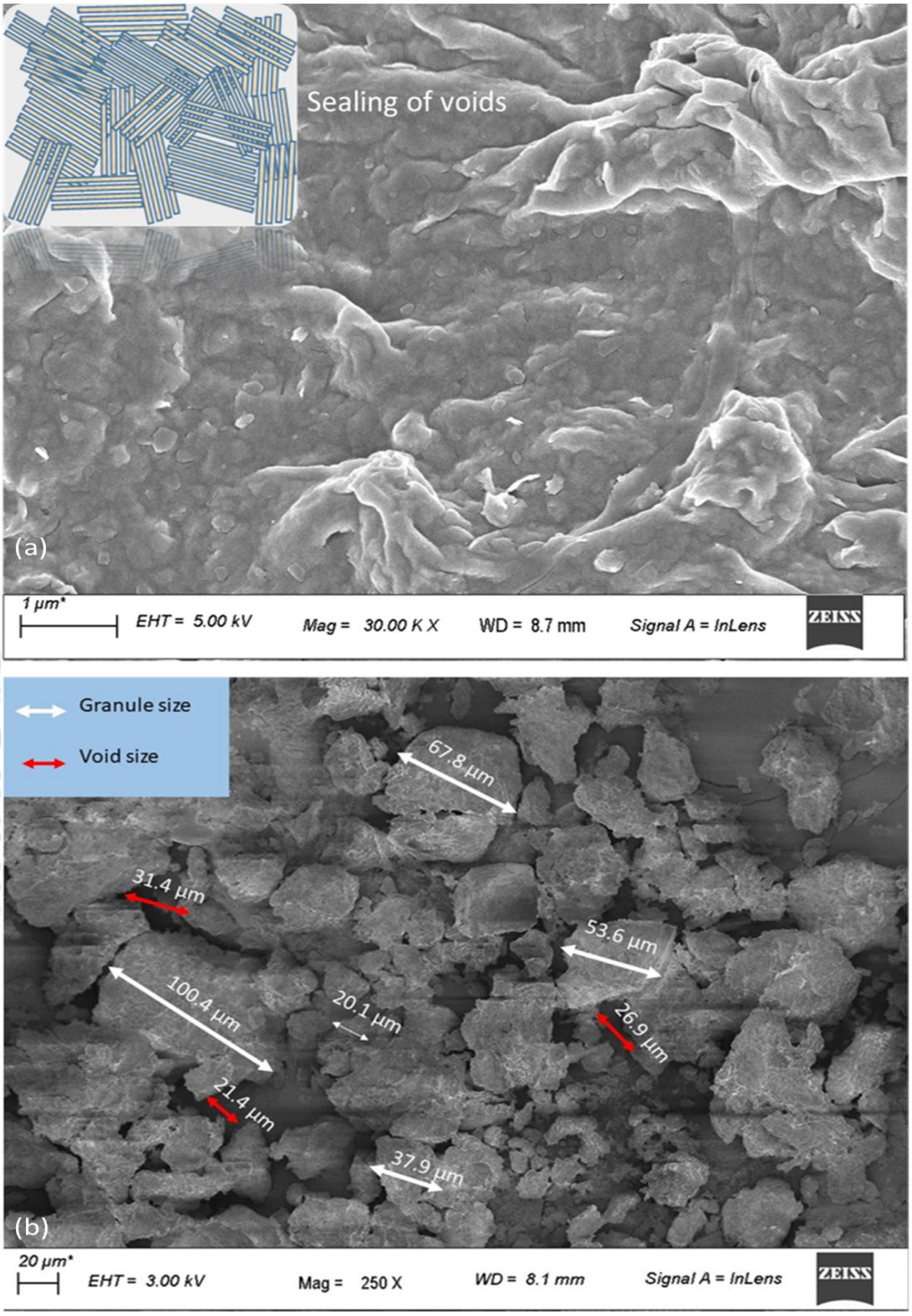

Figure 6.4: FESEM image of GB as an individual layer (a) in the presence of water, (b) in the presence of 0.5M KCl

The aggregates of GB are bonded by vander Waals forces at the dry state. Upon hydration with water or a lower concentration of salts, the developed repulsive forces between the hydrated particles dominated the vander Waals forces and allow the aggregates/granules to disintegrate into smaller particles (Bharat and Sridharan, 2013; Bharat and Das, 2017; Das and Bharat, 2021). The disintegrated, hydrated clay particles swell into the inter-granular voids and restricted the flow of pore-fluids thereby maintained the hydraulic conductivity to $<10^{-9}$ m/s. The specimen exhibited macroscopic swelling once the inter-granular and inter-aggregate voids were completely sealed (Fig. 6.5). However, in the presence of high salt concentration (here, 0.5M KCl), the inter-granular voids could not be sealed. The inability of the large-sized granules to disintegrate into individual particles in the presence of higher salt concentrations was understood to be the primary reason behind the poor sealing ability of the GB. The GB remained in the form of granules when exposed to such high pore-fluid concentrations (Fig. 6.5). Therefore, the GB in the presence of a higher KCl and $CaCl_2$ concentrations showed a negligible sealing and swelling ability under the studied mechanical stresses.

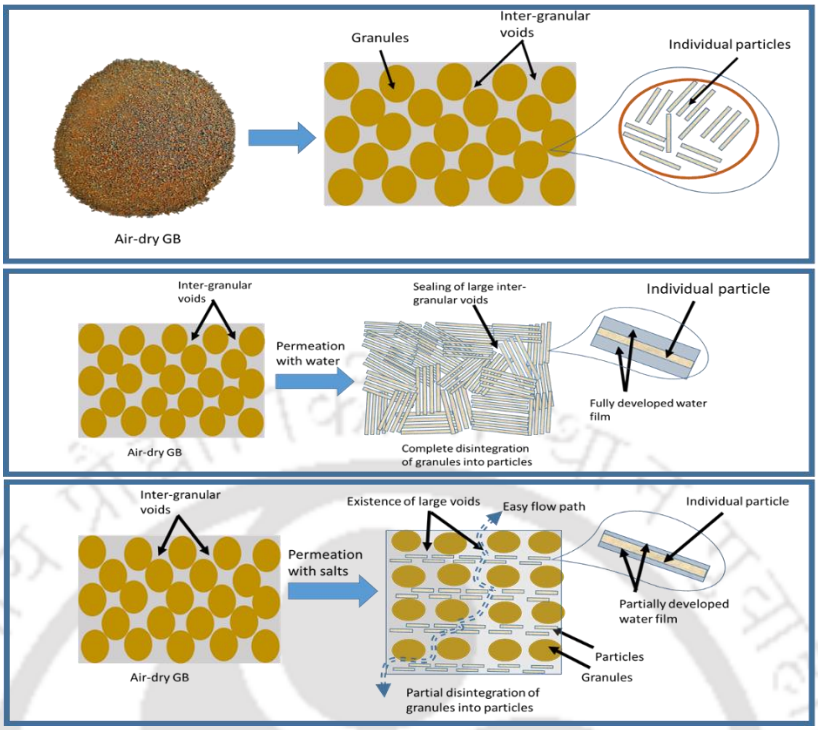

Figure 6.5: Illustration depicting complete and partial disintegration of the granules into particles in the presence of water and salts, respectively

The experimental results from the present study also revealed that the ST reduced slightly and the performance of the GB was improved when the tests were conducted at 100 kPa mechanical stress. The GB in the presence of KCl (*n=0.5M*) and under applied stress of 50 kPa, was not able to undergo complete sealing, however, for the similar pore-fluid, the GB could seal under 100 kPa stress, although at a much later stage of the test. This was due to the assistance of higher mechanical stress in disintegrating the granules against the van der Waals forces. Further, it was observed that the swelling of the GB was initiated after an initial collapse in the presence of all the studied permeants. In the initial phase of the permeation of the GB, the diffused double layers around the particles due to the disintegration of the large granules are not fully developed. Therefore, under the applied stress condition the GB collapsed initially. However, with time, the diffused double layers around the particles were fully formed resulting in swelling of the soil after the initial collapse. On the other hand, in the presence of higher ionic strength solutions of KCl and $CaCl_2$ solution, swelling of the GB after the initial collapse was negligible and more strikingly under the application of 100 kPa stress. This was primarily due to the swelling

pressure of the GB in the presence of a higher concentration of KCl and $CaCl_2$ was lesser than the applied stresses and therefore the collapse was observed.

6.4 Salient observations

- The volume change behaviour and the sealing ability of the compacted granular bentonite were found to be dependent on the cation type, salt concentrations, and the overburden stress
- In the presence of water and a low concentration of a salt solution, the sealing was achieved very quickly. On the other hand, with an increase in the concentration of the permeating fluid, the ST significantly increased.
- Under 100 kPa mechanical stress, the performance of the GB slightly improved in terms of its sealing. However, in the presence of 0.5M KCl and 0.5M $CaCl_2$, the sealing could not be achieved even at 100 kPa mechanical stress. Further, the collapse of the GB in the presence of 0.5M KCl and 0.5M $CaCl_2$ under 100 kPa was more in comparison to the lower mechanical load as the swelling pressure of the GB in the presence of such fluids is lesser than the applied stress.
- The granules were able to disintegrate into individual particles and hence the self-sealing of the GB was achieved at a lower concentration. However, at higher concentrations, the GB could not seal, particularly in the presence of 0.5M KCl and 0.5M $CaCl_2$ at both the stress conditions.
- Significant swelling after an initial collapse was observed for the GB in the presence of water or low concentrations of the studied salt solutions. However, at higher concentrations, the GB showed negligible swelling and collapse was more predominant. Such high collapse is undesirable for the landfill liners as it can cause instability of the landfill slope.

Chapter 7

Kaolin as a protective barrier layer for solid waste landfills

7.1 General

The experimental results from the previous chapter reveal that the sealing ability of the GB was completely lost upon permeation with higher ionic strength salt solutions and under low overburden stress (50 kPa). Moreover, the GB exhibited collapse in the presence of high ionic strength solutions. The applicability of the GB in the form of geosynthetic clay liners as a bottom liner facility in a higher saline environment, therefore, remains a serious concern. The inability of the GB to self-seal in the presence of high ionic strength salt cations would allow easy mobility of other companion ions (as seen in Chapter 5) and also numerous viral pathogens or other companion ions that exist in the landfill due to the disposal of pathogen-contaminated bio-medical waste in recent years. Further, the excessive collapse of the GB can lead to fatal consequences in terms of landfill slope instability.

The applicability of kaolin as a protective layer to the GB was explored, for the first time, to enable the GB to seal to the full potential. Some of the available literature suggests that kaolin exhibit strikingly contrasting behaviour in comparison to the bentonite due to interaction with different pore-fluids. The plasticity of kaolin increase with increased salt concentration, which consequently decreases the hydraulic conductivity (Sridharan et al., 2000; Sridharan, 2014; Li et al., 2013) due to the sorption ability of the termination sites. Moreover, the volume change behaviour of the kaolin in the presence of pore-fluids is found to be opposite in comparison to the bentonite (Choudhury and Bharat, 2018). Therefore, kaolin was considered in this study for potential use as an additional barrier layer to improve the efficiency of GB in the presence of higher salt concentrations.

The proposed barrier system comprising of a densely compacted layer of kaolin (ρ_d=1.6 Mg/m^3) placed over the GB. The recent study reveals that kaolin collapses at lower compaction densities, however, at higher compaction density the kaolin exhibits swelling behaviour under high ionic strength solutions (Choudhury and Bharat, 2018) which is desirable in the field. Moreover, it needs mention here that the maximum dry density (MDD)

of the studied kaolin is ~1.6, which can be achieved in the field by adding the optimum moisture content (OMC). For the present study, a more conservative condition was considered where the kaolin was compacted in the dry condition. Placing the kaolin layer at MDD and OMC state for the laboratory experiments would result in the sealing of the GB layer due to moisture diffusion, and the sealing and swelling ability of the layered system in the salt environment would not be possible.

The present chapter highlights the influence of different permeant fluids on the un-hydrated kaolin-GB system under different applied stresses. The comparison of the swelling and sealing property of the single GB layer and the kaolin-GB layered system under applied stress of 50 kPa was studied in this chapter. As a more detrimental effect on the sealing and swelling ability of the GB in the presence of 0.5M KCl and 0.5M $CaCl_2$ under lower applied mechanical stress (50 kPa), the behaviour of the kaolin-GB layered system was studied under these extreme conditions. Further, the diffusion behaviour of the kaolin-GB layered system in the presence of high concentration salt solution was evaluated and compared with the single layer of compacted granular bentonite under similar conditions.

7.2 Result and discussion

7.2.1 *Sealing and swelling ability of the compacted kaolin-GB layered system*

The temporal variations of fluid permeation rate through a single GB layer and kaolin-GB layered system were presented in the presence of high ionic strength salt solutions (*n=0.5M*) under 50 kPa applied stress in Fig. 7.1 (a-c). The ST was considerably less for the kaolin-GB layered system in comparison to the individual GB layer for any given salt solution. The individual GB layer took ~4000 minutes to seal under the influence of NaCl solution, but the kaolin-GB layered system could undergo sealing in 800 minutes (Fig. 7.1a). Similarly, the kaolin-GB layer took ~900 minutes and 1540 minutes to seal the inter-granular voids in the presence of 0.5M concentration of KCl and $CaCl_2$, respectively, while the individual GB layer could not seal under similar conditions (Fig. 7.1b-7.1c).

Further, the temporal variation of the normalized thickness of GB alone and the kaolin-GB layered system was presented in Fig. 7.2 (a-c). In the presence of 0.5M NaCl solution, the kaolin-GB layer showed a considerable amount of swelling after a period of ~200 minutes.

On the other hand, the individual GB did not swell after the initial collapse (Fig. 7.2a). Moreover, the kaolin-GB layered system experienced a relatively lesser collapse, and slight swelling was observed after ~500 minutes with an equilibrium normalized thickness of ~1 in the presence of 0.5M KCl and $CaCl_2$ (Fig. 7.2b-7.2c). However, under similar conditions, the individual GB layer showed collapse behaviour for a large duration of the test and the equilibrium thickness at the time of termination was 0.95 and 0.93 in the presence of 0.5M KCl and $CaCl_2$, respectively.

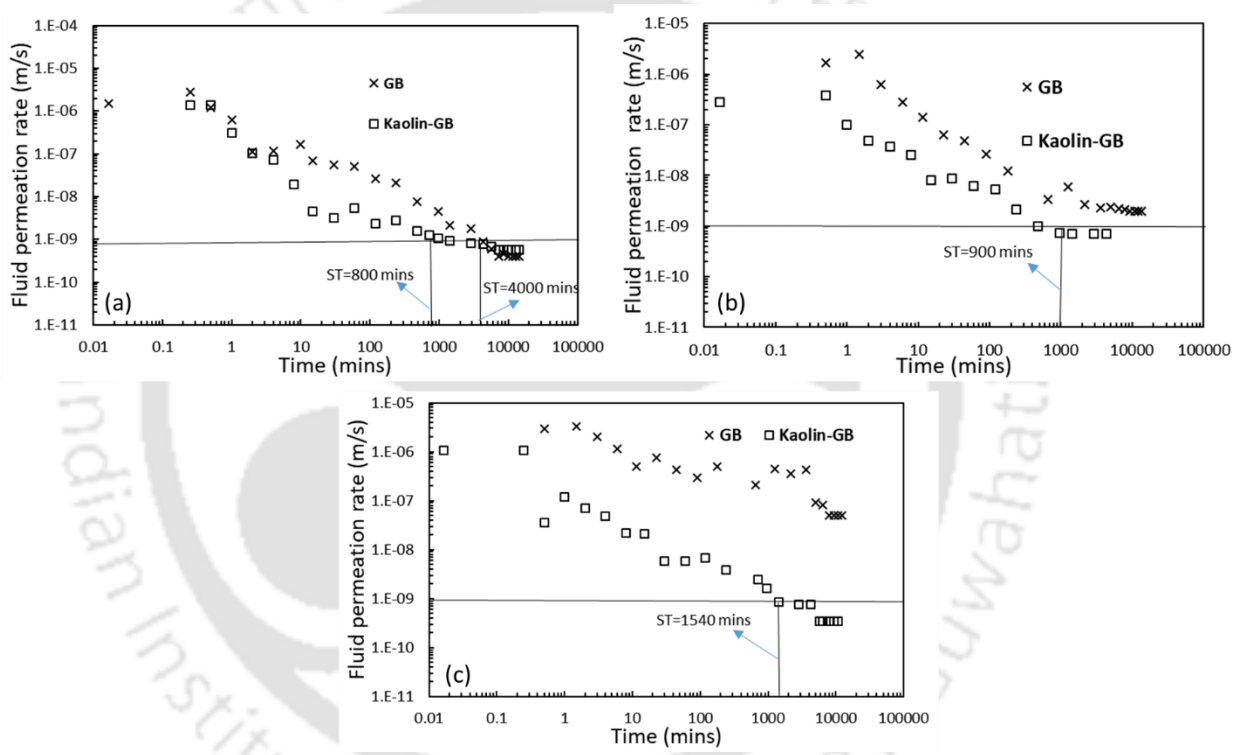

Figure 7.1: Comparison of the temporal variation of the fluid permeation rate for the GB and Kaolin-GB layered system in the presence of 0.5M concentration of (a) NaCl; (b) KCl, (c) $CaCl_2$ under applied stress of 50 kPa

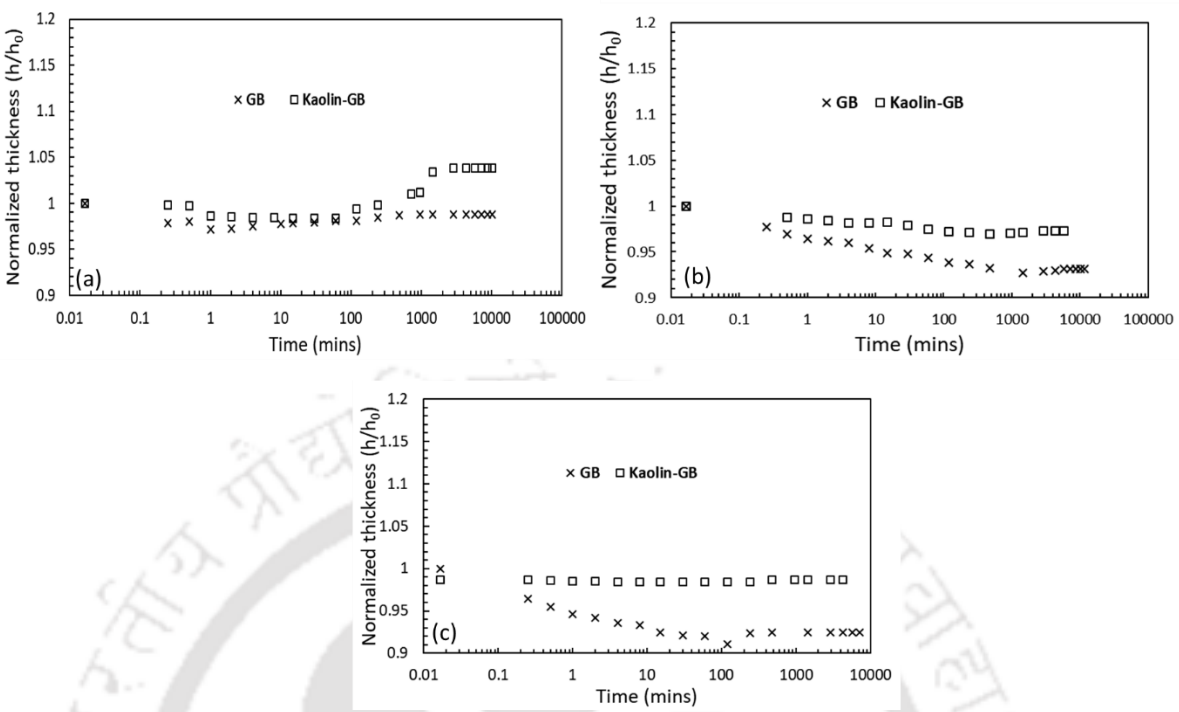

Figure 7.2: Comparison of the temporal variation of the normalized thickness for the GB and kaolin-GB layered system in the presence of 0.5M concentration of (a) NaCl; (b) KCl, (c) $CaCl_2$ under applied stress of 50 kPa

7.2.2 *Microstructural and elemental compositional analysis*

The sealing ability for the kaolin-GB layered system improved significantly even in the presence of higher concentrations of KCl and $CaCl_2$ and lower mechanical stress. In order to understand the behaviour of the studied kaolin-GB layered system in the presence of various pore-fluids, the microstructure and elemental compositional analysis were performed using Field Emission Scanning Electron Microscope (FESEM) the Energy-Dispersive X-ray (EDX) spectroscopy, respectively. The FESEM image of the GB in the kaolin-GB layered system after equilibration with 0.5M KCl indicated that the granules disintegrated into smaller particles and the particle size varied in the range of 0.173-0.263 μm (Fig. 7.3a). The sealing ability of the GB in the kaolin-GB layered system in the presence of 0.5M KCl was comparable to the individual GB layer in the presence of water (Fig. 7.3b).

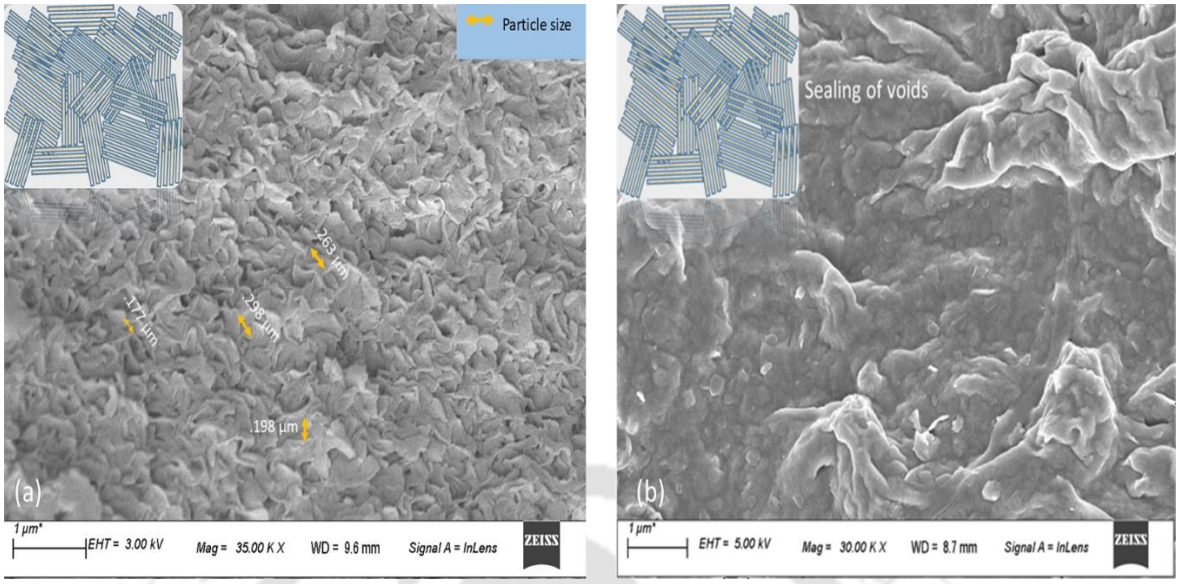

Figure 7.3: (a) Sealing of the GB layer of the kaolin-GB layered system in the presence of 0.5M KCl, (b) Sealing of the individual GB layer in the presence of water

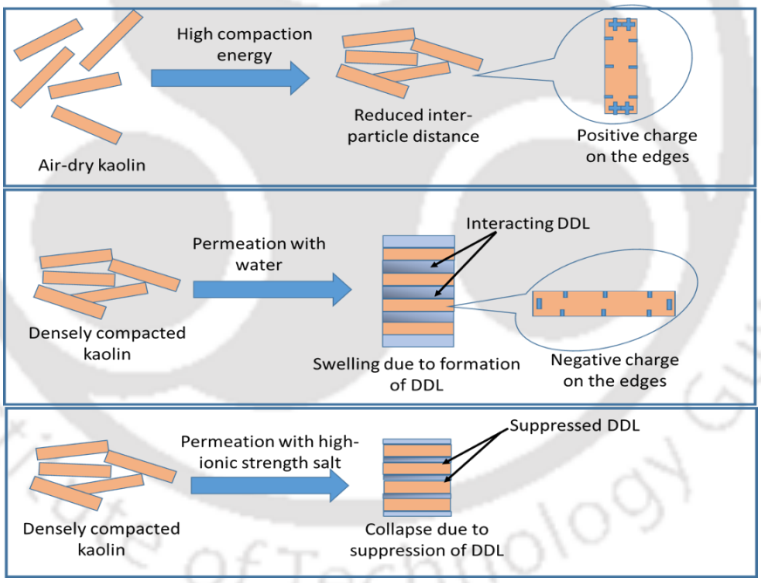

Figure 7.4: Particle orientation of kaolin in the presence of water and high-ionic strength salt solution

The microstructural analysis shows an overall improvement in the sealing behaviour due to the placement of the kaolin layer over the GB. The combination of coulombic and van der Waals' forces predominantly infuences the compacted kaolin behaviour under chemo-mechanical loadings. The higher compaction effort at air-dry kaolin signifcantly increases

the attractive forces while reducing the inter-particle distances. Kaolin hydration by water alters the positive charges to negative on the particle edges and nullifes the coulombic attraction between the basal face–edges (Choudhury and Bharat, 2018). A DDLs formation around the hydrated kaolinite particles in densely compacted kaolin results in osmotic pressure development and subsequent macroscopic swelling (Fig. 7.4). The presence of high ionic strength salts suppresses the diffuse double layer thickness similar to GB and exhibited slight collapse. However, the observed collapse is smaller due to smaller inter-particle distances and thinner DDLs due to the smaller surface charge density of kaolinite.

Elemental analysis of different layers under different chemo-mechanical conditions was undertaken to understand the effect of kaolin inclusion on the sealing ability of adjacent GB layer under high salt concentrations. The adsorption potential of kaolin for the potassium salts was analyzed by EDX spectroscopy for the kaolin sample present in the kaolin-GB layered system after the self-sealing test with 0.5M KCl. The EDX spectra of the kaolin sample as part of the kaolin-GB layered system was presented in Fig. 7.5a. The percentage range of various elements in the kaolin sample was analyzed in the adequate voltage range and was also presented. The spectra was characterized by distinct peaks for oxygen (O), silicon (Si), and aluminum (Al), indicating the presence of gibbsite and silicate sheets in the studied kaolin. Apart from the structural elements, the kaolin in the kaolin-GB layer exhibited a high peak for potassium (K^+) with a weighted percentage of 3.8. On the other hand, the EDX spectra of the kaolin sample in its natural condition showed a negligible peak for potassium with a weight percentage of 0.2 (Fig. 7.5b). It showed the excellent adsorption affinity of kaolin for K^+ ions upon permeation with 0.5M KCl solution. Moreover, a very high peak for potassium with a weight percentage of 5.6 was observed for the individual GB layer post permeation with 0.5M KCl. But, under a similar condition, the weight percentage of potassium for the GB sample of the kaolin-GB layer reduced to 2.7, indicating lesser adsorption from the reduced concentration of the permeant that was allowed in the GB layer (Fig.7.5c-7.5d). The EDX results, therefore, confirmed that the kaolin in the kaolin-GB layered system adsorbed a significant amount of the potassium in the presence of 0.5M KCl due to the formation of inner-sphere complexes while the underlying GB layer underwent complete sealing. The adsorption of the monovalent and divalent cations to form inner-sphere complexes occur mostly in the edge sites of the kaolin minerals where the broken

edges (silanols) and aluminium hydroxyls present (Jorgen, 2002; Vascencelos et al., Li et al, 2015; Matlok et al., 2015; Doi et al., 2020). Due to the adsorption of the salt cations on the edge of kaolin soil, it allowed only the reduced concentration of the permeant into the GB layer. The reduced concentration of the permeant makes it possible for the GB layer to seal the inter-granular voids completely. Complete closure of the inter-granular voids enables the GB layer to allow only diffusion mechanism for the ion transport and makes it suitable for slowing down the contaminant migration rates significantly.

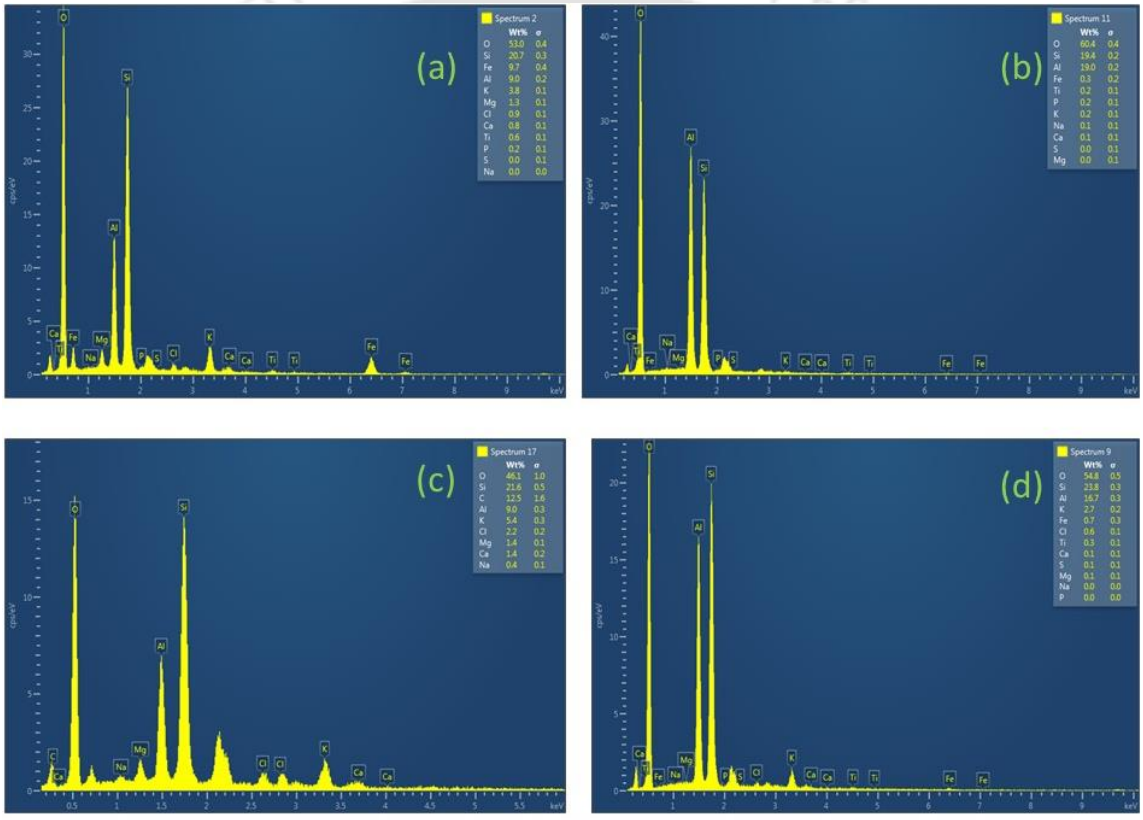

Figure 7.5: EDX spectra post permeation with 0.5M KCl for (a) kaolin sample in the kaolin-GB layered system, (b) kaolin sample in the natural condition, (c) Individual GB layer. and (d) GB sample of the kaolin-GB layer

Thus the sealing of the kaolin-GB layered system was achieved even at high ionic strength salt solutions, while the GB layer alone failed to seal under similar conditions. It is, however, worth noting that the individual kaolin would not achieve the permeation rate $<10^{-9}$ m/s in low concentration pore-fluid/water and would not be suitable as a liner material. Therefore,

the combination of kaolin and the GB as a layered system was able to perform satisfactorily in adverse conditions such as high salt concentrations and low mechanical stress. Moreover, the kaolin-GB layered system showed swelling behaviour after a period of ~500 minutes and the magnitude of the initial collapse was also considerably reduced for the proposed kaolin-GB layered system even in extreme saline conditions. The proposed layer system should be adapted in the landfills as the inability of the GB to self-seal in the presence of high salt concentrations would allow easy mobility of numerous viral pathogens.

7.2.3 *Diffusion characteristics of the compacted kaolin-GB layered system*

Salt diffusion through the compacted kaolin-GB layered system was also performed to evaluate the diffusion characteristics of such layered systems. The diffusion behaviour of the kaolin-PB layered system in the presence of salt solutions is expected to be similar to the kaolin-GB layered system as both PB and GB under saturated conditions exhibit similar diffusion characteristics.

As the compacted PB and GB were found to exhibit higher D_e in the presence of aggresive salt concentrations (n>0.1M), the diffusion behaviour of the kaolin-GB layered system was evaluated for the studied salts (LiCl, NaCl, and KCl) having a concentration of 0.5M. The temporal variation of the theoretical concentration plots of 0.5M LiCl, 0.5M NaCl, and 0.5M KCl through the kaolin-GB layered system was shown in Fig. 7.5 a-c. The estimated model parameters obtained by inverse analysis through CONTRADIS was also presented. It was observed that the migration rate through the layered system was significantly reduced for all the salts in comparison to the individual layer. A significant reduction was observed in the presence of NaCl and KCl solutions. Further, the estimated D_e was found to be much less for the kaolin-GB layered system compared to the case when only GB was used as an individual layer (Fig. 7.5 c-d). The maximum reduction in the D_e was observed in the presence of NaCl and KCl solution. Moreover, the R_d was relatively higher for the kaolin-GB layered system in comparison to the individual GB layer, indicating a higher amount of sorption.

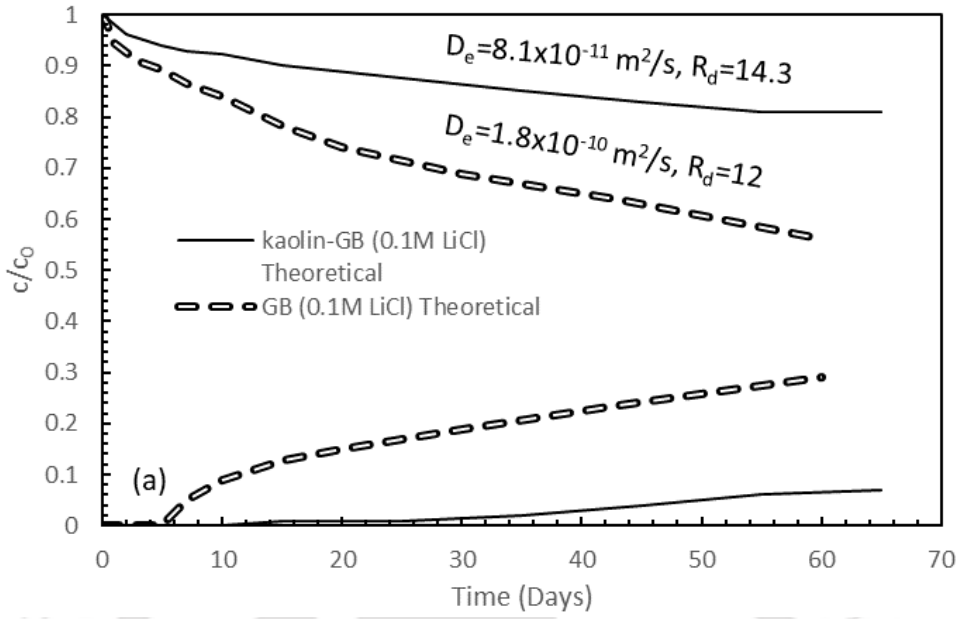

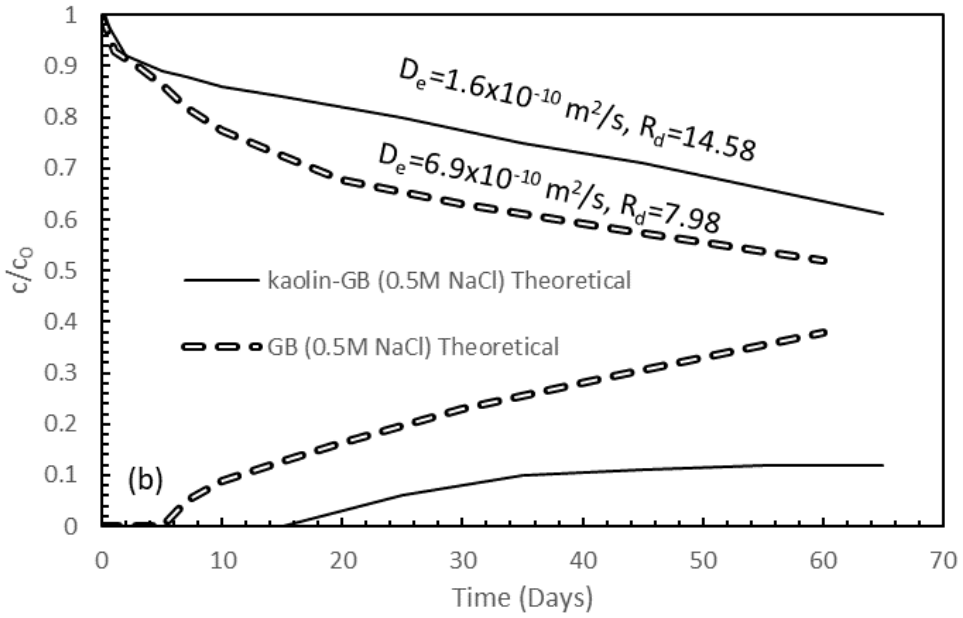

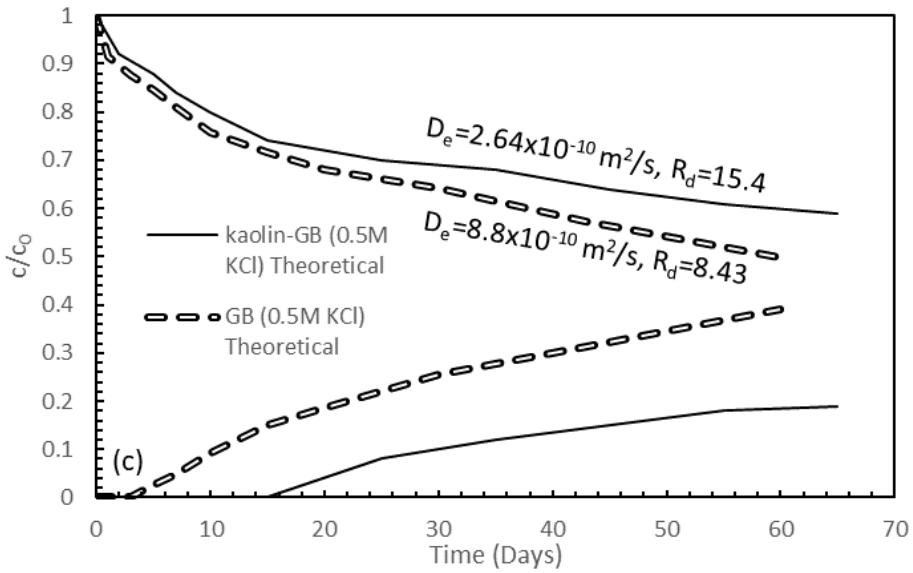

Figure 7.6: Comparison of the theoretical concentration profile through the individual GB and kaolin-GB layered system in the presence of (a) 0.5M LiCl, (b) 0.5M NaCl, (c) 0.5M KCl

Apart from the tortuous pathway through densely compacted kaolin in the kaolin-GB layered system, the high adsorption of the salt cations on the edges of kaolinite contributed to the overall reduction in the migration rate of the solute. As the diffusion of the solute occurred through the kaolin layer first it allowed only a reduced concentration of the salt ions into the GB layer. Under such a reduced concentration of the salt ions, the DDL thickness does not get suppressed significantly during the cation exchange process. Hence, the overall flow path for the diffusing ion is limited resulting in a lesser D_e for the layered system in comparison to an individual GB layer. Moreover, the higher R_d was due to the combined adsorption ability of both the layers for the salt cations.

7.3 Salient observations

- The sealing and swelling ability were improved significantly with the addition of a kaolin layer above the GB. Even upon permeation with a higher concentration of KCl and $CaCl_2$, the underlying GB in the kaolin-GB layered system was able to seal.

- For a higher concentration of the pore-fluid, the proposed layered system showed swelling after initial collapse compared to the individual GB layer which did not experience any swelling.
- The microstructural and elemental compositional analysis indicated that the top kaolin layer behaved as a protective layer for the underlying GB by allowing a reduced concentration of the permeant into the GB.
- The D_e for the compacted kaolin-GB layer was very less in comparison to the single GB layer indicating a more tortuous pathway. Moreover, the R_d for the layered system was also very high suggesting higher adsorption.

Chapter 8

Qualitative assessment of Clay Mineral Attenuation Capacity for Human Viral Pathogens

8.1 General

The previous chapters discussed the fate of inorganic salt cations through the compacted bentonite clays. It was seen that the performance of the bentonite-based liner system could be significantly improved by the addition of a kaolin layer on top of the PB/GB layer. However, apart from the salt leachates, clay-based barrier systems are expected to attenuate several other contaminants, including the toxic and hazardous viral pathogens as the current guidelines adopted by most of the countries to curb this passive transmission of the contagious viruses rely on landfilling. The attenuation potential of the bentonite-based barriers for the virus-contaminated solid waste is unknown till now.

In this chapter, the effectiveness of compacted clay-based barrier systems was qualitatively assessed for the encapsulation of virus-contaminated biomedical waste (BMW) for the first time. The existing data of the virus interaction with the montmorillonite and kaolinite minerals from the batch-sorption studies for drug delivery applications were utilized to understand the diffusion behaviour of the clay minerals in the presence of the human viral pathogens. The model parameters essential for designing such virus-contaminated BMW containment facilities, viz., effective diffusion coefficient (D_e), and retardation factor (R_d) for different clay minerals were evaluated for the first time based on the available limited data on some common pathogens that might enter the landfills. The model parameters were utilized to understand the attenuation of various viral pathogens (Coronavirus, poliovirus, and reovirus), and bacteriophages (MS2 and φx-174) in montmorillonite and kaolinite mineral barriers under various conditions.

8.2 Characteristics of the studied pathogens

The common viral pathogens which cause disruptions to the human CNS, viz. coronavirus, poliovirus, and reovirus were considered in the present study for understanding their sorption

behavior on the clay minerals. The adsorption and transport characteristics of phage viruses viz., MS2, and φx-174 were also studied to understand the applicability of such phages in predicting the behaviour of the human viruses. The surface morphology of φx-174 is characterized by a single-stranded DNA with an outer protein coat. On the other hand, the other studied pathogens are characterized by inner single/double-stranded RNA encapsulated by a protein coat.

The amino acid of the protein envelope/coat comprises of various hydrophobic and hydrophilic groups. The hydrophobic groups of the virus surface determine the extent of the virus interaction with other charged particles. The nature of the amino acid chain in the outer protein coat for different viruses varies in their hydrophobicity, and the hydrophobicity is expected to be higher due to the non-polar amino group of the protein capsid (Israelachvili, 2011; Armanious et al., 2016). The non-polar amino acid chain of the virus-protein undergoes unfolding in an aqueous environment due to the induced tensile stress from the fluid, exposing the hydrophobic group, which otherwise remains shielded. The presence of hydrophobic groups in the protein capsid gives the virus an impetus to interact with other hydrophobic charged particles. Apart from the hydrophobicity, the interaction of viral pathogens with any charged particles is also pH-dependent due to the amphoteric nature of the virus surface (Burge and Enkiri, 1978; Gerba, 1984).

8.3 Clay mineral characteristics

Two prominent naturally available clay minerals, viz., montmorillonite and kaolinite, are considered for understanding the sorption and diffusion behaviour for attenuating different studied human pathogens. As the surface properties of the studied clay minerals are not available, the assessment was only qualitative. Both montmorillonite and kaolinite mineral exhibit contact angle (β) hysteresis, wherein the clay minerals are hydrophilic in nature in an aqueous environment with β=0° (complete wetting) during the wetting and exhibit hydrophobicity during drying with $\beta\approx$65°. The contact angle increases significantly by the exclusion of water exclusion from the clay surface during the clay-pathogen interaction and is found to be exhibiting hydrophobic characteristics (Chrysikopoulos and Syngouna, 2012). Although the siloxane layer in the clay mineral is hydrophobic at $\beta\approx$65°, the surface is

wetting (β<90°), for the formation of a diffused double layer in the presence of water. Such characteristics of the clay minerals govern their interaction with other hydrophilic and hydrophobic biological entities (Stotzky, 1985; Yu et al., 2013).

In the clay-based compacted barrier systems, the virus transport is governed by the diffusion mechanism due to the low saturated hydraulic conductivity for clay minerals if all the inter-granular voids are sealed in the presence of a protective kaolin layer. As diffusion is a slow process, where sufficient time is available for the virus to interact with the clay minerals, the equilibrium sorption data provide an accurate assessment of the virus sorption potential on the clay minerals. During the virus-clay mineral interaction, the equilibrium sorption data are often studied using the batch equilibrium tests for different applications, such as drug delivery applications. The experimental batch-test results from the available literature were utilized to evaluate the sorption potential of the compacted clay-based barrier systems in this study for the waste containment application

8.4 Equilibrium sorption isotherm for different human pathogens

Sorption isotherm represents a plot between the equilibrium liquid phase virus concentration (c_e) and the adsorbed virus per mass of the clay mineral (q_e). The amount of solute adsorbed (q_e) by the adsorbent material is obtained from the solution phase concentration difference as given by:

$$q_e = \frac{(c_0 - c_e) \times V_s}{w} \tag{8.1}$$

where w is the mass of the adsorbent material, V_s is the volume of the suspension, and C_0 is the initial concentration of the virus. For ease of comparison, the units of sorbed and equilibrium concentration of the viruses were consistently expressed in plaque-forming units (pfu). The liquid phase virus concentration is expressed in pfu/ml, and the adsorbed virus per mass of the clay was expressed as pfu/mg.

The sorption data for different pathogens viz., bovine-coronavirus (Clark et al., 1998), poliovirus (Vilker et al., 1983), reovirus (Lipson and Stotzky, 1983), MS2 (Stagg et al., 1977; Park et al., 2015), and φx-174 (Syngouna and Chrysikopoulos, 2010) were utilized from the

literature studies to establish the linear and non-linear sorption isotherm model parameters. The isotherm models provided the nature of the surface sorption for various types of viruses on both the studied clay minerals. The equation describing the linear sorption model is given by:

$$q_e = k_d c_e \tag{8.2}$$

The slope of the linear isotherm provides the distribution coefficient, K_d, which indicates the amount of virus sorbed on the clay mineral. The non-linear Freundlich isotherm model defining the relationship of active adsorption sites and their energies are given by (Freundlich, 1936):

$$q_e = k_f c^{\frac{1}{n}} \tag{8.3}$$

where k_f and $1/n$ are the relative retention capacity and the intensity of retention of the adsorbent material, respectively. The log-log form of Eq. 8.3 was used to obtain the parameters k_f and $1/n$ to evaluate the non-linear sorption behaviour. The linear variation of virus sorption with equilibrium concentration for all the studied viruses was shown in Fig. 8.1 along with the measured data. The measured data from the literature studies (Fig. 8.1) indicated that the retention capacity of the montmorillonite increased with the increase in the virus concentration. The linear isotherm model provided a good approximation to the measured data exhibiting the regression coefficient (R^2), which varied between 0.83-1 for the studied viruses. The sorption data for bovine-coronavirus was found to match with poliovirus data due to the similar surface morphology of the pathogens. The percent adsorption of polio and bovine-coronavirus on the montmorillonite mineral was ~95% and 99.99%, respectively, for the virus titer of 10^6 pfu/ml (Clark et al., 1998; Vilker et al., 1983). The adsorption behaviour of the bovine-coronavirus and human poliovirus being identical, the montmorillonite is also expected to be an excellent adsorbent for human coronaviruses (SARS-CoV, SARS-CoV-2) due to their similar hydrophobic characteristics. The limited available data and recent molecular dynamic simulations also supported this conclusion (Abduljauwad, 2020).

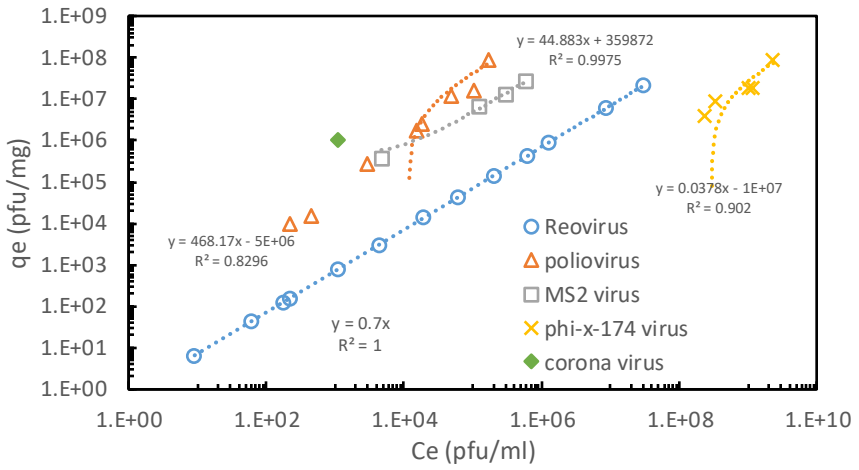

Figure 8.1: Equilibrium linear isotherm for different virus retention on montmorillonite

The distribution coefficient (K_d) for all the viruses obtained from the linear isotherm model was provided in Table 8.1. Among the studied viruses, the maximum K_d was found for poliovirus and MS2, indicating a very strong interaction with the montmorillonite surface. This observation further reaffirms that the coronavirus has a strong affinity for montmorillonite clay surface due to similar surface hydrophobicity as poliovirus. On the other hand, the sorption potential of reovirus and φx-174 was found to be negligible for montmorillonite having a very low K_d value in comparison to the other viruses.

Table 8.1: Sorption isotherm parameters for linear and Freundlich model

Virus	Montmorillonite			Kaolinite		
	Linear distribution coefficient, K_d (ml/mg)	Freundlich parameters		Linear distribution coefficient, K_d (ml/mg)	Freundlich parameters	
		K_f	$1/n$		K_f	$1/n$
Polio	468.17	5.54	1.33	-	-	-
MS2	44.88	224.38	0.8674	294.15	810027	0.4298
Reo	0.7	0.71	1	0.7	0.71	1
Φx-174	0.038	0.00067	1.17	0.0737	1.31	0.117
Corona	-	-	-	-	-	-

The experimental sorption data for the viruses were also fitted with the Freundlich isotherm model to understand the retention capacity of montmorillonite-rich clays for the different viruses (Fig. 8.2). The experimental data fitted well with the Freundlich isotherm model with the R^2 value ranging from ~0.92-1 for the studied viruses. The non-linear sorption parameters for the considered viruses obtained from the Freundlich isotherm model were also provided in Table 8.1. The retention capacity indicated by the non-linear model was qualitatively similar to the linear model, wherein the retention capacity for both the clay mineral was found to be low for reovirus and φx-174.

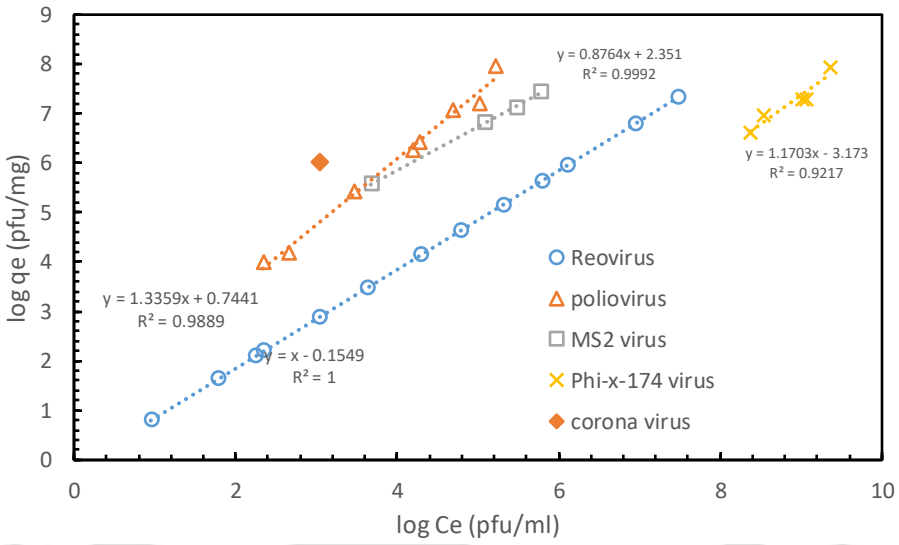

Figure 8.2: Equilibrium Freundlich isotherm for different virus retention on montmorillonite

The retention capacity of the montmorillonite-rich clays for different viruses varied due to the varied hydrophobicity of the virus surfaces. The hydrophobic interaction mainly governs the adhesion of the virus to the clay surface. The viruses are negatively charged when the pH of the virus suspension is higher than the isoelectric point of the virus. Thus, the adsorption of the negatively charged virus to the negatively charged clay surface is governed by strong hydrophobic interaction. The negatively charged viruses approach the clay surface due to cation bridging and H-bonds, during which the hydrophobic group of the virus interacts with the hydrophobic siloxane surface of the clay mineral by the exclusion of water (drying phenomenon). The amino acid of the protein coat in the poliovirus, MS2, and

coronaviruses (CoVs) contains long pockets of the exposed hydrophobic group, which facilitates the strong hydrophobic interaction with the clay (Lama and Carrasco, 1995; Liemann et al., 2002; Martinez-Gil et al., 2011). On the other hand, the affinity of reovirus and φx-174 was found to be the bare minimum due to the least hydrophobic nature of such viruses (Schijven and Hassanizadeh, 2000).

The linear and non-linear sorption isotherms for virus interaction with kaolinite mineral were presented in Fig. 8.3 and Fig. 8.4. The percentage adsorption of coronavirus on montmorillonite and kaolinite minerals was 99.99% (Clark et al., 1998). However, the adsorption capacity of kaolinite mineral for poliovirus was found to be higher (~99.53%) in comparison to montmorillonite (94.1%) (Moore et al., 1981). The linear and Freundlich isotherm parameters as presented in Table 8.1, also indicated a higher retention capacity of kaolinite mineral for MS2 and φx-174 in comparison to montmorillonite. The sorption parameters for both montmorillonite and kaolinite mineral were similar for MS2. The higher affinity of the kaolinite was attributed to the higher composition of positive edge sites than montmorillonite-rich soils. Kaolinite possesses pH-dependent charges on the edges and alumina basal surface due to the presence of reactive termination sites. The isoelectric point of the kaolinite edge ranges from 5.8-10, and when the virus suspension in buffer media (pH=6-7) interacts with the kaolinite, it renders a higher amount of positive charge on the edges (Palomino and Santamarina, 2005; Choudhury and Bharat, 2017). Such positive adsorption sites are expected to have a higher affinity towards the negatively charged viruses. Therefore, apart from the hydrophobic interaction, electrostatic interaction also plays a major role in the virus adsorption to kaolinite mineral. Moreover, the IEP of the kaolin surface at air-dried condition, being in the acidic range, transfers proton to the virus. The protonation is then followed by the electrostatic interaction between the negatively charged clay surface and the net positively charged virus. As a result of strong electrostatic and hydrogen bonding between the kaolinite and the virus protein surface, kaolinite proves to be a slightly better adsorbent than montmorillonite for the studied viruses.

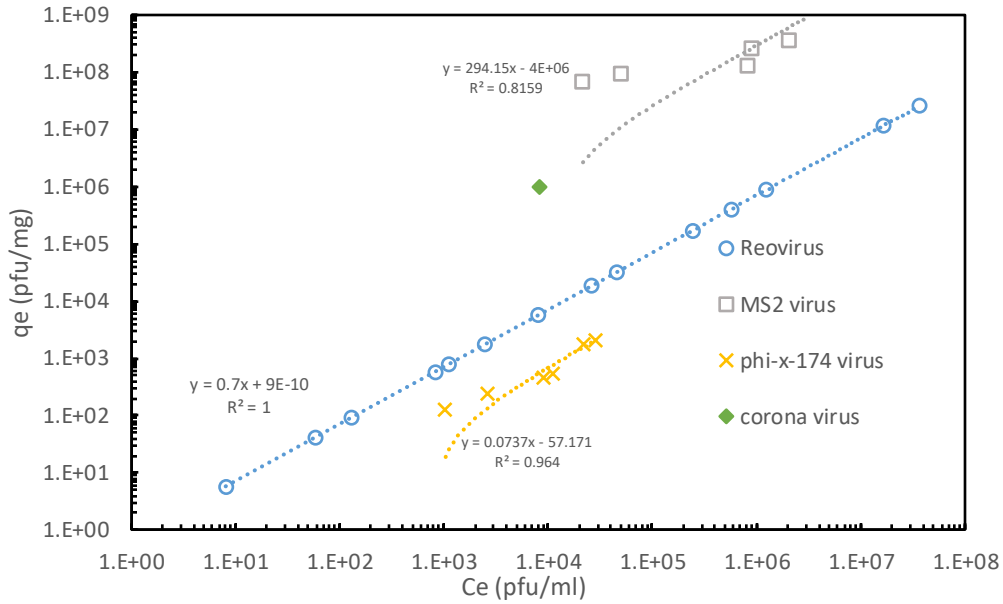

Figure 8.3: Linear isotherm for different virus retention on kaolinite

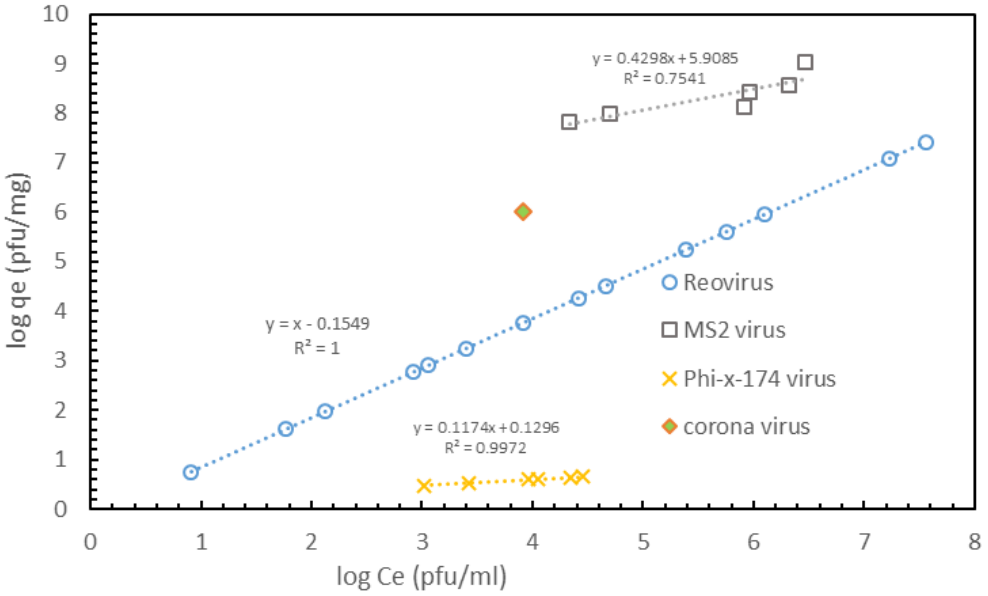

Figure 8.4: Equilibrium Freundlich isotherm for different virus retention on kaolinite

From the sorption studies of different viruses on montmorillonite and kaolinite minerals, it is evident that both the clay minerals exhibited a strong affinity for different viruses, especially for bovine-coronavirus, and poliovirus. Thus, the SARS-CoV-2, a serotype of coronaviridae family (CoVs) is expected to be adsorbed appreciably on the surface of the

studied clay minerals, owing to its similar surface morphology and surface hydrophobicity as bovine-coronavirus.

In order to address the ongoing waste disposal problem of SARS-CoV-2 BMW and the subsequent prevention of the passive transmission of the virus, disposal in the landfills comprising of clay-based barrier facility can prove to be an effective solution. Diffusion is a dominant mechanism that governs virus transport through the compacted clay barrier systems. For the design of such compacted clay barriers, the sorption and diffusion parameters are generally evaluated by performing laboratory through-diffusion or in-diffusion tests with different contaminant species (Shackelford and Daniel., 1991; Rowe et al., 1997). However, the diffusion studies pertaining to virus migration through compacted clay mineral are not available yet. The sorption parameters for the present study were estimated from the batch sorption results based on the following methodology. Similarly, the effective diffusion coefficient (D_e) estimation was discussed in sec. 8.6.

8.5 Estimation of sorption potential (R_d) for compacted clays

The sorption potential of the clay-based barrier system is characterized by the retardation factor (R_d). The R_d values for montmorillonite and kaolinite clays were evaluated based on the available batch test results. As the commonly adopted field density (air-dried) for the design of a clay-based barrier system vary in the range of 1.0-1.3 Mg/m^3 (Alonso et al., 2011; Seiphoori et al., 2014), a compaction density (ρ_d) of 1.3 Mg/m^3 was assumed for the estimation of R_d for both montmorillonite and kaolinite mineral. The R_d values of the montmorillonite rich bentonite and kaolinite clays for inorganic salts at compaction density ranging from 1-1.4 Mg/m^3 obtained from the batch sorption test is comparable to the R_d of the same clay in the compacted state (Kau et al., 1999). As the compaction density increases the available surface area for interaction with the contaminant species decreases, although the amount of clay in a given volume increases. Therefore, the R_d values with different compaction densities are generally comparable to the batch sorption results. Thus, in the absence of data, the author assumes the R_d value obtained from the available equilibrium batch test for understanding the diffusion behaviour of the studied clay minerals in the virus environment.

The R_d from the batch sorption test assuming linear isotherm (Shackelford and Daniel, 1991; Rowe and Booker, 1985; Bharat, 2013) and Freundlich isotherm (Rao, 1974; Shackelford et al., 1989) is given by Eq. 8.4 and 8.5 respectively.

$$R_d = 1 + \frac{\rho_d K_d}{n} \tag{8.4}$$

$$R_d = 1 + \frac{\rho_d K_f c_o^{\left(\frac{1}{n}-1\right)}}{n} \tag{8.5}$$

where n is the effective porosity of the soil, ρ_d is the dry density of the soil, K_d is the linear sorption parameter expressed in ml/mg, K_f and $1/n$ are the Freundlich isotherm coefficients. The term $K_f c_0^{(1/n-1)}$ has the same units as K_d (Shackelford et al., 1989). The R_d associated with the Freundlich isotherm is a function of the initial concentration under consideration. The initial concentration of 10^6 pfu/ml was considered in the pathogen-contaminated waste for the estimation of R_d from the non-linear isotherm. The linear sorption parameter K_d and the non-linear sorption parameters K_f and $1/n$ vary significantly for the same virus in the presence of different buffer solutions. The K_d for the MS2 adsorption on montmorillonite in the presence of low ionic strength phosphate buffer solution (PBS) was found to be ~500-700 times lower than MS2 adsorption on the same mineral in the presence of magnesium chloride (Fig. 8.5). On the other hand, the K_d was found to be 4000-5000 times lower for the MS2 adsorption on kaolinite mineral in the presence of low ionic strength PBS in comparison to artificial water (Fig. 8.6). Phage virus, viz., MS2 is commonly used as a surrogate to understand the sorption behaviour of various human viral pathogens, viz., poliovirus, and reovirus on clay minerals. Therefore, it is expected that such human pathogens would also exhibit varied adsorption behaviour in the presence of different buffer media. In order to account for such disparity in the adsorption potential of clay minerals in the presence of different buffer solutions, the linear and non-linear terms K_d and $K_f c_0^{(1/n-1)}$ were reduced by 1000 times for the practical estimation of the retardation factor. The linear and non-linear R_d obtained from the batch test results, after the reduction in the sorption coefficients were presented in Table 8.2. Due to the unavailability of the sorption data for human-coronavirus (SARS-CoV-2), the clay minerals were assumed to have a similar R_d as that of poliovirus. The assumption was justified as the percentage adsorption of the poliovirus and bovine

coronavirus (belonging to the family of CoVs), at a higher concentration by montmorillonite mineral was nearly similar.

The R_d for both the studied clays was found to be maximum for poliovirus followed by MS2, and the least R_d was exhibited by φx-174. On the other hand, the R_d for kaolinite mineral was higher than the montmorillonite-rich clay for the same type of virus. The minimum value of R_d obtained from the linear and Freundlich isotherm was used for understanding the migration of a virus through compacted barrier systems.

Table 8.2: Model parameter for various pathogens

Virus	Retardation factor (R_d)				Effective diffusion coefficient D_e (m^2/sec)	
	Montmorillonite		kaolinite			
	Linear	Non-linear	Linear	Non-linear	Montmorillonite/kaolinite τ=0.11	Montmorillonite/kaolinite τ=0.64
Polio	1339	1513	-	-	3.08×10^{-13}	1.79×10^{-12}
MS2	129	104	896	936	1.29×10^{-12}	7.5×10^{-12}
Reo	3	3	3.13	3.16	9.1×10^{-13}	5.3×10^{-12}
Φx-174	1.1	1.02	1.22	1	1.29×10^{-12}	7.5×10^{-12}
Corona	1339	1513	-	-	3.85×10^{-14}	2.24×10^{-13}

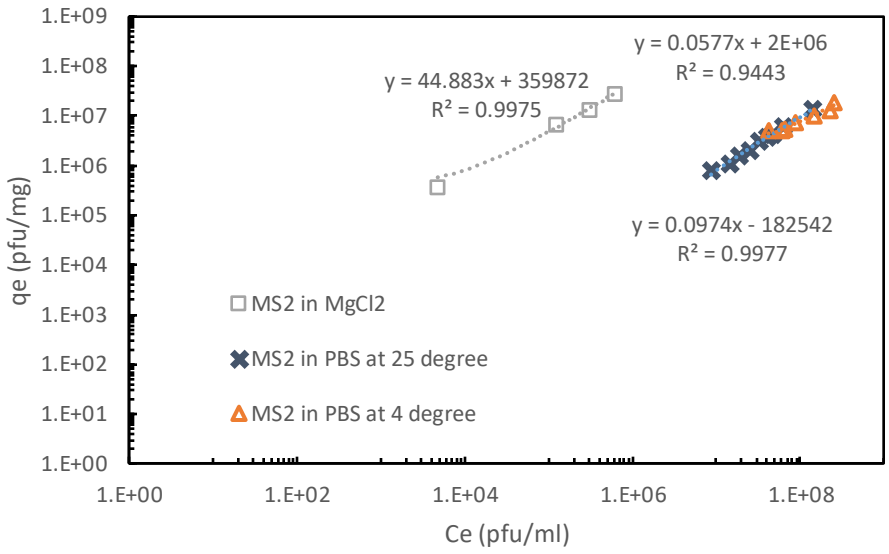

Figure 8.5: Sorption isotherm for MS2 retention on montmorillonite in the presence of (a) MgCl2 (Stagg et al., 1977) (b) phosphate buffer solution (PBS) at 25°c, (Syngouna and Chrysikopoulos, 2010), (c) phosphate buffer solution (PBS) at 4°c (Syngouna and Chrysiko

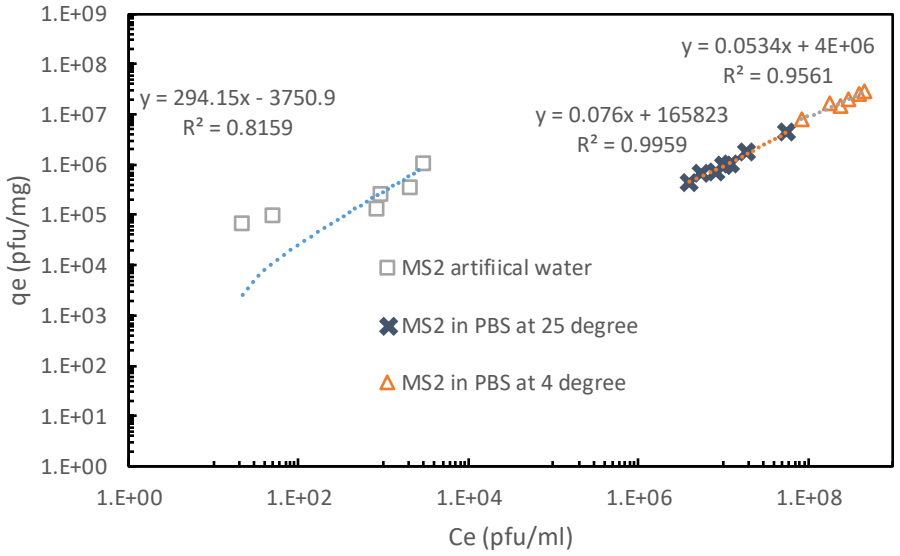

Figure 8.6: Sorption isotherm for MS2 retention on kaolinite in (a) artificial water (Park et al., 2015), (b) phosphate buffer solution (PBS) at 25°c (Syngouna and Chrysikopoulos, 2010), (c) phosphate buffer solution (PBS) at 4°c (Syngouna and Chrysikopoulos, 2010)

8.6 Estimation of the effective diffusion coefficient for compacted clays

Diffusion is a process in which any viral pathogen transports from a region of higher concentration to a region of low concentration. Eq. 2.5 also describes the governing

differential equation describing the 1-Dimensional flow of the virus through the saturated clay mineral.

The D_e was estimated for both the clays from the existing knowledge of the free solution diffusion coefficient (D_0) of the virus and the tortuosity (τ) of the clays for different compaction densities. The D_0 for six different studied viral pathogens were considered from the available literature data (Gomatos and Tamm, 1963; Moller, 1964; Cui et al., 2005; Costello et al., 2013; Buchta et al., 2019). The D_0 values for polio and reovirus were 2.8×10^{-12} and 8.3×10^{-12}, respectively. Due to the paucity of data for phage virus Φx-174, it was assumed to have a similar D_0 as MS2 which is 1.17×10^{-11} m^2/sec. Further, the D_0 for the human coronavirus (SARS-COV-2) was assumed to be similar to that of feline coronavirus ($D_0 = 3.5 \times 10^{-13}$ m^2/sec) due to the similar surface morphology of the viruses. The effective porosity of the clay minerals for a compaction density of 1.3 Mg/m^3 was evaluated knowing the specific gravity of the soils.

The τ of the clay minerals were based on the porosity-tortuosity relationship for the two extreme conditions for specific species (Mackie and Meares, 1955; Boudreau, 1996). A tortuosity factor of 0.62 and 0.64 was obtained for kaolinite and montmorillonite mineral, respectively, utilizing the relationship given by Boudreau (1996). On the other hand, the τ for the kaolinite and montmorillonite mineral was estimated to be 0.09 and 0.11 utilizing the relationship provided by Mackie and Meares (1955). The tortuosity-porosity relationship established by Mackie and Meares (1955) was based on the diffusion of electrolyte solution through membranes and the diffusive tortuosity relationship of fine-grained unlithified sediments with porosity was given by Boudreau (1996). In the presence of any electrolyte solutions, the diffused double layer thickness of the montmorillonite suppresses significantly which results in higher tortuosity in comparison to kaolinite. However, the τ was assumed to be similar (τ=0.11 and 0.64) for both montmorillonite and kaolinite clays as the tortuosity of montmorillonite minerals is expected to be relatively smaller, for the realistic estimation of the D_e in the presence of a virus. Therefore, the τ in the lower bound was assumed to be 0.11 and the τ in the upper bound was estimated to be 0.64 for both the clay minerals. The D_e for both the clay minerals for different viruses were listed in Table 9.2.

8.7 Assessment of clay barrier attenuation capacity

The influence of the estimated model parameters (D_e and R_d) on the design of barrier facilities for attenuating the virus-contaminated waste, was assessed by considering the spatial distribution of the virus at a given time. Theoretical concentration data of virus with the depth of a barrier layer for 50 years was simulated using the estimated model parameters as presented in Table 8.2 and utilizing the expression described in Eq. 4.1 (Shackelford et al., 1991)

The Eq. 4.1 simulates the concentration profile for flux boundary conditions above the clay liner and semi-infinite boundary conditions at the bottom. The simulated data showed that a considerable variation in the concentration data of different viruses was found with depth. After a period of 50 years, coronavirus could reach a depth of only 1 mm, and on the other hand, the poliovirus diffused to a depth of nearly 3 mm of the compacted montmorillonite layer having τ=0.11 (Fig. 8.7a). Although the considered R_d is the same for both corona and poliovirus, the variation in the D_e resulted in the difference in the attenuation of clay.

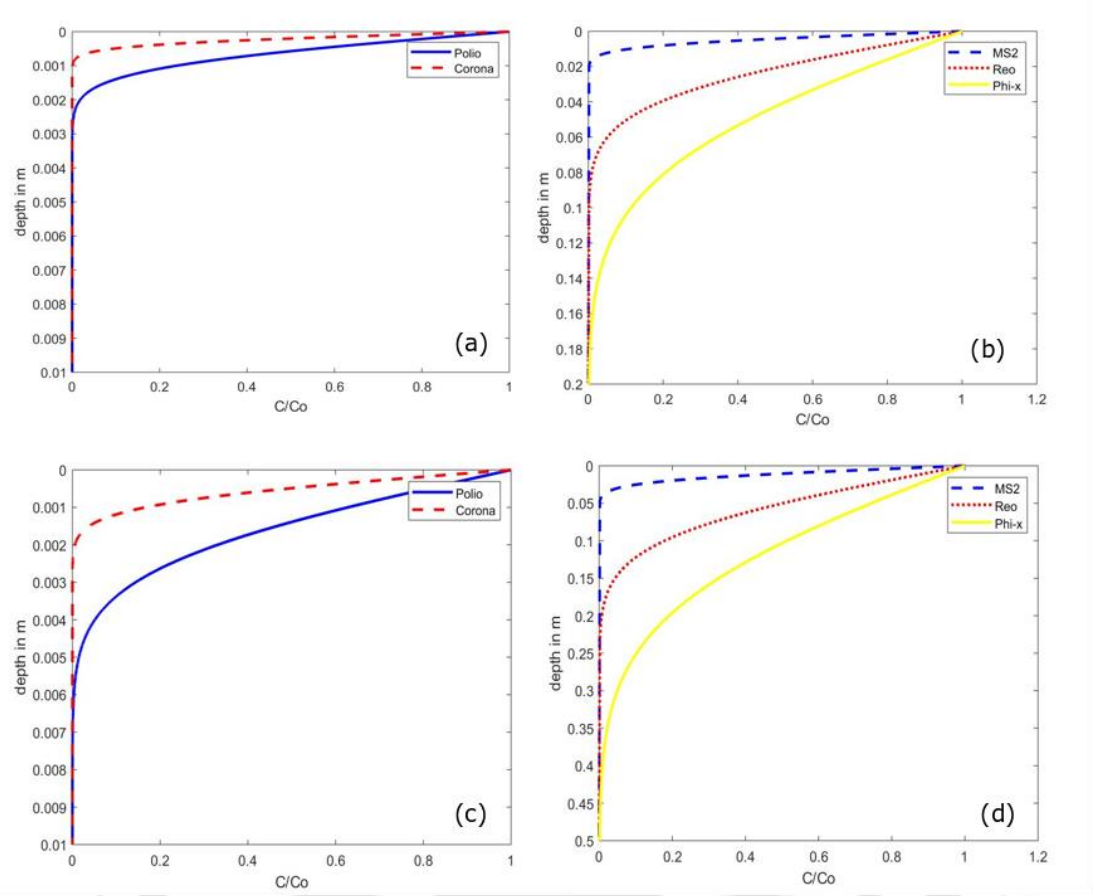

Figure 8.7: Comparison of the migration rate through montmorillonite layer with τ=0.11 for (a) polio and coronavirus; (b) reovirus, MS2, and Φx-174; comparison of migration rate through montmorillonite layer with τ=0.64 for (c) polio and coronavirus; (d) reovirus,

For similar conditions, small concentrations of reovirus and φx-174 were present at a greater depth of ~100 and 140 mm, respectively, while MS2 could diffuse to only a depth of 20 mm of the compacted montmorillonite layer (Fig. 8.8b). Further, the diffusion rates for the studied pathogens through the compacted montmorillonite layer having τ=0.64, was observed to be relatively faster (Fig. 8.7c-d). This was due to the availability of more free path for the pathogens migration. Similar to the earlier case (τ=0.11), the least diffusion rate was exhibited by poliovirus and coronavirus and the maximum rate was exhibited by φx-174. The slower diffusion rate of the poliovirus and coronavirus was due to the higher hydrophobic interaction between the surface protein of the virus and the montmorillonite surface (Fig. 8.7c). On the other hand, φx-174 exhibits the least hydrophobicity among the studied pathogens, and hence the adsorption was minimal which aggravated the diffusion rates. The phage viruses, viz., MS2, and φx-174 are usually utilized as a surrogate virus to

understand the adsorption affinity of human viral pathogens. The migration rate of MS2 bacteriophage could provide a close match with that of poliovirus and coronavirus. Therefore, the MS2 virus can be used as a potential surrogate virus to understand the diffusion rate of poliovirus and coronavirus through compacted montmorillonite and kaolinite mineral. On the other hand, φx-174 would lead to a complete underestimation of the adsorption behaviour of different viral pathogens.

Similar spatial variation for the viruses (reovirus, MS2, and Φx-174) was observed when kaolinite mineral was used as the barrier layer (Fig. 8.8 a-b). The migration rates for these three viruses through the kaolin clay was slightly less compared to the montmorillonite clay. Due to the paucity of literature sorption data for polio and coronavirus at different concentrations, on kaolinite mineral, the modelling could not be performed for these viruses. However, as kaolin was found to be a relatively better adsorbent for the surrogate virus MS2, it is expected that a slightly lesser thickness of the kaolin layer would be required in comparison to the montmorillonite for the attenuation of polio and coronavirus. Kaolinite mineral, owing to its unique pH-dependent surface and edge characteristics exhibits a relatively stronger affinity for the negatively charged viral pathogens in an aqueous environment.

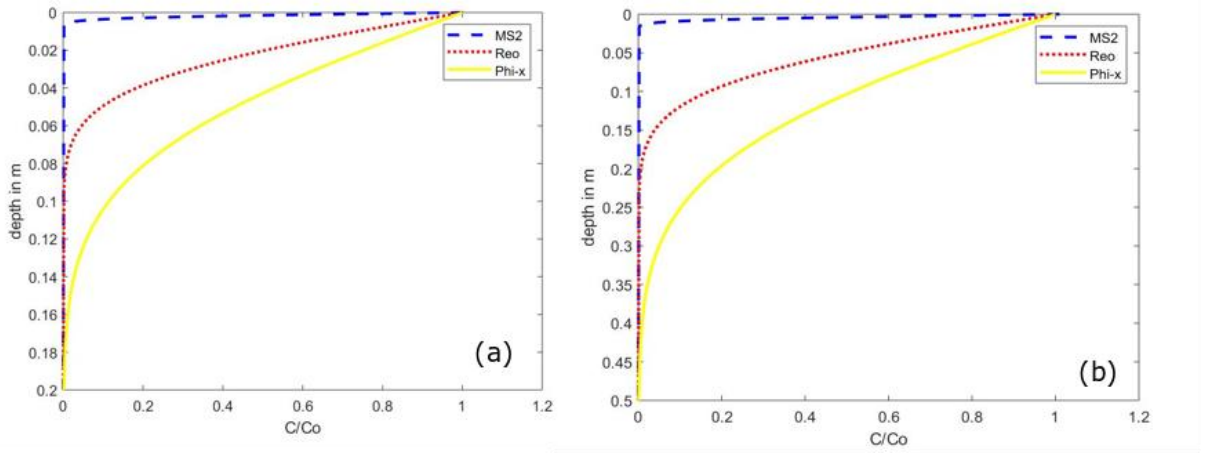

Figure 8.8: Comparison of the migration rate for (a) MS2, reovirus, and Φx-174 through kaolinite layer with τ=0.11; (b) MS2, reovirus, and Φx-174 through kaolinite layer with τ=0.64

Moreover, a tortuosity of 0.64 is not expected in the compacted clay-based barrier facilities, which are exclusively meant for attenuation of the BMW and other sanitary waste generated

from the studied viral pathogens. Therefore, from the spatial concentration variation for human coronavirus and poliovirus, it can be surmised that a compacted montmorillonite or kaolinite liner of ~2-3 mm thickness would be able to attenuate both corona virus and poliovirus completely for 50 years. On the other hand, the spatial variation of reovirus concentration for a period of 50 years (Fig. 8.8b) indicated that a higher barrier thickness is required for its complete attenuation. However, reovirus being a relatively less fatal pathogen in comparison to coronavirus and poliovirus, it is expected that a thickness of 2-3 mm is also sufficient for reovirus, as over a period of 50 years, the viruses are expected to undergo complete inactivation. Therefore, in order to curb the passive transmission of the human viral pathogens from the virus contaminated BMW, such clay-based barrier facilities can be the best alternative to incineration and open dumping under the conditions that the inter-granular voids in the GBs are sealed.

Further, as observed in Chapter 6, the existing barrier systems failed to perform in the extreme saline conditions. The GCLs could not seal the inter-granular voids in the presence of high concentration salts. Such unsealed liner systems can cause detrimental effects to the environment. Therefore, if the virus-contaminated waste is dumped in an existing MSW landfill, where the disposal of the excessive salt-laden solid waste is common then viral pathogens can find an easy path through the unsealed liners to the nearby groundwater table. In order to avoid such a problem, the proposed kaolin-bentonite liner system is expected to attenuate all the possible contaminants if implemented in the landfills. The addition of the kaolin layer above the montmorillonite-rich bentonite layer (GB) will not only allow the underlying GB layer to seal but also adsorb the pathogens as kaolin is found to be a better adsorbent of viruses.

8.8 Application of Montmorillonite for SARS-CoV-2 prevention

Herein, based on the sorption data (Fig. 8.1-Fig. 8.2) we propose bentonite paste, which is a natural and environmentally friendly material, to effectively control the transmission of SARS-CoV-2 and other human viral pathogens through dermal contact. SARS-CoV-2 (Covid-19), a newly discovered human viral pathogen, is found to induce acute neurologic disorder in humans by attacking the central nervous system (CNS). This contagious human pathogen belongs to the family of coronavirus (SARS-CoV) and leads to neurodegenerative

effects on the human nerve and brain cells, causing loss of olfactory functions and severe ischemic stroke. Poliomyelitis or the poliovirus is also a morphologically similar human pathogen, which also has the potential to cause muscle weakness and sometimes complete paralysis of limbs.

The world was recently reeling under the human health and economic crisis caused by the SARS-CoV-2 virus, which reached a stage of a global pandemic. Moreover, another global outbreak of such a virus cannot be shunned. On the other hand, the local outbreak of the poliovirus within the unvaccinated and under-vaccinated population coverage is common. The cessation of human-human transmission of both the viruses during the local outbreak is thus, essential as they are contagious and potential to spread rapidly.

The virus transmission occurs through hand-hand contact, contact to oral and nasal discharges, and dermal contact of contaminated surfaces as the viruses survive for several hours on human skin and other surfaces under ambient conditions. Thus a frequent hand sanitization is required for interruption of the virus transmission chain. The current practice of hand cleansing mostly relies on using alcohol-based hand-sanitizer (ABHS), which contains nearly 70% ethanol or isopropanol (Figure 8.9a). Excessive dermal exposure and nasal inhalation of the high concentred alcoholic mists and vapors lead to severe damage to the CNS, which results in memory disorders, nausea, slurred speech, and hypothermia (Bessonneau et al., 2010). Accidental ingestion of the solution causes alcohol poisoning leading to several liver diseases and death in extreme conditions. Further, irritant contact dermatitis (ICD) and allergic contact dermatitis (ACD) are often reported using ABHS. And, a negative impact of ABHS on the skin microbiota by a significant reduction in bacterial cell counts deter the ABHS application as the skin microbiota is vital for maintaining the immune homeostasis in the skin.

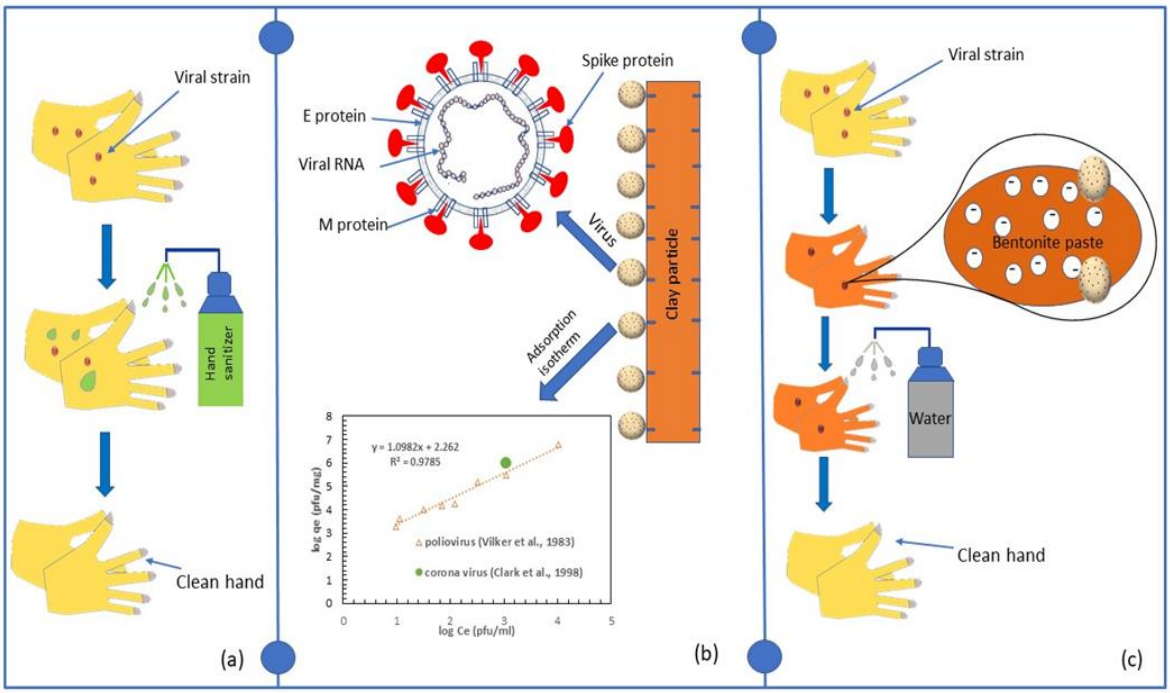

Figure 8.9: (a) The usual practice of hand cleansing with an alcohol-based sanitizer, (b) Virus adsorption unto clay particle, (c) Proposed technique for hand cleansing

The bentonite paste can be used as an effective measure to control virus transmission through dermal contact. The bentonite clays are rich in montmorillonite minerals and characterized by very high specific surface area and cation exchange capacity. As observed in the analysis presented in the previous section, montmorillonite mineral is an excellent adsorbent to SARS-CoV and other human viral pathogens (Table 8.2)

The association of the protein spike with the charged clay mineral due to different clay-virus interactions leads to a very high cohesive energy density between the virus and the clay surface (Abduljauwad, 2020). As both the SARS-CoV and poliovirus pathogens have similar surface morphology, the sorption data match for these viruses on the clay minerals (Fig. 8.1a-8.1b). The percent adsorption of corona and poliovirus on the bentonite soil was nearly 99.99% and 95%, respectively, where the adsorbent dosage was in the range of 0.1-0.2mg/5ml of the virus (Fig. 8.9b). Such a high affinity of bentonite clay for the viruses, where the number of adsorption sites was minimal, indicates a complete (100%) adsorption of the virus in the presence of a higher amount of bentonite. Thus very high interaction energy of 28 J/cm^3 is theoretically estimated for the protein spike of SARS-CoV-2 to the

montmorillonite surface (Abduljauwad, 2020), which is abundant in bentonite clay. On the other hand, the affinity of the SARS-CoV-2 for human enzymes is negligible (0.4 J/cm^3) in comparison to the bentonite clay. The expected binding energy of these viruses for the skin is likely to be ≤0.4 J/cm^2. Thus, the proposed technique of using a bentonite clay paste for sanitization is a natural replacement to the existing hand sanitizers for infection control. And, the ill effects associated with the ABHS on the skin can be avoided. The bentonite paste adsorbs all the available virus strain from the skin, washing with fresh water removes the bentonite clay with the sorbed viruses (Figure. 8.9 c).

The bentonites show several medicinal benefits besides being an effective natural sanitizer for removing the virus from the skin. The application of bentonite paste aids in treating skin infections and shedding the dead skin layers. Further, accidental consumption of bentonite clay does not lead to any side-effects; rather, it would help in alleviating any digestive complications and detoxifying the body. Due to the virtues of bentonite paste as discussed above, it is a potential deterrent to the SARS-CoV-2 transmission arising from the improper disposal of contaminated medical gears. Spraying with bentonite slurry and subsequent washing with water would cater to the problems associated with the disposal of the contaminated medical gear. The application of bentonite slurry would not only make the medical gear reusable and prevent the spread of the contagious virus but also safeguard the environment by maintaining sustainability goals.

8.8 Summary and salient observations

The effectiveness of montmorillonite/kaolinite based liner facilities to contain the studied pathogens was assessed based on the available, limited equilibrium batch sorption isotherm data on different clay minerals for different applications. In this study, the long-term effective diffusion and sorption potential of compacted clay-based barrier systems for the virus-contaminated BMW were evaluated, for the first time, based on the batch sorption data, free-water diffusion coefficients, and tortuosity factors for compacted clays. The model parameters were utilized to assess the attenuation of various viral pathogens (coronavirus, poliovirus, and reovirus), and bacteriophages (MS2 and φx-174) in montmorillonite and kaolinite mineral barriers. The following conclusions are drawn based on the analysis.

- The interaction of any virus with the clay mineral is dictated by the presence of hydrophobic amino acid in the outer protein coat. The retardation factor (R_d) evaluated from the linear and non-linear sorption isotherms suggested that the sorption potential for the studied clay minerals varied for different viral pathogens. The montmorillonite mineral exhibited a very high sorption potential for poliovirus. The montmorillonite is also expected to be an excellent adsorbent for coronavirus as similar hydrophobic and electrostatic interactions are prevalent between the negatively charged spike protein and negatively charged montmorillonite clay mineral and surface cations. The limited available data and recent molecular dynamic simulations also supported this conclusion. Further, the sorption potential for MS2 is significantly high on montmorillonite mineral while a weak interaction is found for reovirus and Φx-174.

- Similar to montmorillonite mineral, the sorption potential of kaolinite for Φx-174 was marginal, while kaolinite exhibited a strong interaction with the other studied pathogens. The R_d for both the clay minerals with Φx-174 was nearly equal to 1. This was due to the negligible hydrophobicity of Φx-174 on the protein layer, which resulted in a very weak interaction with the clay minerals.

- The sorption potential (R_d) of kaolinite for reovirus, MS2, and Φx-174 was found to be relatively higher than montmorillonite. This was attributed to the higher surface area on the edges of the kaolinite. Apart from the hydrophobic interaction on the mineral surface, the iso-electric point of the kaolinite edge and alumina basal surface also play a dominant role in adsorbing the negatively charged virus surface in an aqueous environment by electrostatic interaction.

- The R_d of the kaolinite for poliovirus and coronavirus could not be estimated due to the paucity of the data. However, as the R_d of kaolinite for the surrogate virus, MS2, was very high, it was concluded that kaolinite would exhibit stronger sorption potential for both poliovirus and coronavirus.

- The migration rate of phage virus Φx-174 was found to be very fast even at a low tortuosity of soil (τ=0.11) owing to its weak adsorption affinity for the studied clay minerals. Such phage virus when used as a surrogate virus to study the adsorption behaviour of other morphologically similar human pathogens would lead to a complete underestimation of the adsorption affinity of those pathogens. On the other hand, the MS2 virus provided a good estimation of the migration rates for both poliovirus and coronavirus in clay barriers based on the sorption data and is useful as a surrogate virus.

- The diffusion rate of the viral pathogens through compacted montmorillonite and kaolinite barrier facilities was higher when the tortuosity factor was high. This was due to more accessible pathways for virus transport. However, over a wide range of tortuosity of the clay minerals, a compacted layer of ~2-3 mm was sufficient for the complete attenuation of the studied pathogens under the conditions where the bottom bentonite layer has undergone complete sealing.

- Most of the liner facility adapted across the globe comprises of the GB layer and it was observed in Chapter 6 that in extreme saline conditions the GB is not able to seal and it can allow easy mobility for the viral pathogens to the surrounding geology. Therefore, in order to curb this problem, the addition of kaolin as a protective layer is expected to be effective in allowing the bottom GB layer to seal in the high ionic strength salt solutions and thereby maintain its overall attenuation ability for various salts and human viral pathogens.

Chapter 9

Conclusion and future scope

9.1 Conclusion

- The hydrated cationic size, cation valence, and cation concentration were found to significantly influence the model parameters required for the liner design. Among the salts with monovalent cation, the effective diffusion coefficient (D_e) was found to be highest for potassium ion. However, in the presence of divalent salt cation, the D_e was the maximum. This was due to the preference of higher valence cations on the bentonite surface which satisfies the charge density and also it replaces the exchangeable cations considerably resulting in the suppression of the DDL thickness.
- The D_e increased significantly with the increase in the concentration for both PB and GB for all the salts, which was attributed to the higher replacement of the surface cations by the cations present in the bulk solution as concentration increases leading to greater suppression of the DDL thickness. The long-term diffusion through the PB augmented by the pore-fraction analysis by GRA showed that the accessible void fraction increases with concentration resulting in unreasonably high D_e, detrimental for the environment.
- The diffusion of synthetic salt leachates through compacted bentonite soil indicated that the migration rate of one ion is influenced by the migration rate of the companion ion in the salt mixture. Elemental compositional analysis suggests that in the presence of synthetic leachate comprising of all the studied salts, a significant amount of potassium and calcium ion were adsorbed in the clay surface, resulting in the thinning of the DDL and increasing the D_e for the larger size cations. The increase in the compaction density decreased the overall D_e of the salt mixture particularly in the presence of lithium and sodium ions. However, in the presence of potassium and calcium ions, the decrease in the overall D_e at higher compaction density was marginal.
- The chemo-mechanical behaviour of the compacted granular bentonite under the influence of various salt concentrations indicated that the soil was not able to seal when higher concentrations of KCl and $CaCl_2$ were used as the permeant fluid under a

overburden stress of 50kPa. The sealing was achieved only at lower concentration pore-fluid or with water. This was attributed to the inability of the granules to disintegrate into smaller particles when permeated with high ionic strength salt solutions. The hydraulic conductivity was found to be much higher than the limiting value and hence the applicability of GCL under extreme saline conditions remains a concern.

- The proposed kaolin-GB layered system, however, showed a considerable improvement in the overall performance of the liner system even at high ionic strength salt solutions. The sealing of the GB was achieved at 0.5M KCl and $CaCl_2$ which was not possible when the GB was present as a single layer. The pore-fluid first flows through the kaolin layer and then it reaches the GB layer in the proposed kaolin-bentonite layered system. The adsorption of the salt cations of higher concentrations on the silanol edges of the kaolin results in the reduction of the concentration of a particular ion when it reaches the GB layer and under such concentration, the soil granules were able to disintegrate into particles and the overall sealing was achieved. The microstructural and elemental compositional analyses justified the conclusion.

- The diffusion through the proposed kaolin-GB layered system revealed that the D_e was reduced significantly in comparison to the individual layer. The top densely compacted kaolin layer behaved as a protective layer for the underlying GB by allowing a reduced concentration of the permeant into the GB. Under such conditions, the permeants find a more tortuous pathway resulting in the lower overall D_e. The R_d for the kaolin-GB layered system was also higher in comparison to the single GB layer, indicating higher adsorption potential of both kaolin and GB for inorganic salt cations. Moreover, the PB and GB behaving similarly in the saturated conditions, the diffusion rates through the kaolin-PB layered system are also expected to be lesser in comparison to the single PB layer.

- The clay-based barrier systems were found to completely attenuate several viral pathogens under the assumption that the bottom liner facilities have completely undergone complete sealing. The commonly adapted liner materials, viz. GCL performs very poorly in terms of its sealing behaviour in extreme saline conditions. The viral pathogens from the virus-contaminated BMW can find easy mobility through an

unsealed GCL in the presence of salt leachate. Therefore, to avoid such problems the proposed kaolin-bentonite layered system was found to have the potential to attenuate all the possible contaminants in the landfill even in the presence of high ionic strength salt solutions.

9.2 Future Scope

- The chemo-mechanical behaviour of the granular bentonite was studied for a specific ion/single salt under the expected loading in MSW. However, to simulate the real field scenario, the volume changes and sealing potential of the bentonite must be ascertained for synthetic leachates.
- As many parts of India is rich in kaolin deposits, the applicability of the proposed kaolin-bentonite layered system must be verified with the locally available kaolin soil. The kaolin used in the present study was a commercially available one. Moreover, the density of the kaolin layer was maintained very high and a replica of such a system might be slightly difficult in the field, hence some more studies need to be conducted at some reduced densities of the kaolin layer and come up with a more viable solution.
- The effect of different layering options of the bentonite and kaolin on the sealing behaviour of the overall system needs to be studied. In the present work, kaolin was used above the bentonite layer, however, the behaviour of the layered system when kaolin is placed below the bentonite layer (permeant passing from bentonite to kaolin) is unknown.
- The present study was conducted by extracting the granular bentonite soil from the GCL, however, the effect of salt leachates on the chemo-mechanical behaviour of the overall GCL material is not available yet.
- The present study focused on the long-term diffusion behaviour of the powdered bentonite plug under the influence of specific ions, however, studies relating the effect of bentonite under the influence of synthetic leachates would give a better understanding of the design of liner systems which is effective in the long run.

- The study on the long-term diffusion characteristics and the sealing ability of the kaolin-GB layered system in the presence of real landfill leachates would provide a better assessment of the applicability of such liner systems. Moreover, the fate of the sorbed contaminants considering the aging effect of the bentonite and kaolinite needs to be studied.

List of publications

Journal Publications (From Thesis):

1. **Partha Das** and Bharat TV (2017). *Effect of Counter-ions on the Diffusion Characteristics of a Compacted Bentonite*. Indian Geotechnical Journal, 47(4), 477–484. DOI: 10.1007/s40098-017-0241-y. Publisher: Springer.

2. Tadikonda Venkata Bharat, **Partha Das** and Venkatesh Buragadda (2019*). Specific ion effects on surrogate compatibility indices of bentonite for hydraulic barrier applications*, International Journal of Geotechnical Engineering, 13:4, 360-368, DOI: 10.1080/19386362.2017.1358411. Publisher: Taylor and Francis.

3. **Partha Das** and Bharat Tadikonda Venkata (2020). Bentonite Clay: A Potential Natural Sanitizer for Preventing Neurological Disorders, ACS Chemical Neuroscience, DOI: 10.1021/acschemneuro.0c00609 (In Press). Publisher: American Chemical Society (ACS)
4. **Partha Das** and Bharat TV (2021) Kaolin based protective barrier in municipal landfills against adverse chemo-mechanical loadings. Sci Rep 11, 10354 (2021). https://doi.org/10.1038/s41598-021-89787-z

5. **Partha Das** and Bharat TV (2021). Assessment of Clay Mineral Attenuation Capacity for Human Viral Pathogens, Journal of hazardous, toxic and radioactive waste, ASCE. (**Under Review**)

6. **Partha Das** and Bharat TV (2021). Diffusion characteristics of compacted powdered bentonite in the presence of synthetic leachate. (Under Preparation)

7. **Partha Das a**nd Bharat TV (2021). Influence of salt solutions on the short-term and long-term diffusion characteristics of bentonite-based liner systems (Under Preparation)

Journal Publications (Outside Thesis)

1. **Partha Das** and Bharat TV (2020). Reconstruction of a wetting-induced shallow landslide in Shillong, India. Proceedings of the Institution of Civil Engineers- Forensic Engineering, 173:2, 48-53, https://doi.org/10.1680/jfoen.20.00003. ICE Publishing.

2. **Partha Das,** Deepak Patwa, and Bharat TV. (2021). Numerical Simulation Complemented by Measured Soil Water Characteristics for Rainfall-Induced Landslide Prediction: A Case Study Of Shillong Landslide (Ne India), Bulletin of Engineering Geology and the Environment, (**Under Review**)

Book Chapters

1. **Partha Das** and Bharat TV (2019*). Experimental Analysis of Salt Diffusion in Compacted Clays by Through-Diffusion and Half Cell Technique*. In book: Geotechnical Characterisation and Geoenvironmental Engineering. Chapter: 8, Part II, Springer, Singapore. DOI: 10.1007/978-981-13-0899-4_22, pp: 179-186
2. Bharat T.V., **Das P**., Srivastava A. (2019) *Insights into Contaminant Transport Modeling Through Compacted Bentonites*. In: Latha G. M. (eds) Frontiers in Geotechnical Engineering. Developments in Geotechnical Engineering. Springer, Singapore. DOI: https://doi.org/10.1007/978-981-13-5871-5_6, pp:101-120.
3. **Partha Das** and Bharat TV (2020*). Effect of inorganic salt solutions on the diffusion and hydraulic characteristics of compacted clay*. In book: Problematic Soils and Geoenvironmental Concerns. **(ACCEPTED)**

International Conference Publications

1. **Partha Das**, Manparvesh SR and Bharat TV (2016). *Salt diffusion in compacted plastic clay: Experimental and Theoretical Evaluation*. International conference on soil and Environment, ICSE, **IISC Bangalore.**
2. **Partha Das**, Bharat TV (2016). *Laboratory Experimental Techniques for Determination of Diffusion Coefficients for Landfill Liner Facilities - A Review*. 1st International Conference on Civil Engineering for Sustainable Development Opportunities and Challenges, CESDOC, **AEC Guwahati**
3. **Partha Das**, Bharat TV (2019). *Effect of Mixed Salts on the Long-term Behavior of Compacted Bentonite Clay*. Second International Conference of Environmental

Geotechnology, Recycled Waste Materials and Sustainable Engineering (EGRWSE-2019) **University of Illinois, Chicago**

(Received Best Presenter Award for this publication conferred by Springer)

National Conference Publications

1. **Partha Das** and Bharat TV (2016). *Experimental Analysis of Salt Diffusion in Compacted Clays by Through Diffusion and Half-cell Technique*. Indian Geotechnical Conference, IGC 2016, IIT Madras. Received BEST PAPER AWARD

(Received A.V. Shroff Biennial Best Paper Award for this publication conferred by IGS)

2. **Partha Das** and Bharat TV (2018). *Effect of inorganic salt solutions on the hydraulic conductivity and diffusion characteristics of clays*. Indian Geotechnical Conference, IGC 2018, IISC Bangalore.

(Received Best Presenter Award for this publication conferred by Springer)

References

- Achari, G., R. C. Joshi, L. R. Bentley, and S. Chatterji. (1999). Prediction of the Hydraulic Conductivity of Clays Using the Electric Double Layer Theory. Canadian Geotechnical Journal 36: 783–792.
- Alonso, E., Romero, E., Hoffmann, C., (2011). Hydromechanical behaviour of compacted granular expansive mixtures: experimental and constitutive study. Geotechnique61(4),329–344
- Al-Yaqout A and Townsend F (2001) Strategy for landfill design in arid region. Practice Periodical of Hazardous, Toxic, and Radioactive Waste Management 5(1): 2–13
- Arasan, S., and T. Yetimoglu. (2008). Effect of inorganic salt solutions on the consistency limits of two clays. Turkish J. Eng. Env. Sci. 32 (2): 107–115.
- Armanious, A, Aeppli, M., Jacak, R., Refardt, D., Sigstam, T., Kohn, T., and Sander, M. (2016). Viruses at Solid–Water Interfaces: A Systematic Assessment of Interactions Driving Adsorption, *Environ. Sci. Technol.*, 2016, **50**, 732–743
- ASTM D5856 (2015). Standard Test Method for Measurement of Hydraulic Conductivity of Porous Material Using a Rigid-Wall, Compaction-Mold Permeameter. West Conshohocken, PA: ASTM International
- Babu, G.LS., Sporer, H., Zanzinger, H., and Gartung E. (2001). Self-Healing Properties of Geosynthetic Clay Liners. Geosynthetics International 2001 8:5, 461-470
- Badv K and Abdolalizadeh R. (2004) A Laboratory Investigation on the Hydraulic Trap effect In Minimizing Chloride Migration through Silt. Iranian Journal of Science & Technology, Transaction B, Vol. 28, No. B1.
- Bagchi, A. (1990). Design, Construction and Monitoring of Sanitary Landfill; John Wiley & Sons: New York, NY, USA, ISBN 9780471613862
- Bales, R. C.; Hinkle, S. R.; Kroeger, T. W.; Stocking, K. (1991). Bacteriophage adsorption during transport through porous media: Chemical perturbations and reversibility, Environ. Sci. Technol. 1991, 25, 2088-2095
- Barone FS, Rowe RK and Quigley RM (1992) A laboratory estimation of diffusion and adsorption coefficients for several volatile organics in a natural clayey soil. Journal of Contaminant Hydrology 10: 225–250.

- Beall, G.W., Sowersby, D.S., Roberts, R.D., Robson, M.H., Lewis, L.K., (2009). Analysis of oligonucleotide DNA binding and sedimentation properties of montmorillonite clay using ultraviolet light spectroscopy. Biomacromolecules, 10, 105–112
- Benson C, Zhai H and Wang X (1994) Estimating the hydraulic conductivity of compacted clay liners. Journal of Geotechnical Engineering, ASCE 120: 366–387.
- Benson C. H., Daniel D. E., and Boutwell G. P. (1999). Field performance of compacted clay liners. Journal of Geotechnical and Geoenvironmental Engineering 5 390-403
- Bharat TV (2008) Agents based algorithms for design parameter estimation in contaminant transport inverse problems. IEEE Swarm Intelligence Symposium 1–7.
- Bharat TV (2009) Metaheuristics for parameter estimation in contaminant transport modeling through soils. In Proceedings of 4th International Young Geotechnical Engineers Conference, Alexandria (Egypt), 2009.
- Bharat TV, Sivapullaiah PV and Allam MM (2008) Accurate Parameter Estimation of Contaminant Transport Inverse Problem using Particle Swarm Optimization. IEEE Swarm Intelligence Symposium St. Louis MO USA, September 21-23.
- Bharat, T. V., Sivapullaiah, P. V., Allam, M. M. (2009) Swarm intelligence-based solver for parameter estimation of laboratory through-diffusion transport of contaminants. *Computers and Geotechnics*, **36**, 984-992
- Bharat TV, Sivapullaiah PV and Allam MM (2012). Robust solver based on modified particle swarm optimization for improved solution of diffusion transport through containment facilities. Expert Systems with Applications 39 (12): 10812–10820.
- Bharat T.V. (2013). Analytical model for 1-D contaminant diffusion through clay barriers, Environmental Geotechnics 2014 1:4, 210-221
- Bharat, T. V., Sridharan, A. (2015) Prediction of compressibility data for highly plastic clays using diffuse double-layer theory. *Clays and Clay Minerals*, **63**, 30-42.
- Bharat, T. V., Sivapullaiah, P. V., Allam, M. M. (2013) Novel procedure for the estimation of swelling pressures of compacted bentonites based on diffuse double layer theory. *Environmental Earth Science*, **70**, 303-314.
- Bharat, T. V., Sridharan, A. (2015) A critical appraisal of Debye length in clay-electrolyte systems. *Clays and Clay Minerals*, **63**, 43-50.

- Bharat, T.V. and Das, D.S. (2017). Physicochemical approach for analyzing equilibrium volume of clay sediments in salt solutions, Applied Clay Science, 136, 164-175, https://doi.org/10.1016/j.clay.2016.11.021
- Blight GE (1996). Report: Standards for Landfills in Developing Countries. Waste Management and Research. 14:399-414
- Bohnhoff Gretchen L and Shackelford Charles D (2014) Hydraulic conductivity of chemically modified bentonites for containment barriers. 7th International Congress on Environmental Geotechnics. iceg2014. [Barton, ACT]: Engineers Australia, 2014: 440-447. ISBN: 9781922107237.
- Boopathy, R., Karthikeyan, S., Mandal, A.B. et al., (2013). Characterisation and recovery of sodium chloride from salt-laden solid waste generated from leather industry. Clean Techn Environ Policy 15, 117–124. https://doi.org/10.1007/s10098-012-0489-y
- Bouazza A and Van Impe WF (1998) Liner design for waste disposal sites. Environmental Geology, 35 (1), 41–54, https://doi.org/10.1007/s002540050291
- Bouazza, A. (2002) Geosynthetic Clay Liners , Geotextiles and Geomembranes, 20, 3–17
- Boudreau B.P. (1996). The diffusive tortuosity of fine-grained unlithified sediments," Geochimica et Cosmochimica Acta, vol. 60, no. 16, pp. 3139–3142
- Bowders, Jr., J. J., D. E. Daniel, G. P. Broderick, and H. M. Liljestrand. (1986). Methods for Testing the Compatibility of Clay Liners with Landfill Leachate. In Hazardous and Industrial Solid Waste Testing, edited by J.K. Petros, Jr., W. J. Lacy, and R. A. Conway, ASTM STP 886, 233–250. West Conshohocken, PA.10.1520/STP36375S
- Bradshaw, S. L. and Benson, C. H. (2014) Effect of Municipal Solid Waste Leachate on Hydraulic Conductivity and Exchange Complex of Geosynthetic Clay Liners. *Journal of Geotechnical and Geoenvironmental Engineering*, **140**, 405–417..
- Buchta D, Fuzik T, Hrebik D et al. (2019). Enterovirus particles expel capsid pentamers to enable genome release. Nat. Commun. 10(1), 1138
- Burge, W. D. and Enkiri, N. K. (1978).Virus adsorption to five soils. *J. Environ. Qual.* **7,** 73–76. Caldentey, J., Bamford, J. K. H., and Bamford, D. H. 1990. Structure and assembly of bacteriophage PRD1, an *Escherichia coli* virus with a membrane. *J. Struct. Biol.* **104,** 44–51

- Carlson, J. F., Woodard, F. E., Wentworth, D. F., and Sproul, 0. J. (1968). Virus inactivation of clay particles in natural water. J. Water Pollution, Control Fed. 40, R89-Rl06
- Central Pollution Control Board of India, CPCB (2020). Guidelines for Handling, Treatment and Disposal of Waste Generated during Treatment/Diagnosis/ Quarantine of COVID-19 Patients, Revision 4.
- Cerato, A.B., Lutenegger, A.J. (2002). Determination of surface area of fine-grained soils by the ethylene glycol monoethyl ether (EGME) method. Geotech. Test. J. 25, 315–321
- Chapman, H.D. (1965). Cation-exchange capacity. In: Black, C.A. (Ed.), Methods of Soil Analysis - Chemical and Microbiological Properties. Agronomy. vol. 9, pp. 891–901
- Chattopadhyay, S., and Puls, R. W. (1999). Adsorption of bacteriophages on clay minerals. Environ. Sci. Technol. 33, 3609–3614
- Chen C, Wang T, Lee C and Teng S (2012) The development of a through-diffusion model with a parent–daughter decay chain. Journal of Contaminant Hydrology 138–139: 1–14.
- Chen YG, Zhu CM, Ye WM, Cui YJ, Chen B (2016) Effects of solution concentration and vertical stress on the swelling behavior of compacted GMZ01 bentonite. Appl Clay Sci 124:11–20
- Chen, J., Benson, C., and Tuncer, E. (2019). Hydraulic conductivity of bentonite-polymer geosynthetic clay liners permeated with coal combustion product leachates. J. Geotech. Geoenviron. Eng. 145 (9): 04019038. https://doi.org/10.1061/(ASCE)
- Choudhury, C. and Bharat, T. V. (2017). Wetting-induced collapse behavior of kaolinite: influence of fabric and inundation pressure. Canadian Geotechnical Journal, 55(7), 956-967
- Choy JH, Choi SJ, Oh JM, Park T. (2007). Clay minerals and layered double hydroxides for novel biological applications. Appl Clay Sci, 36:122–32
- Chrysikopoulos, C. V. and Syngouna, V. I., (2012). Attachment of bacteriophages MS2 and ΦX174 onto kaolinite and montmorillonite: Extended-DLVO interactions, Colloids

and Surfaces B: Biointerfaces, 92, Pp: 74-83, https://doi.org/10.1016/j.colsurfb.2011.11.028

- Clark, K.J., Sarr, A.B., Grant, P.G., Phillips, T.D., Woode, G.N., (1998). In vitro studies on the use of clay, clay minerals and charcoal to adsorb bovine rotavirus and bovine coronavirus. Vet. Microbiol. 63, 137–146
- Conner, J.R., Hoeffner, S.L. (1998). A critical review of stabilization/solidification technology. Crit. Rev. Env. Sci. Tec. 28 (4), 397–462
- Costello, D.A., Millet, J.K., Hsia, C.-Y., Whittaker, G.R., Daniel, S., 2013. Single particle assay of coronavirus membrane fusion with proteinaceous receptor-embedded supported bilayers. Biomaterials 34 (32), 7895–7904
- Cui, Z.; Zhang, Z.; Zhang, X.; Wen, J.; Zhou, Y.; Xie, W. (2005). Visualizing the dynamic behavior of poliovirus plus-strand RNA in living host cells Nucleic Acids Res. 2005, 33, 3245
- Daniel, D.E. (1993) Geotechnical Practice for Waste Disposal; Springer: Boston, MA, USA.
- Daniel, D.E. (1993). Case Histories of Compacted Clay Liners and Covers for Waste Disposal Facilities. International Conference on Case Histories in Geotechnical Engineering. 2. https://scholarsmine.mst.edu/icchge/3icchge/3icchge-session15/2
- Darde, B., Roux, JN., Pereira, JM. et al (2020). Investigating the hydromechanical behaviour of bentonite pellets by swelling pressure tests and discrete element modelling. Acta Geotech. https://doi.org/10.1007/s11440-020-01040-5
- Das, P. and Bharat, T.V. (2021). Specific Surface Area of Plastic Clays from Equilibrium Sediment Volume under Salt Environment, Geotechnical Testing Journal (In Press).
- Dashman, T., and G. Stotzky. (1982). Adsorption and binding of amino acids on homoionic montmorillonite and kaolinite. Soil Biol. Biochem. 14:447– 456
- Di Maio, C., L. Santoli, and P. Schiavone. (2004). Volume Change Behaviour of Clays: The Influence of Mineral Composition, Pore Fluid Composition and Stress State. Mechanics of Materials 36: 435–451.

- Doi, A., Khosravi, M., Ejtemaei, M., Tuan A.H., Nguyen, T.A.H., Nguyen, A.V. (2020). Specificity and affinity of multivalent ions adsorption to kaolinite surface, Applied Clay Science, 190, https://doi.org/10.1016/j.clay.2020.105557
- Du, Y.-J., Shen, S.-L., Liu, S.-Y., & Hayashi, S. (2009). Contaminant mitigating performance of Chinese standard municipal solid waste landfill liner systems. Geotextiles and Geomembranes, 27(3), 232–239. doi:10.1016/j.geotexmem.2008.11.007
- Edil, T. B., P. M. Berthouex, J. K. Park, D. L. Hargett, L. K. Sandstrom, and S. Zelmanowitz. (1991). Effects of Volatile Organic Compounds on Clay Landfill Liner Performance. Waste Management Research 9: 171–187.
- Egloffstein, T. (2001). Natural bentonites–influence of the ion exchange and partial desiccation on permeability and self-healing capacity of bentonites used in GCLs. Geotext. Geomembr., 19, 427–444.
- EPA (2005): AP-42, CH 11.25: Clay Processing. URL: http://www.epa. gov/ttnchie1/ap42/ch11/.../c11s25.pdf
- EPA (2015). Draft Environmental Guidelines: Solid Waste Landfills, 2nd ed.; US Environmental Protection Agency: Washington, DC, USA
- Franchi, M., Bramanti, E., Bonzi, L.M., Orioli, P.L., Vettori, C., Gallori, E., (1999). Claynucleic acid complexes: characteristics and implications for the preservation of genetic material in primeval habitats. Origins of Life and Evolution of the Biosphere 29, 297–315
- Freundlich, H. (1936). Adsorptionstechnik. By Franz Krzil. The Journal of Physical Chemistry, 40(6), 857–858. doi:10.1021/j150375a022
- Garcia-Gutierrez M, Cormenzana JL, Missana T and Mingarro M (2004) Diffusion coefficients and accessible porosity for HTO and 36Cl^- in compacted FEBEX bentonite. Applied Clay Science 26(1–4): 65–73.
- Garcia-Gutieirrez M, Missana T, Mingarro M, Samper J, Dai and Z, Molinero J (2005) Overview of laboratory methods employed for obtaining diffusion coefficients in FEBEX compacted bentonite. Journal of Iberian Geology 32 (1): 37–53.

- Gerba, C. P. (1984). Applied and theoretical aspects of virus adsorption to surfaces. Adv. Appl. Microbiol. 30, 133–168

  Gillham RW, Robin MJL, Dytynyshyn DJ and Johnston HM (1984) Diffusion of nonreactive and reactive solutes through fine-grained barrier materials. Canadian Geotechnical Journal 21(3): 541 –550.
- Giroud, J.P. Badu-Tweneboah, K. and Soderman, K.L. (2015). Comparison of Leachate Flow Through Compacted Clay Liners in Landfill Liner Systems, Geosynthetics International, 4:3-4, 391-431.
- Gleason, M. H., D. E. Daniel, and G. R. Eykholt. (1997). Calcium and Sodium Bentonite for Hydraulic Containment Applications. Journal of Geotechnical and Geoenvironmental Engineering 123: 438–445.
- Gomatos, P. J., and Tamm, I. (1963). The secondary structure of reovirus RNA. Proc. Natl. Acad. Sci. U.S. 49, 707-714
- Goyal, S. M., & Gerba, C. P. (1979). Comparative adsorption of human enteroviruses, simian rotavirus, and selected bacteriophages to soils. Applied and environmental microbiology, 38(2), 241–247. https://doi.org/10.1128/AEM.38.2.241-247.1979
- Haque, M. S., Uddin, S., Sayem, S. M., & Mohib, K. M. (2020). Coronavirus disease 2019 (COVID-19) induced waste scenario: A short overview. Journal of environmental chemical engineering, 104660. Advance online publication. https://doi.org/10.1016/j.jece.2020.104660
- Imamura, S., Sueoka, T., and Kamon, M. (1996). Long-term stability of bentonite/sand mixtures at L.L.R.W. storage. Proc., 2nd Int. Congress on Environmental Geotechnics, M. Kamon, ed., Balkema, Rotterdam, The Netherlands, 545–550.
- Indian Standard (IS). (1973). Methods of Test for Soils: Determination of specific gravity, IS 2720, Part III
- Indian Standard (IS). (1985). Methods of Test for Soils: Determination of liquid limit and plastic limit, IS 2720, Part V
- Indian Standard (IS). (1985). Methods of Test for Soils: Determination of shrinkage limit, IS 2720, Part VI

- Institute for Global Environmental Strategies. IGES (2020). Waste Management during the COVID-19 Pandemic From Response to Recovery, ISBN No: 978-92-807-3794-3, Job No: DTI/2292/PA
- Israelachvili, J.N. (2011). Intermolecular and surface forces. Elsevier/Academic Press 3rd ed. Amsterdam
- Itakura T, Airey DW, Leo CJ (2003). The diffusion and sorption of volatile organic compounds through kaolinitic clayey soils. J Contam Hydrol 65:219–243
- Jingjing, F. (2014). Leakage Performance of the GM + CCL Liner System for the MSW Landfill, The Scientific World Journal, vol. 2014, Article ID 251465, 9 pages, 2014. https://doi.org/10.1155/2014/251465
- Jo, H. Y., Benson, C. H., Shackelford, C. D., Lee, J.-M., and Edil, T. B. (2005). Long-term hydraulic conductivity of a geosynthetic clay liner (GCL) permeated with inorganic salt solutions. *Journal of Geotechnical and Geoenvironmental Engineering*, **131**, 405–417.
- Jo, H.Y., Katsumi, T., Benson C.H., and Edil, T.B. (2001). Hydraulic Conductivity of Nonprehydrated Geosynthetic Clay Liners Permeated with Inorganic Solutions and Waste Leachates, Journal of Geotechnical and Geoenvironmental Enginering, ASCE, 127 (7), 557-567
- Jorgen, R. (2002). Surface chemistry of Al and Si (hydr)oxides, with emphasis on nano-sized gibbsite (α-Al(OH)3), PhD Thesis, Umeå University, Faculty of Science and Technology, Chemistry
- Katsumi Takeshi, Ishimori Hiroyuki, Onikata Masanobu, Fukagawa Ryoichi (2007) Long-term barrier performance of modified bentonite materials against sodium and calcium permeant solutions. Geotextiles and Geomembranes 26 (2008): 14-30.
- Kau PMH, Binning PJ, Hitchcock PW and Smith DW (1999) Experimental analysis of fluoride diffusion and sorption in clays. Journal of Contaminant Hydrology 36: 131–151.
- Kolstad, D., Benson, C., and Edil, T. (2004) Hydraulic conductivity and swell of nonprehydrated GCLs permeated with multi-species inorganic solutions. *Journal of Geotechnical and Geoenvironmental Engineering*, **130**, 1236–1249.
- Kong, D. J., H. N. Wu, J. C. Chai, and A. Arulrajah. (2017). State-of-the-art review of geosynthetic clay liners, Sustainability 9 (11): 2110. https://doi.org/10.3390/su9112110

- Kutlic A., Bedekovic G. and Sobota I., (2012). Bentonite processing, professional paper 24, 61-65
- Lake, C. B., and Rowe, R. K. (1999). Diffusion of sodium and chloride through geosynthetic clay liners. Geotextiles and Geomembranes, 18(2-4), 103-131.
- Lake, C. B., and Rowe, R. K. (2004). Volatile organic compound diffusion and sorption coefficients for a needle-punched GCL. Geosynthetics International, 11(4), 257-272.
- Lake, C.B. and Rowe, R.K. (2000). Swelling characteristics of needlepunched, thermally treated geosynthetic clay liners. Geotextiles and Geomembranes, 18 (2–4), https://doi.org/10.1016/S0266-1144(99)00022-9
- Lama, J., and L. Carrasco. (1995). Mutations in the hydrophobic domain of poliovirus protein 3AB abrogate its permeabilizing activity. FEBS Lett. 367: 5–11
- Lange, K.; Rowe, R.K.; Jamieson, H. (2009). Diffusion of metals in geosynthetic clay liners. Geosynth. Int., 16, 11–27.
- Lee, J. M., and Shackelford, C. D. (2005). Impact of bentonite quality on hydraulic conductivity of geosynthetic clay liners. Journal of Geotechnical and Geoenvironmental Engineering, 131(1), 64-77
- Lee, J., Shackelford, C., Benson, C., Jo, H., and Edil, T. B. (2005) Correlating index properties and hydraulic conductivity of geosynthetic clay liners. *Journal of Geotechnical and Geoenvironmental Engineering*, **131**, 1319–1329.
- Li, T.K. and Rowe, R.K. (2020). GCL self-healing: fully penetrating hole/slit hydrated with RO water and 10 mM Ca solution, Geosynthetics International, 27:1, 34-47
- Li, X., Li, H. & Yang, G. (2015). Promoting the Adsorption of Metal Ions on Kaolinite by Defect Sites: A Molecular Dynamics Study. Sci Rep 5, 14377, https://doi.org/10.1038/srep14377
- Li, Z., Katsumi, T. Inui, T., Takai, A. (2013). Fabric effect on hydraulic conductivity of kaolin under different chemical and biochemical conditions, Soils and Foundations, 53 (5), 680-691, https://doi.org/10.1016/j.sandf.2013.08.006
- Liemann S, Chandran K, Baker TS, Nibert ML, Harrison SC. (2002). Structure of the reovirus membrane-penetration protein, Mu1, in a complex with is protector protein, Sigma3. Cell; 108: 283-295

- Lipson, S. M. and Stotzky, G. (1983). Adsorption of reovirus to clay minerals: effects of cationexchange capacity, cation saturation and surface area. *Appl. Environ. Microbiol.* **46,** 673–682
- Lorenzetti, R. J., Bartelt-Hunt, S. L., Burns, S. E., & Smith, J. A. (2005). Hydraulic Conductivities and Effective Diffusion Coefficients of Geosynthetic Clay Liners with Organobentonite Amendments. Waste Containment and Remediation. doi:10.1061/40789(168)2
- Lyklema, J. 1995. Fundamentals of Interface and Colloid Science Volume II: Solid-Liquid Interfaces. Academic Press, New York.
- Ma, C. and Eggleton, R.A. (1999) Cation exchange capacity of kaolinite, Clays Clay Miner. 47 174–180
- Mackie, J.S. and Meares, P. (1955) The diffusion of electrolytes in a cation-exchange resin membrane. I. Theoretical, Proceedings of the Royal Society A: Mathematical, Physical and Engineering Sciences, vol. 232, no. 1191, pp. 498–509
- Mallik, K. (2020). Use of Isoelectric Point for Fast Identification of Anti-SARS CoV-2 Coronavirus Proteins. Preprints, 2020050270, doi: 10.20944/preprints 202005.0270.v1
- Manassero: controlled landfill design," in Environmental Geotechnics, pp. 77–112, Technical Committee TC 5 on Environmental Geotechnics, Bochum, Germany, 1997
- Martinez-Gil, L. et al. (2011) Membrane integration of poliovirus 2B viroporin. J. Virol. 85, 11315–11324.
- Matlok, M., Petrus, R., Warchoł, J. K. (2015). Equilibrium Study of Heavy Metals Adsorption on Kaolin. Ind. Eng. Chem. Res. 2015, 54, 6975-6984
- Mazzieri, F., and Pasqualini, E. (2000). Permeability of Damaged Geosynthetic Clay Liners, Geosynthetics International 2000 7:2, 101-118
- Mesri, G., and R. E. Olson. (1971). Mechanisms Controlling the Permeability of Clays. Clays and Clay Minerals 19: 151–158.
- Mieszkowski R (2003) Diffusion of lead ions through the Poznań Clay (Neogene) and through glacial clay. Geological Quarterly 47(1): 111–118.

- Mishra, A. K., M. Ohtsubo, L. Li, and T. Higashi. (2005). Effect of salt concentrations on the permeability and compressibility of soil-bentonite mixtures. J. Fac. Agric. Kyushu Univ. 50 (2): 837–849.
- Mishra, A. K., Ohtsubo, M., Li, L. Y., Higashi, T., and Park, J. (2009). Effect of salt of various concentrations on liquid limit, and hydraulic conductivity of different soil-bentonite mixtures. Environmental geology, 57(5), 1145-1153
- Mitchell JK (1993) Fundamentals of Soil Behavior, second ed. John Wiley and Sons, New York.
- Mitchell, J. K., and Soga, K. (2005). Fundamentals of soil behavior. Fundamentals of soil behavior. (Ed. 3).
- Moller, W. J. (1964). Determination of Diffusion Coefficients and Molecular Weights of Ribonucleic Acids and Viruses, Proc. Nut1 Acad. Sci. U.S.A. 51, 501-509
- Moore RS, Taylor DH, Sturman LS, Reddy MM, Fuhs GW (1981). Poliovirus adsorption by 34 minerals and soils. Appl. Environ. Microbiol., 42:963-975.
- Moridis GJ (1999) Semianalytical solutions for parameter estimation in diffusion cell experiments. Water Resources Research 35(6): 1729-1740.
- Munns, R., Wallace, P. A., Teakle, N. L., & Colmer, T. D. (2010). Measuring Soluble Ion Concentrations (Na+, K+, Cl−) in Salt-Treated Plants. Plant Stress Tolerance, 371–382. doi:10.1007/978-1-60761-702-0_23
- Ozgunay H, Colak S, Mutlu MM, Akyuz F (2007). Characterization of leather industry waste. Pol J Environ Stud 16(6):867–873
- Palomino, A.M., and Santamarina, J.C. (2005). Fabric map of kaolinite: Effects of pH and ionic concentration on behavior. Clays and clay minerals, 53(3): 209-222
- Parastar, F., Hejazi, S.M. Sheikhzadeh, M. Alirezazadeh, A. (2017). A parametric study on hydraulic conductivity and self-healing properties of geotextile clay liners used in landfills, Journal of Environmental Management, 202 (1), 29-37, https://doi.org/10.1016/j.jenvman.2017.07.013
- Park, J. A., Kim, J. H., Lee, C. G., & Kim, S. B. (2014). Pyrophyllite clay for bacteriophage MS2 removal in the presence of fluoride. Water Science and Technology: Water Supply, 14, 485–492

- Park, J.A., Kang, J.K., Kim, J.H., Kim, S.B., Yu, S., and Kim, T.H. (2015). Bacteriophage removal in various clay minerals and clay-amended soils. Environ. Eng. Res. 20, 133-140
- Peirce, J.J., Sallfors, G., and Murray, L. (1986). Overburden Pressures Exerted on Clay Liners. Journal of Environmental Engineering, 112 (2), 264-279, DOI: 10.1061/(ASCE)0733-9372(1986)112:2(280)
- Petrick, M. and B.S. Swanson, B.S. (1958) Radiation attenuation method of measuring density of a two-phase fluid, Rev. Sci. Instrum. 29 (12) (1958) 1079–1085
- Petrov RJ, Rowe RK, Quigley RM (1997) Selected factors influencing GCL hydraulic conductivity. ASCE. Journal of Geotechnical and Geoenvironmental Engineering. 123(8):683–695
- Pires, L.F. and Pereira, A.B. (2014) "Gamma-Ray Attenuation to Evaluate Soil Porosity: An Analysis of Methods", *The Scientific World Journal*, vol. 2014, Article ID 723041, 10 pages. https://doi.org/10.1155/2014/723041
- Pusch R, (1992) Use of bentonite for isolation of radioactive waste products. Clay Miner 27: 353–361.
- Rao, P S C. (1974). Pore geometry effects on solute dispersion m aggregated soils and evaluation of a predmtlve model Ph D Thems, Umv Hawan, Honolulu, HI, pp: 195
- Rao, S. N., and P. K. Mathew, P.K. (1995). Effects of Exchangeable Cations on Hydraulic Conductivity of a Marine Clay. Clays Clay Minerals 43: 433–437.
- Reddy Akhileshwari (2020). Delhi to Vijayawada, India has started dumping Covid-19 infected waste in public places, The Print, 5th September, 2020
- Robin MJL, Gillham, RW and Oscarson, DW (1987) Diffusion of strontium and chloride in compacted clay-based materials. J. Soil Sci. Soc. Am., 51: 1102–1108.
- Rowe RK and Booker JR (1985) 1-D pollutant migration in soils of finite depth. Journal of Geotechnical Engineering 111(4): 479–49.
- Rowe, R.K., Quigley, R.M., Booker, J.R. (1997). Clayey Barrier Systems for Waste Disposal Facilities; CRC Press, Taylor and Francis: Boca Raton, FL, USA; ISBN 9780419226000

- Rowe, R.K., and AbdelRazek, A.Y. (2020). Performance of multicomponent GCLs in high salinity impoundment applications. Geotextiles and Geomembranes, https://doi.org/10.1016/j.geotexmem.2020.10.007 (In Press)
- Rowe, R.K., and Li, T.-K. (2020). Self-healing of circular and slit defects in GCLs upon hydration from silty sand under applied stress. Geotextiles and Geomembranes, 48 (5), 667-683, https://doi.org/10.1016/j.geotexmem.2020.05.001
- Ruhl, J. L., and Daniel, D. E. (1997). Geosynthetic clay liners permeated with chemical solutions and leachates. Journal of Geotechnical and Geoenvironmental Engineering, 123(4), 369-381.
- Rushbrook P, and Pugh M (1999) Solid Waste Landfills in Middle and Lower Income Countries. The World Bank, Washington D.C
- Sabiha-Javied, Tufail, M and Sofia Khalid (2008). Heavy metal pollution from medical waste incineration at Islamabad and Rawalpindi, Pakistan, Microchemical Journal, 90 (1), 77-81, https://doi.org/10.1016/j.microc.2008.03.010
- Safari, E., Ghazizade, M. J., & Abdoli, M. A. (2012). A performance-based method for calculating the design thickness of compacted clay liners exposed to high strength leachate under simulated landfill conditions. Waste Management & Research, 30(9), 898–907. doi:10.1177/0734242x12448520
- Salemi, N., Abtahi, S.M., Rowshanzamir, M., Hezaji, S.M. (2018). Geosynthetic clay liners: effect of structural properties and additives on hydraulic performance and durability. Environ Earth Sci 77, 168. https://doi.org/10.1007/s12665-018-7364-z
- Salihoglu, H., Chen, J. N., Likos, W. J., & Benson, C. H. (2016). Hydraulic Conductivity of Bentonite-Polymer Geosynthetic Clay Liners in Coal Combustion Product Leachates. Geo-Chicago 2016. doi:10.1061/9780784480144.043
- Samper J, Dai Z, Dai J, Molinero J, Garcia Gutierrez M, Missana T, Mingarro M (2006) Inverse modeling of tracer experiments in FEBEX compacted Ca-bentonite. Physics and Chemistry of the Earth 31: 640–648.
- Sapna J , Bhawna Y. L. , Sanjeev K. and Deepanmol S. (2020). Strategy for repurposing of disposed PPE kits by production of biofuel: Pressing priority amidst COVID-19 pandemic, Biofuels, DOI: 10.1080/17597269.2020.1797350

- Sardini P, Delay F, Hellmuth K, Porel G and Oila E (2003). Interpretation of out-diffusion experiments on crystalline rocks using random walk modeling. Journal of Contaminant Hydrology 61: 339–350.
- Scalia, J., and Benson, C. H. (2010). Preferential flow in geosynthetic clay liners exhumed from final covers with composite barriers. Canadian Geotechnical Journal, 47(10), 1101–1111
- Schaub, S. A. and Sagik, B. P. (1975). Association of enteroviruses with natural and artifically introduced colloidal solids in water and infectivity of solids-associated virions, Appl. Environ. Microbiol., 30, 212
- Schijven, J.S. & Hassanizadeh, S.M. (2000) Removal of Viruses by Soil Passage: Overview of Modeling, Processes, and Parameters, Critical Reviews in Environmental Science and Technology, 30:1, 49-127, DOI: 10.1080/10643380091184174
- Seiphoori, A., Ferrari, A. and Laloui, L. (2014). Water retention behaviour and microstructural evolution of MX-80 bentonite during wetting and drying cycles, Géotechnique 2014 64:9, 721-734
- Setz, M.C., Tian, K., Benson, C.H., Bradshaw, S.L. (2017). Effect of ammonium on the hydraulic conductivity of geosynthetic clay liners. Geotextiles and Geomembranes, 45 (6), 655-673, https://doi.org/10.1016/j.geotexmem.2017.08.008
- Shackelford CD (1988) Diffusion of Inorganic Chemical Wastes in Compacted Clay. PhD Dissertation, Department of Civil Engineering, University of Texas, Austin, TX, USA
- Shackelford C, Daniel DE and Liljestrand HM (1989) Diffusion of inorganic chemical species in compacted clay soil. Journal of Contaminant Hydrology 4(3): 241–273.
- Shackelford C.D. (1991). Laboratory diffusion testing for waste disposal—a review. J Contam Hydrol 7:177–217
- Shackelford CD and Daniel DE (1991) Diffusion in saturated soil. I. Results for compacted clay. Journal of Geotechnical Engineering 117(3**)**: 485–506.
- Shackelford CD and Daniel DE (1991) Diffusion in saturated soil. II. Results for compacted clay. Journal of Geotechnical Engineering 117(3): 485–506.

- Shackelford CD, Benson CH, Katsumi T, Edil T B, and Lin L (2000) Evaluation the hydraulic conductivity of GCLs permeated with non-standard liquids. Geotextiles. Geomembrane 18 (2000): 133–161.
- Shackelford, C. D., Lee, J. M. (2003). The destructive role of diffusion on clay membrane behavior. *Clays and Clay Minerals*, **51**, 187-197.
- Shan, Hsin-Yu and Lai, Yen-Jing. (2002). Effect of hydrating liquid on the hydraulic properties of geosynthetic clay liners. Geotextiles and Geomembranes, 20 (1), 19-38, https://doi.org/10.1016/S0266-1144(01)00023-1
- Shariatmadari, N., M. Salami, and F. M. Karimpour. (2011). Effect of inorganic salt solutions on some geotechnical properties of soil-bentonite mixtures as barriers. Int. J. Eng. Sci. Technol. 9 (2): 103–110.
- Sharifzadeh, M., Khalafi, H., Afarideh, H. et al. (2017). Two-phase flow component fraction measurement using gamma-ray attenuation technique. NUCL SCI TECH 28, 88. https://doi.org/10.1007/s41365-017-0237-4
- Sharma HB, Vanapalli KR, Cheela VRS, Ranjan VP, Jaglan, KA, Dubey B, Goel S and Bhattacharya J (2020) Challenges, opportunities, and innovations for effective solid waste management during and post COVID-19 pandemic. Resources, Conservation and Recycling 162: 105052, https://doi.org/10.1016/j.resconrec.2020.105052.
- Sparks, D. L. 1999. Soil Physical Chemistry. Boca Raton, FL: CRC Press.
- Sridharan A and Prakash K (1999) Influence of clay mineralogy and pore medium chemistry on clay sediment formation. Canadian Geotechnical Journal 36(5): 961–966.
- Sridharan A., Rao SM, Murthy NS (1986) Compressibility behavior of homoionized bentonites. Geotechnique 36: 551–564.
- Sridharan, A., and K. Prakash. (1999). Percussion and Cone Methods of Determining the Liquid Limit of Soils: Controlling Mechanisms. Geotechnical Testing Journal 23: 236–244.
- Sridharan A, El-Shafei, Miura N (2000) Geotechnical behaviour of Ariake Clay and its comparison to typical clay minerals. In: Proceedings of the international symposium on low land technology, Saga University, Saga, pp 121–128
- Sridharan, A., and Prakash, K. (2004). Free Swell Ratio and Clay Mineralogy of Fine-grained Soils. Geotechnical Testing Journal 27: 220–225.

- Sridharan, A., and Choudhury, D. (2008). Computation of Hydraulic Conductivity of Montmorillonitic Clays by Diffuse Double Layer Theory. International Journal of Geotechnical Engineering 2: 1–10
- Sridharan, A. (2014). Fourth IGS-Ferroco Terzaghi Oration: 2014. Indian Geotech J 44, 371–399 (2014). https://doi.org/10.1007/s40098-014-0136-0
- Stagg, C. H., C. Wallis, and C. H. Ward. (1977). Inactivation of clay-associated bacteriophage MS-2 by chlorine. Appl. Environ. Microbiol. 33:385-391
- Stern, R. T., and C. D. Shackelford. (1998). Permeation of sand-processed clay mixtures with calcium chloride solutions. J. Geotech. Geoenviron. Eng. 124 (3): 231–241. https://doi.org/10.1061/(ASCE)1090-0241(1998)124:3(231).
- Stotzky G. (1985). Mechanisms of Adhesion to Clays, with Reference to Soil Systems. In: Savage D.C., Fletcher M. (eds) Bacterial Adhesion. Springer, Boston, MA. https://doi.org/10.1007/978-1-4615-6514-7_8
- Syngouna, V. I., and Chrysikopoulos, C. V. (2010). Interaction between viruses and clays in static and dynamic batch systems. Environ. Sci. Technol. 44, 4539–4544
- Technical Code for Liner System of Municipal Solid Waste Landfill, CJJ113-2007, China Architecture and Building Press, Beijing, China, 2007.
- Thammathiwat, A., and Chim-oye, W. (2010). Effect of permeant liquid on the swell volume and permeability of geosynthetic clay liners. J. EJGE, 15, 1183-1197.
- Thiyagarajan, T.K., Dixit, N.S., Satyamurthy, P., Venkatramani, N., & Rohatgi, V.K. (1991). Gamma-ray attenuation method for void fraction measurement in fluctuating two-phase liquid metal flows. Measurement Science and Technology, 2(1), 69-74.
- Tian, K., Likos, W.J., Benson, C.H., 2019. Polymer elution and hydraulic conductivity of bentonite–polymer composite geosynthetic clay liners. J. Geotech. Geoenviron. Eng.145 (10), 04019071.
- Turkyilmaz, A., Guney, M., Karaca, F., Bagdatkyzy, Z., Sandybayeva, A., & Sirenova, G. (2019). A comprehensive construction and demolition waste management model using PESTEL and 3R for construction companies operating in central Asia. Sustainability (Switzerland), 11(6), [1593]. https://doi.org/10.3390/su11061593

- Van Loon LR, Jakob A (2005). Evidence for a second transport porosity for the diffusion of tritiated water (HTO) in a sedimentary rock (Opalinus clay-OPA): application of through- and out-diffusion techniques. Transp Porous Media 61:193–214
- van Olphen, H. (1963). An Introduction to Clay Colloid Chemistry. New York: Interscience.
- Vasconcelos, I. F.; Bunker, B. A.; Cygan, R. T. (2007). Molecular Dynamics Modeling of Ion Adsorption to the Basal Surfaces of Kaolinite. J. Phys. Chem. C, 111, 6753−6762
- Velde, B. (1995). Origin and Mineralogy of Clays: Clays and the Environment. Berlin: Springer-Verlag
- Vilker VL, Meronek GC, Butler PC. (1983). Interactions of poliovirus with montmorillonite clay in phosphate-buffered saline. Environ Sci Technol. 1983 Oct 1;17(10):631-4. doi: 10.1021/es00116a014. PMID: 22288711
- Wang, B., Xu, J., Chen, B., Dong, X., Dou, T. (2019). Hydraulic conductivity of geosynthetic clay liners to inorganic waste leachate. Applied Clay Science. 168, 244-248, https://doi.org/10.1016/j.clay.2018.11.021
- Wang, Q and Su, M. (2020). A preliminary assessment of the impact of COVID-19 on environment - A case study of China, Sci. Tot. Environ., 728 (2020), Article 138915**,** doi:10.1016/j.scitotenv.2020.138915
- Wang, Y.H., and Siu, W.K. (2006). Structure characteristics and mechanical properties of kaolinite soils. I. Surface charges and structural characterization. Canadian Geotechnical Journal, 43(6): 587-600. 10.1139/t06-026
- Wanyoike S, Ramirez Gonzalez A, Dolan SB, et al. (2017). Disposing of Excess Vaccines After the Withdrawal of Oral Polio Vaccine. *J Infect Dis*.; 216(suppl_1): S202-S208. doi:10.1093/infdis/jiw572
- Weber, W.J; Jang, Y.C.; Townsend, T.G.; Laux, S. (2002). Leachate from Land Disposed Residential Construction Waste. Journal of Environmental Engineering, 128:3
- WHO. (2004). WHO global action plan for laboratory containment of wild polioviruses, Vaccines and Biologicals, January, 2004
- WHO (2014). Safe management of wastes from health-care activities, ISBN 978 92 4 154856 4.

- Williams R.T. (2018). Hydraulic performance of geo-synthetic clay liners, MS Thesis, University of Virginia, USA
- Worrell, W.A., Vesilind, P.A., (2012). Solid Waste Engineering, second ed. Cengage Learning, Stamford, CT
- Wyoming Mining Association, Bentonite mining. URL: http://www. wma-minelife.com/bent/bentmine/bentmine.htm
- Wysokinski, L. (2007). (Ed.) Principles of Assessing the Suitability of Cohesive Soils of Poland for the Construction of Mineral Insulating Barriers; ITB, Ministry of Environment: Warsaw, Poland, 2007; ISBN 978-83-249-1125-7.
- Xie, H., Zhang, C., Sedighi, M., Hywel, R., Chen, Y., (2015). An analytical model for diffusion of chemicals under thermal effects in semieinfinite porous media. Comput. Geotech. 69, 329e337
- Yeheyis, M., Hewage, K., Alam, M.S. et al. (2013). An overview of construction and demolition waste management in Canada: a lifecycle analysis approach to sustainability. Clean Techn Environ Policy 15, 81–91, https://doi.org/10.1007/s10098-012-0481-6
- Yu, W.H., Li, N., Tong, D.S., Zhou, C.H., Lin, C.X., Xu, C.Y., (2013). Adsorption of proteins and nucleic acids on clay minerals and their interactions: a review. Appl. Clay Sci. 80–81, 443–452
- Zainab, B. and Tian, K. (2015). Hydraulic Conductivity of Bentonite-Polymer Geosynthetic Clay Liners to Coal Combustion Product Leachates, Geo-Congress 2020 : Engineering, Monitoring, and Management of Geotechnical Infrastructure